The Parkinson's disease-related kinase Pink1 mediates mitochondrial quality control

Dissertation

zur Erlangung des Doktorgrades
der Mathematisch-Naturwissenschaftlichen Fakultät
der Rheinischen Friedrich-Wilhelms-Universität Bonn

vorgelegt von

CORNELIA RÜB

Bonn, Mai 2016

universitätbonn

Angefertigt mit Genehmigung der Mathematisch-Naturwissenschaftlichen Fakultät der
Rheinischen Friedrich-Wilhelms-Universität Bonn

1. Gutachter: Prof. Dr. Wolfgang Voos
2. Gutachter: Prof. Dr. Jörg Höhfeld

Tag der mündlichen Prüfung: 8. August 2016
Erscheinungsjahr: 2016

Publications

Original articles

Hallmann, K., Kudin, A. P., Zsurka, G., Kornblum, C., Reimann, J., Stüve, B., Waltz, S., Hattingen, E., Thiele, H., Nürnberg, P., Rüb, C., Voos, W., Kopatz, J., Neumann, H., Kunz, W. S. (2016) Loss of the smallest subunit of cytochrome c oxidase, COX8A, causes Leigh-like syndrome and epilepsy. **Brain** 139: 338-45

Fedorowicz, M. A., de Vries-Schneider, R. L. A., Rüb, C., Becker, D., Huang, Y., Zhou, C., Wolken, D. M. A., Voos, W., Liu, Y. H., Przedborski S. (2014) Cytosolic cleaved PINK1 represses Parkin translocation to mitochondria and mitophagy. **EMBO Rep** 15: 86-93

Guardia-Laguarta, C., Area-Gomez, E., Rüb C., Liu, Y., Magrane, J., Becker, D., Voos, W., Schon, E. A., Przedborski S. (2014) alpha-Synuclein is localized to mitochondria-associated ER membranes. **J Neurosci** 34: 249-59

Nargang, F. E, Adames, K., Rüb, C., Cheung, S., Easton, N., Nargang, C. E., Chae, M. S. (2012) Identification of genes required for alternative oxidase production in the Neurospora crassa gene knockout library. **G3 (Bethesda)** 2: 1345-56

Review articles

Rüb, C., Schröder, N., Voos, W. (2015) Biochemical properties of the kinase PINK1 as sensor protein for mitochondrial damage signalling. **Biochem Soc Trans** 43: 287-291

Voos, W., Rüb, C., Bruderek, M. (2014) Chaperones and Proteases of Mitochondria: From Protein Folding to Degradation and Mitophagy. **The Molecular Chaperones Network in Protein Degradation and Folding** (Ed.: Houry, W. A.), Springer Science+Business Media, New York, p. 303-327

Poster

Rüb, C., Schröder, N., Becker, D., Fedorowicz, M. A., Przedborski, S., Voos, W. Reconstitution of Pink1 localization and function. “Pink1-Parkin Signalling in Parkinson’s Disease and Beyond”. Biochemical Society, London 2014

Table of contents

Table of figures

1 Introduction

1.1 Mechanisms of mitochondrial homeostasis

In eukaryotic cells, mitochondria fulfill a multitude of essential functions, ranging from energy production to mediating apoptotic cell death. Thus, cells employ a sophisticated system of organelle-specific molecular chaperones and proteases to maintain mitochondrial biogenesis and protein quality control (PQC) under normal and stress conditions. These processes collectively contribute to mitochondrial protein homeostasis. On the one side, mitochondrial chaperones of the Hsp60 and Hsp70 type assist import and folding of nuclear-encoded proteins, which constitute the fast majority of the mitochondrial proteome. On the other side, these chaperones work together with specialized soluble and membrane-associated proteases to prevent the accumulation of damaged or superfluous proteins through refolding or degradation (Voos, 2013). In particular under intrinsic or externally imposed stress conditions, the biochemical mechanisms of mitochondrial PQC may be exhausted. The resulting accumulation of denatured or even aggregated polypeptides constitutes a severe danger for mitochondrial and cellular health. Apart from the loss of important metabolic functions, damaged mitochondrial may exert a negative influence on cellular survival by releasing large amounts of reactive oxygen species (ROS) or apoptotic proteins including cytochrome *c* (Andersen & Kornbluth, 2013, Halliwell, 2006). Thus, cells possess an additional mechanism of organellar quality control. This process, which utilizes the reactions of cellular autophagy to remove irrevocably damaged mitochondria as a whole, is termed mitophagy. At the beginning of a putative signaling pathway, arguably deciding about “life or death” of defective mitochondria, stands the mitochondrial kinase Pink1 (Ashrafi & Schwarz, 2013). The question, how Pink1 signals mitochondrial damage and which events lead to its activation has been addressed in the present work.

1.2 Mitochondrial dysfuction in Parkinsons's disease

Over the last years, mitochondrial dysfunction has emerged as a common feature of aging-related neurodegenerative diseases like Parkinson's disease, Alzheimer's disease, Huntington's disease or amyotrophic lateral sclerosis (ALS) (Lin & Beal, 2006). With a prevalence estimated at 0.3 % of the entire population and 1 % in people over the age of 60, Parkinson's disease (PD) is the second most common neurodegenerative disorder (de Lau & Breteler, 2006). PD is clinically characterized by four key symptoms: rigidity, postural instability, tremor and a typical slowness in executing movements termed bradykinesia. These neurological symptoms are collectively caused by the progressive loss of dopaminergic neurons in the *substantia nigra pars compacta* (Lang & Lozano, 1998a, Lang & Lozano, 1998b).

First evidence for a link between Parkinson's disease and mitochondria dates back to the late 1970s, when accidental exposure to 1-methyl-4-phenyl-1,2,3,6-tetrahydropyridine (MPTP), a synthesis byproduct of the illegal drug 1-methyl-4-phenyl-4-propionoxy-piperidine (MPPP) was shown to cause PD-like symptoms and degeneration of dopaminergic neurons (Langston, Ballard et al., 1983). MPTP was later demonstrated to be oxidized to MPP^+, which is selectively taken up by dopaminergic neurons via the dopamine transporter (Javitch & Snyder, 1984), and inhibits complex I of the mitochondrial respiratory chain (Nicklas, Vyas et al., 1985). Accordingly, a similar effect results from exposure to complex I inhibitors like rotenone or paraquat, developed as pesticide and herbicide, respectively. Both chemicals cause Parkinsonism in animal models (Berry, La Vecchia et al., 2010, Betarbet, Sherer et al., 2000). A second line of evidence for the exceptional role of mitochondria in the etiology of PD comes from mutations in the mitochondrial genome (mtDNA). The 16,500 base pairs comprising circular mtDNA encodes 13 genes for subunits of respiratory chain complexes I, III, IV and V along with 22 mitochondrial tRNAs and two rRNAs, respectively (Anderson, Bankier et al., 1981). High levels of large-scale somatic mtDNA deletions, causing mitochondrial dysfunction, were found in *substantia nigra* neurons from post-mortem brains of PD patients (Bender, Krishnan et al., 2006). Moreover, patients with mutations in the mitochondrial polymerase γ accumulate excessive levels of mtDNA mutations as a result of defective mitochondrial replication and this defect coincides with an increased risk for developing PD (Luoma, Melberg et al., 2004).

Table 1: Overview of PARK-designated Parkinson's disease-related loci, mode of inheritance, gene names and names of encoded proteins. Bold: Loci linked to monogenic PD. AD: autosomal dominant, AR: autosomal recessive. Asterisk: erroneous locus (identical to *PARK1*). Modified after (Klein & Westenberger, 2012).

Symbol	Inheritance	Gene name	Protein name (short name)	UniProt entry number
PARK1	AD	*SNCA*	Alpha-synuclein	P37840
PARK2	AR	*PARKN*	E3 ubiquitin-protein ligase parkin (Parkin)	O60260
PARK3	AD	unknown	unknown	-
PARK4*	AD	*SNCA*	Alpha-synuclein	P37840
PARK5	AD	*UCHL1*	Ubiquitin carboxyl-terminal hydrolase isozyme L1 (UCH-L1)	P09936
PARK6	AR	*PINK1*	Serine/threonine-protein kinase Pink1, mitochondrial (Pink1)	Q9BXM7
PARK7	AR	*DJ-1*	Protein-deglycase DJ-1 (DJ-1)	Q99497
PARK8	AD	*LRRK2*	Leucine-rich repeat serine/threonine- protein kinase 2 (LRRK2)	Q5S007
PARK9	AR	*ATP13A2*	Probable cation-transporting ATPase 13A2	Q9NQ1
PARK10	risk factor	unknown	-	-
PARK11	AD	unknown	-	-
PARK12	risk factor	unknown	-	-
PARK13	AD or risk factor	*HTRA2 OMI*	Serine protease HtrA2, mitochondrial (HtrA2/Omi)	O43464
PARK14	AR	*PLA2G6*	85/88 kDa calcium-independent phospholipase A2 (CaI-PlA2)	O60733
PARK15	AR	*FBX07*	F-box only protein 7	Q9Y3I1
PARK16	risk factor	unknown	-	-
PARK17	AD	*VPS35*	Vacuolar protein sorting-associated protein 35 (hVPS35)	Q96QK1
PARK18	AD	*EIF4G1*	Eukaryotic translation initiation factor 4 gamma1 (eIF-4G1)	Q04637

While about 90 % of PD cases are sporadic, studying the rare hereditary cases has led to the identification of several genes contributing to onset and progress of Parkinson‘s disease. The 18 loci demonstrated or suspected to relate to the disease shown in Table 1, were termed PARK and numbered chronologically in order of their identification (Klein & Westenberger, 2012).

In brief, six genes are linked to monogenic PD, meaning a form of the disease for which a mutation in a single gene is sufficient to cause the phenotype. Among them is *SNCA* (*PARK1*), encoding α-synuclein. Point mutations in the α-synuclein-encoding gene *SNCA* as well as gene duplications or triplications, respectively, have been shown to cause PD (Klein & Westenberger, 2012). The 140 aa α-synuclein protein is the major component of the so-called Lewy bodies. These intraneuronal proteinaceous inclusions are the morphological characteristic of PD and related diseases, summarized as α-synucleinopathies (Goedert, 2001). In Lewy bodies, which represent insoluble deposits of the protein, α-synuclein is present in fibrils with a β-sheet like structure (Der-Sarkissian, Jao et al., 2003). It is thought that the pathogenicity of the aggregation-prone α-synuclein involves the formation of small neurotoxic oligomers, which eventually mature to larger aggregates (Haass & Selkoe, 2007). In addition to its predominantly cytosolic localization, α-synuclein has been proposed to localize at or in mitochondria (Devi, Raghavendran et al., 2008, Li, Yang et al., 2007). Functional links between the protein and mitochondria stem from the observation, that mutant α-synuclein sensitizes neurons to mitochondrial toxins like MPP^+. Moreover, effects of α-synuclein on mitochondrial dynamics, meaning the fusion and fission of mitochondria, have been reported (Nakamura, 2013). Another gene accountable for monogenic PD is *DJ-1* (*PARK7*). The DJ-1 protein is sensitive to oxidative stress and may act as a redox-responsive chaperone, which can prevent protein misfolding (Shendelman, Jonason et al., 2004). Notably, DJ-1 was found to reloaclize to mitochondria in the presence of reactive oxygen species (Canet-Aviles, Wilson et al., 2004) and mitochondrial defects were observed in DJ-1-deficient *Drosophila* and mouse models (Hao, Giasson et al., 2010). Mutations in *PARK8*, encoding the serine/threonine kinase LRRK2, are the most common cause of autosomal dominant PD (Klein & Westenberger, 2012). LRRK2 interacts with regulators of mitochondrial fusion and fission. Accordingly, PD-related mutations of the protein alter mitochondrial dynamics (Ryan, Hoek et al., 2015). Intriguingly, LRRK2

inhibits the removal of proteins by chaperone-mediated autophagy (CMA), leading to accumulation of CMA substrates, including α-synuclein (Orenstein, Kuo et al., 2013). Through this mechanism, LRRK2 may contribute to α-synuclein aggregation and α-synuclein-dependent mitochondrial damage (Ryan et al., 2015) *HTRA2* (*PARK13*) encodes the stress-inducible mitochondrial serine protease HtrA2 (Omi), which resides in the intramembrane space. Proteins of the HtrA family have the remarkable property to switch between protease and chaperone activity. It is speculated that the mitochondrial HtrA2 functions in protein quality reactions, comparable to the bacterial HtrA homologs, including DegP. However, clear evidence for a role of HtrA2 in PQC is lacking so far (Voos, 2013). Moreover, upon apoptotic stimuli, HtrA2 is released into the cytosol to promote apoptosis (Vande Walle, Lamkanfi et al., 2008). Loss-of-function mutations, affecting the regulation of the proteolytic activity of HtrA2 were identified in the *HTRA2* gene from heterozygous PD patients (Strauss, Martins et al., 2005). Finally, mutations in two genes, encoding the mitochondrial serine/threonine-protein kinase Pink1 (PARK6) and the cytosolic E3 ubiquitin-protein ligase Parkin (PARK2), respectively, cause autosomal recessive PD (Kitada, Asakawa et al., 1998, Valente, Abou-Sleiman et al., 2004). Pink1, which collaborates with Parkin to mediate the removal of damaged mitochondria by mitophagy, has been in the focus of this work.

In summary, out of the six gene products associated with monogenic PD, five are linked to mitochondrial function and at least one additional mitochondrial protein may contribute to the etiology of the disease. Thus, functional insight from PD-related proteins strongly supports prior evidence for a role of mitochondrial dysfunction in Parkinson's disease.

1.3 Identification of Pink1

Pink1 was initially identified in a screen for proteins transcriptionally regulated by the tumor suppressor PTEN (phosphatase and tensin homolog) and predicted to contain a highly conserved serine/threonine-protein kinase domain. Accordingly, the protein was termed PTEN-induced putative kinase 1 (Pink1) (Unoki & Nakamura, 2001). Further analysis revealed that Pink1 consists of 581 amino acids, with a predicted molecular mass of 62.8 kDa and is ubiquitously expressed, with highest expression in heart, skeletal muscle and testis (Unoki & Nakamura, 2001). Pink1 is conserved among eukaryotes ranging from *C. elegans* and *D. melanogaster* to humans but absent from the model

organism yeast. While a role in PTEN-signaling was excluded by Unoki et al., the protein gained major attention ever since mutations in the *PINK1* (*PARK6*) gene affecting the Pink1 kinase domain, were shown to be responsible for hereditary early onset Parkinson's disease (Valente et al., 2004). In the same study, and in agreement with a predicted mitochondrial targeting signal, Pink1 was demonstrated to localize to mitochondria.

1.4 Import, processing and submitochondrial localization of Pink1

Initial reports on the mitochondrial localization of Pink1 motivated further investigations regarding import and suborganellar localization of the protein. Like most mitochondrial proteins, Pink1 is encoded in the nuclear genome and synthesized at cytosolic ribosomes. In the classical presequence import pathway, a matrix-destined mitochondrial preprotein is directed to the cytosol-exposed receptors of the outer mitochondrial membrane by an N-terminal mitochondrial targeting signal (MTS). Translocation across the outer- and inner membrane (OMM and IMM) then occurs via the TOM and TIM23 translocase complexes, respectively. Insertion of the preprotein into the TIM23 channel implicitly requires the presence of a mitochondrial membrane potential ($\Delta\psi$), as the electrochemical gradient drives translocation of the positively charged targeting signal. Moreover, complete translocation of the polypeptide into the matrix is dependent on ATP hydrolysis by the import motor complex at the inner face of the inner membrane translocase complex. Upon crossing of the preprotein through the IMM, the targeting sequence is usually cleaved off by the matrix processing peptidase (MPP). This processing reaction gives rise to the mature protein, which is released into the matrix compartment. Apart from transport into the matrix, multiple other import pathways direct proteins to their specific mitochondrial subcompartment (Becker, Böttinger et al., 2012b).

The very N-terminal segment of the Pink1 sequence resembles a mitochondrial targeting signal (Figure 1) (Valente et al., 2004), which was reported to be sufficient for mitochondrial localization of the protein (Silvestri, Caputo et al., 2005). Moreover, an N-terminal Pink1 processing product of apparently 55 kDa was identified in addition to the 64 kDa full-length Pink1 (Beilina, Van Der Brug et al., 2005). Although both observations theoretically agree with import of Pink1 into the mitochondrial matrix, a

more complex and partially controversial picture of Pink1 import and processing emerged from subsequent studies.

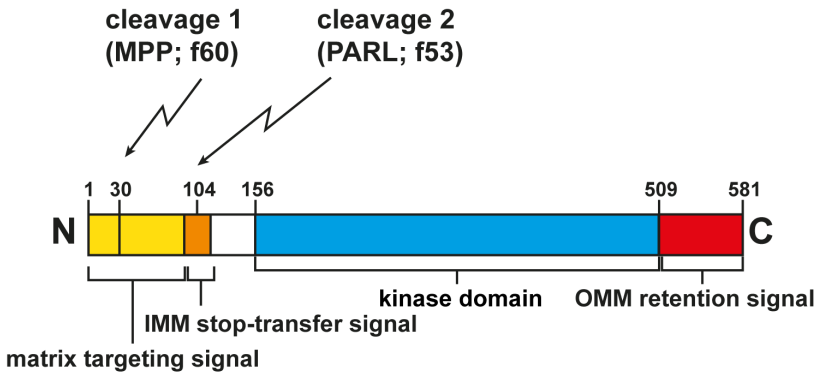

Figure 1: Schematic representation of domain structure and cleavage sites within the Pink1 sequence. The N-terminal mitochondrial targeting signal is followed by a hydrophobic transmembrane domain, which comprises residues 85 to 110 and acts as an inner membrane stop-transfer signal. Residues 156 to 509 constitute the Ser/Thr kinase domain, followed by a C-terminal domain, which may act as an OMM retention signal. Protease cleavage sites for MPP and PARL and the resulting Pink1 fragments are indicated. Note that the MPP cleavage site was estimated from the molecular mass of the MPP processing product.

First, different submitochondrial localizations of Pink1 were reported, making it difficult to define an import pathway for the protein. While both full-length and processed Pink1 are predominantly located at the outer face of the OMM with the kinase domain facing the cytoplasm (Becker, Richter et al., 2012a, Zhou, Huang et al., 2008), the protein was alternatively found in the intermembrane space (IMS) (Meissner, Lorenz et al., 2011) and in the IMM (Silvestri et al., 2005). In addition, a fraction of the processed Pink1 fragment was shown to localize to the cytosol (Lin & Kang, 2008). Secondly, a role of the mitochondrial membrane potential in import, localization and arguably stability of Pink1 was proposed. While under basal conditions, endogenous Pink1 is barely, if at all detectable by Western blot or immunofluorescence (Becker et al., 2012a, Zhou et al., 2008), the protein accumulates on mitochondria upon dissipation of $\Delta\psi$ (Jin, Lazarou et al., 2010, Narendra, Jin et al., 2010b). Thirdly, different proteases were demonstrated to sequentially process Pink1, possibly influencing its submitochondrial localization and suggesting a complex interplay of import and processing reactions (Deas, Plun-Favreau et al., 2010a, Greene, Grenier et al., 2012).

Using an *in vitro* assay, Becker et al. elucidated the mitochondrial import pathway of Pink1 in detail (Becker et al., 2012a). The results of the latter and other studies suggest that in the presence of an inner membrane potential, the Pink1 polypeptide is partially inserted into the IMM through the TOM and TIM23 complexes (Figure 2). An N-terminal hydrophobic segment adjacent to the presequence-like signal, acts as a stop-transfer signal, preventing full translocation of Pink1 over the IMM (Zhou et al., 2008). When the N-terminal portion reaches the matrix, it is cleaved by MPP, resulting in the formation of a 60 kDa cleavage product ($Pink1_{f60}$) (Greene et al., 2012). The IMM resident protease PARL (Presenilin-associated rhomboid-like protein) then catalyzes a second cleavage between positions 103 and 104 within the Pink1 sequence, generating a 53 kDa fragment ($Pink1_{f53}$) (Deas et al., 2010a). Upon cleavage by PARL, the processed fragment is released from the import machinery. $Pink1_{f53}$ then associates with the OMM via its very C-terminal hydrophobic portion (Becker et al., 2012a). $Pink1_{f53}$ was further demonstrated to be degraded by the proteasome, a process that would require its full translocation to the cytosol (Matsuda, Sato et al., 2010, Yamano & Youle, 2013). By contrast, in depolarized mitochondria, the 64 kDa full-length Pink1 ($Pink1_{p64}$) associates with the OMM, possibly through binding of the presequence-like N-terminal segment of Pink1 to cytosol-exposed TOM receptors. As further translocation of Pink1 is arguably prevented in the absence of Dy, full-length Pink1 accumulates on the OMM and recruits cytosolic Parkin. In turn, Parkin initiates the downstream mitophagy process (Jin et al., 2010).

In summary, Pink1 is directed to the outer mitochondrial membrane by a non-canonical import pathway. Partial insertion into the inner mitochondrial membrane and processing of the protein are at least to some extent dependent on the mitochondrial membrane potential.

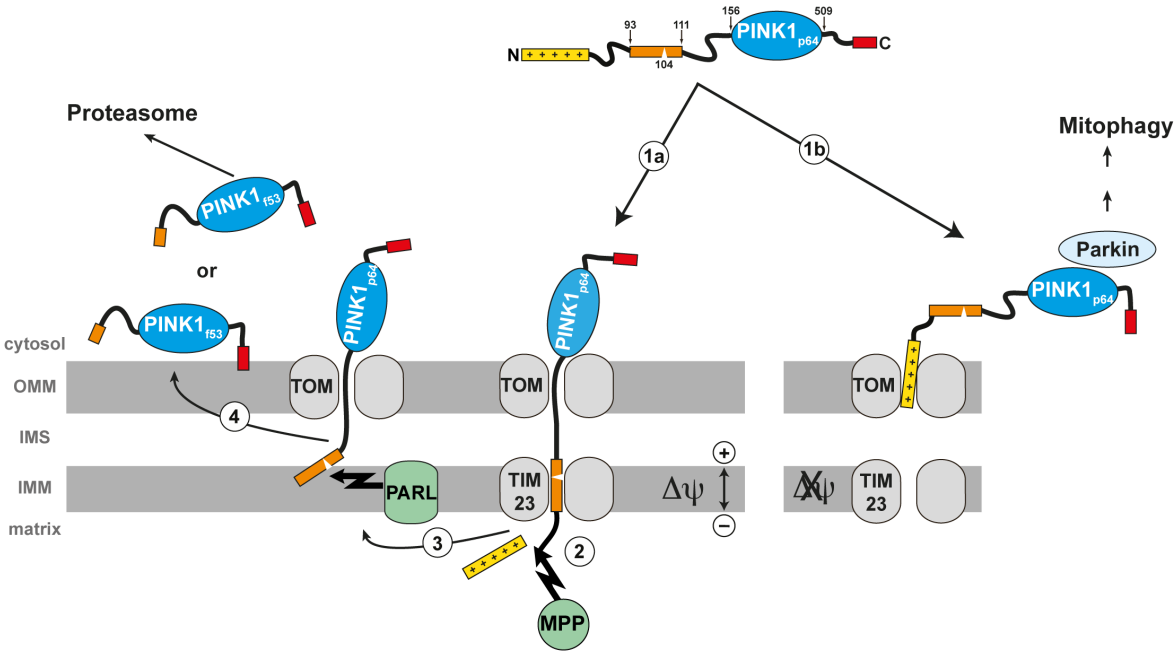

Figure 2: Model of Pink1 import in the presence and absence of Δψ, respectively. In the presence of Δψ (left side), the presequence-like N-terminal segment of the Pink1 precursor ($Pink1_{p64}$) drives the translocation of Pink1 across the OMM via the TOM complex and its insertion into the IMM via the TIM23 complex (1a). The inner membrane stop-transfer signal prevents complete translocation of Pink1 over the IMM. The N-terminus of Pink1 reaches the matrix, allowing cleavage of the mitochondrial targeting signal by the matrix processing peptidase (MPP) (2). The IMM protease PARL cleaves $Pink1_{p64}$ at position 104, generating the processed form $Pink1_{f53}$, which is released from the import machinery (3). A fraction of $Pink1_{f53}$ associates with the OMM as a peripheral membrane protein, possibly assisted by the very C-terminal fraction of the polypeptide. Alternatively, $Pink1_{f53}$ is degraded by the proteasome. In depolarized mitochondria (right side), the Pink1 precursor ($Pink1_{p64}$) associates with the OMM, possibly via TOM components. Accumulating Pink1 recruits Parkin, which in turn induces mitophagy (1b). OMM, outer mitochondrial membrane; IMS, intramembrane space; IMM, inner mitochondrial membrane. Modified after (Becker et al., 2012a).

1.5 Degradation of Pink1

The electrochemical potential over the inner mitochondrial membrane is not only a requirement for import of mitochondrial preproteins into the matrix compartment but also indicative of active oxidative phosphorylation and mitochondrial integrity. Therefore, the loss of Δψ has traditionally been used as a measure for the degree of mitochondrial dysfunction. Vice versa, chemical uncoupling of Δψ e.g. by the ionophore valinomycin or the protonophore carbonyl cyanide *m*-chlorophenyl hydrazone (CCCP) is routinely utilized to simulate mitochondrial damage in cell culture models. While both full-length and processed Pink1 are virtually undetectable under normal conditions, the full-length

form accumulates upon depletion of Δψ by exposure of cells to CCCP (Jin et al., 2010, Narendra et al., 2010b, Zhou et al., 2008). Moreover, a relatively fast decrease in Pink1 levels upon recovery of Δψ was reported. These observations led to the initial hypothesis that the low steady-state levels of Pink1 in healthy mitochondria result from constitutive and rapid degradation of the imported and processed form of Pink1 (Matsuda et al., 2010). By this mechanism, Pink1 was postulated to accumulate specifically on depolarized mitochondria to signal mitochondrial damage (Narendra et al., 2010b). Concerning the protease responsible for Pink1 degradation, several publications proposed an involvement of the proteasome, as proteasomal inhibitors stabilize the processed form of Pink (Lin & Kang, 2008, Takatori, Ito et al., 2008). Degradation of Pink1 was further demonstrated to follow the N-end rule, meaning that susceptibility of a protein to degradation via the ubiquitin-proteasome system is determined by its N-terminal amino acid (Yamano & Youle, 2013). By contrast, another study postulated degradation of Pink1 inside the matrix compartment, catalyzed by the mitochondrial protease Lon (Thomas, Andrews et al., 2014). Notably, the latter observation is largely inconsistent with a localization of Pink1 at the outer mitochondrial membrane described above.

Taken together, according to the current model, mitochondrial Pink1 amounts are regulated through Δψ–dependent import and degradation of the protein. By this mechanism, Pink1 is postulated to accumulate on depolarized mitochondria to act as a sensor of mitochondrial damage. Notably, this hypothesis is based on the inner membrane potential as the sole measure for mitochondrial damage. However, it is not clear how the complete depolarization of virtually all mitochondria within a cell, experimentally caused by CCCP translates to physiological and pathophysiological conditions. Thus, the authentic cause for the fast increase in Pink1 levels in response to mitochondrial perturbations is not yet clear. In addition, the proposed import/turnover model raises the question if the 53 kDa major cleavage product of Pink1 represents merely a degradation intermediate or if it fulfills any specific function.

1.6 Pink1/Parkin-mediated mitophagy

After Pink1 accumulates on depolarized mitochondria, it recruits the usually cytosolic E3 ubiquitin-protein ligase Parkin. In turn, Parkin initiates a downstream pathway that eventually leads to mitophagy, a mitochondria-specific type of macroautophagy. In brief,

autophagy describes the sequestration of a portion of the cytoplasm, protein aggregates or whole organelles in a double membrane structure, termed autophagosome. The autophagosome then fuses with a lysosome, delivering its content to degradation by lysosomal enzymes (Figure 3). While non-specific autophagy of intracellular components occurs in response to nutrient starvation, autophagy can be highly selective for specific organelles, including mitochondria (Wang & Klionsky, 2011). Mitophagy mediates the removal of mitochondria during erythrocyte development (i), eliminates paternal mitochondria in fertilized oocytes (ii) and is responsible for the clearance of irrevocably damaged mitochondria (iii). While all three mitophagy pathways are thought to utilize core components of the autophagic machinery, the preceding events that lead to the initiation of mitophagy are likely distinct. In response to mitochondrial damage, Pink1 and Parkin function together to mediate mitophagy (Ashrafi & Schwarz, 2013).

Using *Drosophila* knockout models, loss of Pink1 or Parkin, respectively, was demonstrated to result in similar mitochondrial defects, namely muscle degeneration, cell death and mitochondrial abnormalities. Complementation analysis further revealed that Pink1 functions upstream of Parkin in a common pathway (Clark, Dodson et al., 2006, Park, Lee et al., 2006). In human cells exposed to CCCP, Parkin was subsequently shown to translocate from the cytosol to mitochondria upon loss of $\Delta\psi$. Moreover, Parkin was proposed to mediate the autophagic removal of damaged mitochondria (Narendra, Tanaka et al., 2008). Providing an explanation for their genetic interaction, Pink1 was finally demonstrated to be responsible for Parkin translocation to depolarized mitochondria (Geisler, Holmstrom et al., 2010b, Matsuda et al., 2010, Narendra et al., 2010b, Vives-Bauza, Zhou et al., 2010, Ziviani, Tao et al., 2010). In addition, the usually repressed ubiquitin ligase function of Parkin was activated upon its Pink1-mediated translocation to mitochondria (Narendra et al., 2010b).

Pink1-dependent recruitment of Parkin to mitochondria and subsequent induction of mitophagy require the kinase function of Pink1 (Geisler et al., 2010b, Matsuda et al., 2010, Narendra et al., 2010b). This notion raised questions concerning Pink1 phosphorylation targets and a putative mechanism of Pink1-mediated mitochondrial translocation and activation of Parkin. As an E3 ubiquitin ligase, Parkin catalyzes the transfer of the of the 76 aa protein ubiquitin (Ub) from an E2 ubiquitin-conjugating

enzyme to the ε- amino group of a substrate protein's lysine residue. The acceptor protein can be another ubiquitin, in which case polyubiquitin chains are formed (Ciechanover, 2005). Depending on the length and linkage type of Ub modifications, substrate proteins are tagged for signaling processes or degradation, by the proteasome, the lysosome or autophagy (Clague & Urbe, 2010). Parkin is capable of catalyzing monoubiquitination, as well as the addition of different types of polyubiquitin chains, including Lys48- and Lys63-linked chains to its substrate proteins (Hampe, Ardila-Osorio et al., 2006, Seirafi, Kozlov et al., 2015). Parkin consists of an N-terminal ubiquitin-like (Ubl) domain, linked to four zink-finger domains, three of which form a RING1-In-Between-RING2 (RBR) motif (Figure 37, appendix). Accordingly, it is classified as an RBR-type E3 enzyme (Trempe & Fon, 2013). Using *in vitro* and *in vivo* techniques, Pink1 was demonstrated to directly phosphorylate Parkin at Ser65 within the UBL domain (Kondapalli, Kazlauskaite et al., 2012). This phosphorylation was initially proposed to relieve an autoinhibitory mechanism of Parkin, thereby promoting its enzymatic activity (Kondapalli et al., 2012, Shiba-Fukushima, Imai et al., 2012). Intriguingly, Parkin carrying a Ser65Ala mutation to abolish its phosphorylation, as well as a Parkin mutant lacking the Ubl domain, still translocate to mitochondria in a Pink1-kinase dependent manner (Kane, Lazarou et al., 2014). An explanation for this observation lies within a recently discovered novel mechanism, in which Pink phosphorylates ubiquitin at Ser65 (homologous to Ser65 in the Parkin Ubl domain) and in turn, phospho-ubiquitin activates the Parkin E3 ligase activity (Kane et al., 2014, Kazlauskaite, Kondapalli et al., 2014, Koyano, Okatsu et al., 2014). According to a recently proposed feed-forward model, Pink1-mediated phosphorylation activates Parkin, which in turn, ubiquitinates proteins on the mitochondrial surface. Pink1 then phosphorylates these newly formed polyubiquitin chains, generating phospho-ubiquitin, which further promotes Parkin activity (Ordureau, Sarraf et al., 2014).

Once activated, Parkin ubiquitinates proteins at the outer face of the outer mitochondrial membrane (Geisler, Holmstrom et al., 2010a, Narendra, Kane et al., 2010a, Sarraf, Raman et al., 2013). Notably, the broad spectrum of Parkin OMM substrates identified in a proteomics approach by Sarraf et al. suggests that the overall ubiquitination pattern, rather than a specific substrate is crucial for the subsequent signaling process (Sarraf et al., 2013). The current model of Pink1/Parkin-mediated mitophagy is illustrated in Figure 3. Although the events downstream of Parkin activity still have to be worked out in detail, it is proposed that cellular autophagic components recognize the ubiquitin chains attached to

OMM proteins and eventually mediate the mitophagy process (Ashrafi & Schwarz, 2013, de Vries & Przedborski, 2012, Geisler et al., 2010a, Pickrell & Youle, 2015). In general, mitophagy utilizes the core autophagy machinery, comprising numerous so-called autophagy-related (Atg) proteins, which were initially identified in yeast. Among them is LC3, one of several human Atg8 homologs, which is conjugated to phosphatidylethanolamine residues of the forming autophagic membrane. Adaptor proteins that interact with both mitochondrial and autophagic proteins, including LC3, mediate organelle specificity of the mitophagy process (Wang & Klionsky, 2011). In case of Pink1/Parkin-dependent mitophagy, the autophagy adaptor p62 may be recruited to ubiquitinated mitochondria albeit its requirement for the mitophagy process as such remains controversial (de Vries & Przedborski, 2012, Geisler et al., 2010a, Narendra et al., 2010a). Other candidate adaptor proteins are the Bcl-2 family member Nix, NBR1, Tax1BP1, NDP52, and optineurin (de Vries & Przedborski, 2012, Pickrell & Youle, 2015). In case of NDP52 and optineurin, a recent study elucidated their direct recruitment by Pink1 to phospho-ubiquitin. Remarkably, Parkin was dispensable for this process, which emphasizes a more direct function of Pink1 in the mitophagy process (Lazarou, Sliter et al., 2015). Notably, most of the work characterizing the Pink1/Parkin system has been carried out in immortalized cell lines and frequently utilizing overexpression of at least on of the two proteins. Hence the question to what extent endogenous Pink1 and Parkin contribute to mitophagy in neurons remains to be answered (Grenier, McLelland et al., 2013).

It should be noted that recruitment of Parkin and the autophagic machinery is likely only one of several functions of Pink1 in a broader context of mitochondrial quality control. Within the cell, mitochondria do not exist as isolated organelles but constitute a dynamic network, which is constantly recomposed by fusion and fission (Youle & van der Bliek, 2012). Fusion of the outer membrane is mediated by the GTPases Mitofusin 1 and Mitofusin 2 (Mfn1 and Mfn2). Both proteins are ubiquitinated in a Pink1/Parkin-dependent manner to be degraded by the proteasome (Gegg, Cooper et al., 2010, Tanaka, Cleland et al., 2010) and at least Mfn2 is also a direct Pink1 substrate (Chen & Dorn, 2013). Abolishing fusion through degradation of Mfn1/Mfn2 prevents severely damaged mitochondria from refusing with and poisoning the mitochondrial network (Youle & van der Bliek, 2012). Moreover, the resulting smaller mitochondria are thought to be better accessible targets for the mitophagy process (de Vries & Przedborski, 2012). Transport of

mitochondria along microtubules confers mitochondrial motility, as exemplified by axonal transport. The mitochondrial Rho GTPase Miro1 acts as an adaptor between mitochondria and kinesin motor proteins. Upon loss of $\Delta\psi$, Pink1, together with Parkin, activates the proteasomal degradation of Miro1, which results in a halt of mitochondrial motility. The resulting spatial isolation may facilitate removal of the damaged organelle by mitophagy (Wang, Winter et al., 2011).

Finally, the mitochondrial Hsp90 chaperone TRAP1 and the IMM protease HtrA2 (see 1.2) were demonstrated to be phosphorylated by Pink1 (Plun-Favreau, Klupsch et al., 2007, Pridgeon, Olzmann et al., 2007). A spatial interaction of the cytosol-exposed Pink1 kinase domain with the matrix resident TRAP1 is unlikely. However, TRAP1 overexpression completely rescues the Pink1-deficient phenotype in flies, pointing towards a certain functional redundancy of Pink1 and TRAP1 (Costa, Loh et al., 2013). Similarly, regulation of HtrA2, a candidate constituent of PQC may implicate a function of Pink1 in mitochondrial homeostasis beyond mitophagy.

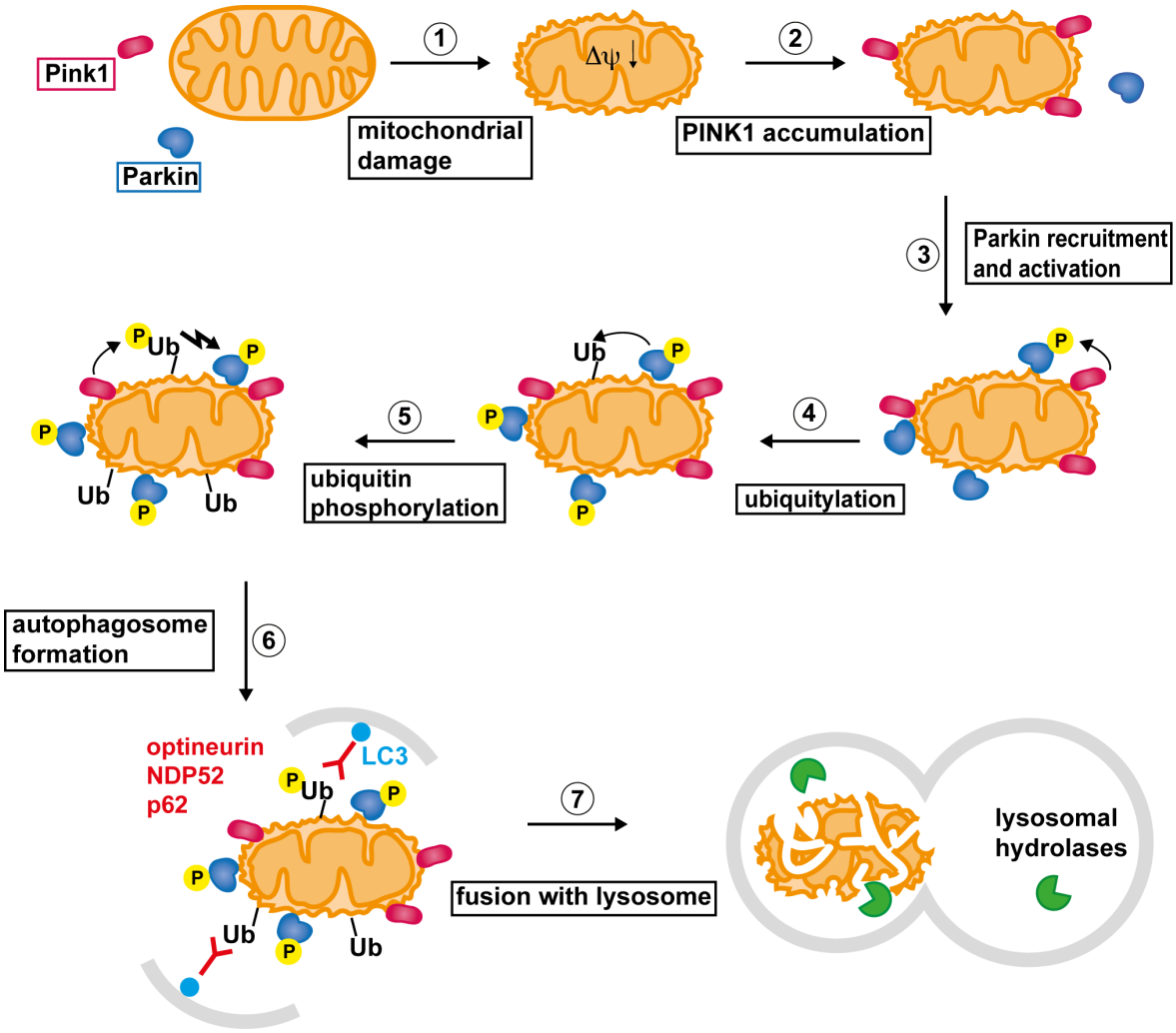

Figure 3: Current model of Pink1/Parkin-mediated mitophagy. Under normal conditions, Pink1 levels are very low. Mitochondrial stress conditions may lead to mitochondrial damage, accompanied by a decrease or loss of the mitochondrial membrane potential (Δψ) (1). In the absence of Δψ, Pink1 accumulates at the outer mitochondrial membrane (OMM) (2). Pink1 recruits and activates the usually cytosolic E3 ubiquitin ligase Parkin in a process involving Pink1-mediated phosphorylation of Parkin at Ser65 (3). Parkin conjugates ubiquitin (Ub) to various OMM proteins (4). Pink1 phosphorylates Ub attached to OMM proteins, and the resulting phospho-Ub further activates Parkin (5). Adaptor proteins (candidate proteins are indicated) that bind to both ubiquitin and the autophagic protein LC3 mediate sequestration of the organelle in an autphagosomal membrane (6). The autophagosome then fuses with a lysosome, delivering its complete content to degradation by lysosomal hydrolases (7).

2 Objectives of this work

The mechanisms, whereby the PD-related mitochondrial kinase Pink1 initiates the autophagic removal of defective mitochondria via the recruitment and activation of Parkin, have been extensively studied. By contrast, the preceding events, leading to a significant increase in the amount of Pink1 polypeptides at the outer mitochondrial membrane of impaired mitochondria are by far less understood. The current model states that Pink1 amounts are regulated via membrane potential-dependent import and concomitant fast turnover of the protein. The considerations leading up to this thesis were 1) that the proposed model presumes complete depolarization of virtually all mitochondria for the activation of the Pink1/Parkin system, a condition that seems unlikely to occur under physiological conditions and 2) that the constitutive synthesis and degradation of Pink1 would consume an enormous amount of cellular energy. Thus, in my thesis I aimed at identifying conditions that elicit an increase in Pink1 protein levels. The main experimental strategy was to treat cultured human cells with diverse chemicals that modulate mitochondrial or cellular functions and monitor Pink1 protein levels under the respective conditions. Analyzing the functional state of mitochondria upon perturbations that elicit Pink1 accumulation would then possibly allow identifying a common trigger for Pink1 accumulation and concomitant mitophagy. In a second approach, the biochemical mechanism underlying the regulation of Pink1 protein amounts should be revisited. To this end, cellular and mitochondrial degradation assays were employed to directly assess the turnover of Pink1 both under normal conditions and mitochondrial perturbations that lead to elevated Pink1 levels. A third approach aimed at establishing a model for mitochondrial perturbations with a direct relevance for PD. The PD-related cytosolic protein α-synuclein, which has been proposed to exert harmful effects on mitochondria, represents a prominent candidate for such a model. As a prerequisite for future experiments, the putative interaction of α-synuclein with mitochondria should be analyzed by means of a radioactive *in vitro* import assay.

3 Materials

3.1 Laboratory devices

Device	Name	Manufacturer
CCD camera	LAS-400 mini	Fujifilm
Cell counter	Scepter	Milipore
Flow cytometer	CyFlow space CY-S3001	Partec
Fluorescence microscope	EVOS fl	PeqLab
Homogenizer	Minilys	PeqLab
Microplate reader	Infinite M200 pro	TECAN
Phosphorimager	FLA-5100	Fujifilm
Ultracentrifuge	Optima Max-XP	Beckman Coulter

3.2 Chemicals

Compound	Supplier
1-Methyl-4-phenylpyridinium iodide (MPP^+)	Sigma-Aldrich
Actinomycin D	Sigma-Aldrich
Antimycin A	Sigma-Aldrich
Apyrase	Sigma-Aldrich
Atractyloside	Calbiochem
Carbonyl cyanide 3-chlorophenylhydrazone (CCP)	Sigma-Aldrich
Creatine	Roche
Creatine Kinase	Roche
Cycloheximide	Sigma-Aldrich
Digitonin	Calbiochem
Dodecyl- β -D-maltosid	Carl Roth
Menadione	Sigma-Aldrich
1-Methyl-4-phenylpyridinium iodide (MPP^+ iodide)	Sigma-Aldrich
MG132 (Z-leu-leu-leu-al)	Sigma-Aldrich

Oligomycin	Sigma Aldrich
Phenylmethylsulfonyl fluoride (PMSF)	Carl Roth
Proteinase K	Sigma-Aldrich
Protease inhibitor cocktail plus	Carl Roth
Rotenone	Sigma-Aldrich
Tetramethylrhodamine ethyl ester (TMRE)	Life technologies

3.3 Reagents

Name	Supplier
ATP determination kit	Life technologies
EXPRESS [^{35}S] protein labeling mix	Perkin Elmer
iScript Select cDNA synthesis kit	BioRad
Lipofectamine	Life technologies
MitoSOX mitochondrial superoxide detector	Life technologies
MitotrackerRed	Life technologies
mMESSAGE mMACHINE SP6 Transcription kit	Life technologies
Molecular Weight Marker, low range	Sigma Aldrich
NativeMark protein standard	Life technologies
NucBlue® Live ReadyProbes™ Reagent	Life technologies
Plasmid DNA isolation kit	Life technologies
Rabbit Reticulocyte Lysate System	Promega
RNeasy Mini Kit	Qiagen
RotiQuant universal	Carl Roth
ServaLight EoSUltra CL HRP WB Substrate Kit	Serva
T_NT-coupled reticulocyte lysate	Promega
TRIzol	Life technologies
TurboFect transfection reagent	Theromo Scientific

3.4 Cell culture media and reagents

Name	Supplier
Dulbeco's modified Eagel's medium (DMEM), high glucose	Life technologies
RPMI medium	Life technologies
Fetal calf serum (FCS)	Life technologies
Penicillin/Streptomycin	Life technologies
L-glutamine	Life technologies
0.005 % Trypsin-EDTA	Life technologies
10 x PBS	Life technologies

3.5 Primary antibodies

Immunogen	Type	Specification	Source
BiP/GRP78	mouse	610978	BD Biosciences
COX1	mouse	459600	Invitrogen
COX4	mouse	3E11	Cell Signaling
COX5a	mouse	A21363	Molecular Probes
DJ1	mouse	-	gift from S. Przedborski
GAPDH	mouse	E1C603-1	EnoGene
GRP75/Mortalin	mouse	SPS-825	Stressgen
Hsp60	rabbit	sc-13966	Santa Cruz Biotechnology
Lon	rabbit		Gramsch
Mfn2	mouse		Abcam
Parkin	rabbit	2132	Cell Signaling
Pink1	rabbit	BC100-494	Novus Biologicals
PMPCA (MPP)	rabbit	HPA021648	Sigma-Aldrich
SDHA	mouse	459200	Invitrogen
Smac	rabbit	sc-22766	Santa Cruz Biotechnology
Tim23	mouse	611222	BD Biosciences
Tom40	rabbit	sc-11414	Santa Cruz Biotechnology
TRAP1	rabbit	GR2387	Gramsch

α -Tubulin	mouse	T5168	Sigma-Aldrich
FLAG-tag	mouse	FLAG M2 affinity gel A2220	Sigma

3.6 Peroxidase-coupled secondary antibodies for Western blot

Immunogen	Type	Specification	Source
Rabbit IgG	goat	A6154	Sigma-Aldrich
Mouse IgG	goat	A4416	Sigma-Aldrich

3.7 Mammalian cell lines

Name	Description	Source
SH-SY5Y	human neuroblastoma	German Collection of Microorganisms and Cell Cultures (DSMZ), ACC-209
HeLa	human cervix carcinoma	DSMZ, ACC-57
MEF *PARL* -/-	mouse embryonic fibroblast	Serge Przedborski

3.8 Plasmids

Name	Description	Source
pHSPINK1	vector: pCMV-SPORT6, insert: human Pink1, CMV promoter for mammalian expression	Imagenes
pHSMDH2	vector: pOTB7, insert: human Mdh2; T7 promoter for *in vitro* transcription	Invitrogen
pPINK1-FLAG	vector: pIRES-hrGFP-1, insert: human Pink1 with C-terminal FLAG-tag, CMV promoter for mammalian expression	Serge Przedborski
pPINK1DN103	vector: pCMV, insert: human Pink1 with	Serge

	deletion of 103 N-terminal amino acids, CMV promoter for mammalian expression	Przedborski
pSNCA-A30P	vector: pCMV, insert: human α-synuclein with A30P mutation and C-terminal HA-tag, CMV promoter for mammalian expression	Serge Przedborski
pSNCA-A53T	pCMV vector, insert: human α-synuclein with A53T mutation and C-terminal HA-tag, CMV promoter for mammalian expression	Serge Przedborski
pSNCA-HA-WT	vector: pCMV, insert: human α- synuclein with C-terminal HA tag, CMV promoter for mammalian expression	Serge Przedborski
pSU9-GFP	vector: pcDNA3.1, insert: GFP fused to first 70 amino acids of *N.crassa* ATPase subunit 9 (Su9(70)),CMV promoter for mammalian expression	Ursula Gerken
pSU9-GFP-DHFR	vector: pcDNA3.1, insert: mouse full length DHFR with *N.crassa* Su9(70) and GFP fused to N-terminus, CMV promoter for mammalian expression	Nadja Schröder
pSU9-GFP-DHFRds	vector: pcDNA3.1, insert: destabilized mouse full length DHFR with *N.crassa* Su9(70) and GFP fused to N-terminus, CMV promoter for mammalian expression	Nadja Schröder

Primers for qRT-PCR

Name	Sequence
PINK1 fwd	5’-AACATCCTTGTGGAGCTGGACCCAGACG-3’
PINK1 rev	5’-CATCAGCCTTGCTGTAGTCAATCACTG-3’
GAPDH fwd	5’- TCAGACACCATGGGGAAGGTGAA-3’
GAPDH rev	5’- GAATCATATTGGAACATGTAAACCATG-3’

3.9 Primers for PCR

Name	Sequence
SP6-Koz-SNCA- fw	5’- GAATTCATTTAGGTGACACTATAGAATACGC CGCCACCATGGATGTATTCATGAAAGGAC-3’
SNCA-stop-rev	5’-TCATCATCATTAGGCTTCAGGTTCGTAGT-3’

3.10 siRNA

Transcript	specification	Source
Mortalin (HspA9)	SR30004	amsbio
control		amsbio

4 Methods

4.1 Protein biochemical methods

4.1.1 Glycine SDS-PAGE

Discontinuous glycine sodium dodecyl sulfate polyacrylamide gel electrophoresis (SDS-PAGE) was routinely utilized to separate proteins according to their molecular weight and under denaturing conditions.

Large Gel	Resolving gel (12.5 %)	Stacking Gel
Acrylamide / bisacrylamide (37.5:1) mix	6.9 ml	0.83 ml
1.875 M Tris pH 8.8	3.5 ml	-
0.8 M Tris pH 6.8	-	0.5 ml
10 % [w/v] SDS	0.17 ml	50 µl
ddH_2O	6.3 ml	3.55 ml
10 % [w/v] APS	100 µl	50 µl
TEMED	10 µl	10 µl
Total volume	17 ml	5 ml

Samples were resolved in 1 x SDS-PAGE sample buffer (8 % SDS, 40 % glycerol, 240 mM Tris-HCl, pH 6, 0.08 % Bromphenol blue, 20 % β-mercaptoethanol) and heated to 95 °C for 5 min. Electrophoresis was conducted in 1 x SDS-buffer (25 mM Tris, 0.191 mM glycine) at 25 mA for 3 -4 h.

4.1.2 Tricine SDS-PAGE

Tricine SDS-PAGE was used for the separation of small proteins, specifically α-synuclein. A 16.5 % acrylamide separation gel was overlaid with a 10 % acrylamide spacer gel and a stacking gel. Samples were prepared as described for glycine SDS-PAGE and electrophoresis was conducted in a two buffer system consisting of anode buffer

(0.2 M Tris-HCl, pH 8.9) and cathode buffer (0.1 M Tris, pH 8.25, 0.1 M tricine and 0.1 % SDS) at 25 mA for 12-14 h.

Acrylamide stock (32:1)	200 ml	final concentration
acrylamide	96 g	49.5 %
bis-acrylamide	3 g	3 %
ddH_2O	to 200 ml	

3 x gel buffer	500 ml	final concentration
Tris-HCl, pH8.5	181.71	3 M
SDS	1.5 g	0.3 %
ddH_2O	to 500 ml	

Gel	16.5 %	10 %	stacking (4ml)
acrylamide (32:1)	5 ml	1 ml	0.417 ml
3 x gel buffer	5 ml	1.67 ml	1.25 ml
glycerol	2 ml	-	-
ddH_2O	3 ml	2.33 ml	3.33 ml
10 % APS	75 µl	17 µl	42 µl
TEMED	7.5 µl	1.7 µl	4.2 µl
total volume	15 ml	5 ml	5 ml

4.1.3 Blue native PAGE of mitochondrial proteins and protein complexes

Mitochondrial proteins and protein complexes were analyzed by Blue native polyacrylamide gel electrophoresis (BN-PAGE). A 5-16.5 % polyacrylamide gradient resolving gel was prepared as following, by help of a gradient mixer, and overlaid with a stacking gel.

3 x gel buffer	500 ml	final concentration
ε -amino n-caproic acid	13.12 g	200 mM
Bis-Tris/HCl pH 7.0	15.7 g	150 mM
ddH_2O	to 500 ml	

Gel	5 %	16.5 %	stacking gel
3 x gel buffer	3 ml	3 ml	2.5 ml
acrylamide (32:1)	0.91 ml	3.05 ml	0.6 ml
glycerol	-	1.8 ml	-
ddH_2O	5.048 ml	1.117 ml	4.367 ml
10 % APS	38 µl	30 µl	30 µl
TEMED	3.8 µl	3 µl	3 µl
total volume	9 ml	9 ml	7 ml

50 µg mitochondria per sample were solubilized in lysis buffer (1 % digitonin, 10 mM HEPES, pH 7.4, 2 mM EDTA, pH 8.0, 50 mM NaCl, 10 % glycerol, 1 mM PMSF). After a clarifying spin to remove non-solubilized material, 10 x loading dye (5 % Coomassie blue G-250, 500 mM ε-amino n-caproic acid, 100 mM Bis-Tris-HCl, pH 7.0) was added and samples applied to the gel. The chamber was filled with pre-chilled anode buffer (50 mM Bis-Tris, pH 7.0) and samples overlaid with cathode buffer with Coomassie (50 mM Tricine, pH 7.0, 15 mM Bis-Tris/HCl, pH 7.0, 0.2 % Coomassie blue G-250), which was replaced by cathode buffer w/o Coomassie after the running front had reached the separation gel. The gel temperature was maintained at 4 °C using a cold water pump and electrophoresis conducted at 70 V for 16 to 20 h. The gel was finally soaked in 1 x SDS buffer for 5 min and subjected to Western blotting as described below.

4.1.4 Western blot and immunodetection of specific proteins

Proteins separated by acrylamide gel electrophoresis were transferred to a polyvinylidene fluoride (PVDF) membrane using semi-dry Western blot technique. PVDF membranes were activated in methanol and pre-soaked in transfer buffer (20 mM Tris, 150 mM glycin, 0.1 % SDS, 20 % methanol), placed on three layers of filter paper soaked in transfer buffer, followed by the gel and three more layers of filter paper. Transfer was

conducted 220 mA for 2 h. After staining in Coomassie solution (0.25 % Coomassie Brilliant Blue R250, 40 % methanol, 10 % acetic acid) and destaining in destaining solution (40 % methanol, 10 % acetic acid) for visualization of total proteins, the membrane was incubated in blocking solution (5 % milk, 0.5 % Tween 20 in TBS) for 1 h. After incubation with a specific primary antiserum diluted in TBS containing 0.5 % Tween 20 at 4 °C o/N, membranes were washed three times in TBS, followed by incubation with anti-mouse- or anti-rabbit IgG antibody coupled to horseradish peroxidase diluted 1:5000 for 1 h at RT, and washing three times in TBS. Western blot membranes were developed using enhanced chemiluminescence (ECL) substrates and a charge coupled device (CCD) camera.

4.1.5 Quantification of Western blot signals

Where indicated, Western blot signals were quantified by means of MultiGauge software (Fujufilm).

4.1.6 TCA precipitation of proteins

TCA precipitation was used to concentrate proteins from dilute samples. 1/5 of final volume of 72 % trichloroacetic acid (TCA) was added to samples and mixed. After 30-40 min incubation on ice, samples were centrifuged at 20,000 g for 40 min at 4 °C. Pellets were washed with ice-cold acetone and centrifuged at 20,000 x g for 12 min. Pellets were air-dried for 2 min and finally resuspended in 1 x SDS-PAGE sample buffer.

4.1.7 Determination of protein concentration by modified BCA assay

Protein concentration was routinely determined by means of modified BCA (bicinchoninic assay) assay (RotiQuant universal, Carl Roth). 5 µl of each sample or of a BSA serial dilution were pipetted in a 96 well plate. A RotiQuant working solution containing 15 parts of reagent 1 and 1 part of reagent 2 was prepared and 200 µl of the working solution added to each well. After 30 min incubation at 37 °C, the absorbance at 492 nm was read in a microplate reader.

4.1.8 Alkaline extraction of proteins

For alkaline extraction of mitochondrial proteins, 50 µg of isolated mitochondria (see 2.4.2) were resuspended in 500 µl of 0.1 M sodium carbonate (Na_2CO_3) / sodium bicarbonate ($NaHCO_3$) solution at pH 7.3, 10, 11.5 or 12, respectively and briefly mixed by vortexing. After 30 min incubation on ice, samples were subjected to ultra-centrifugation at 100,000 x g for 1 h at 4 °C. Supernatants were TCA-precipitated and all samples analyzed by SDS-PAGE and Western blot.

4.1.9 *In vitro* transcription and translation

Radiolabeled precursor proteins for *in vitro* import were synthesized in cell-free transcription and translation systems. For uncoupled transcription and translation, mRNA was produced from linearized plasmid DNA using the SP6-transcription kit (Promega). The obtained mRNA was used as a template for *in vitro* translation in the presence of [^{35}S]-methionine/cysteine by means of reticulocyte lysate system (Promega). For transcription of SNCA constructs, transcription template DNA was amplified from the HA-tagged plasmids by standard PCR reaction, introducing SP6 promoter and Kozak sequence via the 5'-primer followed by uncoupled transcription and translation reactions as described. Coupled transcription/translation was conducted using the T_NT-coupled reticulocyte lysate system (Promega) and linearized plasmid DNA as a template.

4.2 Cell culture methods

4.2.1 Cell culture conditions

Cell line	Culture medium
SH-SY5Y	DMEM, 10 % FCS, 1 mM L-glutamine, 100 units/ml penicillin, 100 µg/ml streptomycin
HeLa	RPMI, 10 % FCS, 2 mM L-glutamine, 100 units/ml penicillin, 100 µg/ml streptomycin
MEF	DMEM, 10 % FCS, 2 mM L-glutamine, 100 units/ml penicillin, 100 µg/ml streptomycin

All cell lines were maintained in 10 cm or 15 cm diameter tissue culture dishes at 37 °C in a saturated humidity atmosphere containing 5 % CO_2. Cells were passaged by trypsinization at ratios of 1:3 to 1:6 every 48 to 72 h and routinely tested for *Mycoplasma* contamination by PCR.

4.2.2 Chemical treatment of cells

SH-SY5Y cells were grown to 70-80 % confluency and then incubated in complete DMEM medium supplemented with the respective compound or corresponding amounts of EtOH/DMSO for control samples. Concentrations and incubation times were as specified in the figure legends.

4.2.3 Transient transfection of cultured cells

For transfection with plasmid DNA, cells were grown to a confluency of 70 to 90 % and transfected by means of TurboFect™ transfection reagent (Thermo Scientific) according to the manufacturer's instructions and used for experiments 24 to 72 h post-transfection.

4.2.4 Knock-down of protein expression by siRNA

For knock-down of protein expression, cells were grown in 6-well plates to a confluency of 50 to 70 % in growth medium w/o antibiotics and transfected with siRNA by means of Lipofectamine™ reagent according to the manufacturer's instructions using 100-pmol of siRNA and 5 µl transfection reagent per well. Cells were used for experiments 24 to 72 h post-transfection.

4.3 Cell biology methods

4.3.1 Lysis of cultured cells

Cells were harvested using a cell scraper, washed twice in PBS and resuspended in lysis buffer (0.5 % Triton X-100, 20 mM Tris-HCl, pH 7.4, 2 mM EDTA, 50 mM NaCl, 0.5 mM PMSF, 1 x protease inhibitors). Incubation at 4 °C with shaking at 1400 x rpm was followed by a clarifying spin at 1200 x g for 5 min to remove unlysed cells. The

protein concentration of the cleared lysate was determined (see 4.1.7) and 20 mg protein per lane were loaded for SDS-PAGE.

4.3.2 Subcellular fractionation of cultured cells

After harvesting, cells were washed twice in ice-cold PBS and resuspended in HMS-A buffer (220 mM mannitol, 70 mM sucrose, 20 mM HEPES, pH 7.6, 1 mM EDTA, 0.2 % BSA, 1 mM PMSF). Cells were homogenized using a glass/Teflon homogenizer and cell lysates subjected to a clarifying spin at 1500 x g for 5 min. The supernatant was separated into mitochondrial and cytosolic fraction at 12,000 x g. The resulting mitochondrial pellet was washed once in HMS-B buffer (220 mM mannitol, 70 mM sucrose, 20 mM HEPES, pH 7.6, 1 mM EDTA, 1 mM PMSF) and finally resuspended in HMS-B. When analyzed in the respective experiment, cytosolic fraction were TCA-precipitated.

4.3.3 Preparation of mitochondrial fractions from muscle biopsies

To obtain mitochondria-enriched fractions from human muscle biopsies, 25-100 mg of muscle tissue was homogenized in 20 µl ice-cold HMS-B buffer per mg tissue by means of a Minilys® homogenizer using 1.4 mm ceramic beads. After pelleting of cell debris at 600 x g for 80 s, the supernatant was re-centrifuged at 17,000 x g for 5 min. The resulting mitochondrial pellet was washed twice in HMS-B. For subsequent analysis by Blue native PAGE, mitochondrial fractions were resuspended in DDM lysis buffer (0.02 M Tris-HCl, pH 7.4, 2 mM EDTA, 0.05 M NaCl, 10 % glycerol, 1 mM PMSF, 2.5 mg/ml n-dodecyl b-D-maltoside) to a final concentration of 1 µg protein / µl. Experiments with patient samples were carried out under supervision of Prof. Dr. W. Kunz (Department of Epileptology and Life and Brain Center, University of Bonn) and according to the guidelines of the Ethical committee of the University of Bonn Medical Center.

4.3.4 *In vitro* import of [^{35}S]-labeled precursor proteins into isolated mitochondria

For *in vitro* import of [^{35}S]-Met/Cys-labeled precursor proteins, 50 µg of freshly isolated mitochondria were resuspended in 100 µl import buffer (20 mM HEPES, pH 7.6, 0.25 M

sucrose, 5 mM magnesium acetate, 80 mM potassium acetate), supplemented with 5 mM glutamate, 5 mM malate, 1 mM DTT, 5 mM KP_i, pH 7.4 and 2 mM ATP. Where indicated, the mitochondrial membrane potential ($\Delta\psi$) was dissipated by the addition of 8 µM antimycin A, 0.5 µM valinomycin, and 20 µM oligomycin prior to import. Following the addition of radiolabeled precursor proteins, reactions were incubated at 37 °C for the indicated times. Mock samples contained radiolabeled pre-proteins diluted in import buffer but no mitochondria. Mtochondria were re-isolated at 12,000 x g, washed once in import buffer and samples analyzed by SDS-PAGE and digital autoradiography. Where indicated, mitochondria were incubated in the presence of 100 µg/ml trypsin for 30 min on ice after import to digest protease-accessible proteins (post-treatment). In order to access dependency of the import reaction on protease-accessible components of the TOM translocation complex, mitochondria were treated with trypsin or proteinase K at concentrations indicated in the respective figures for 25 min on ice prior to import (pre-treatment).

4.3.5 Mitochondrial re-translocation assay

For the mitochondrial re-translocation assay, import of [^{35}S]-labeled precursor proteins was performed as described for 30 min at 30 °C. After completion of the import reaction, mitochondria were re-isolated at 12,000 x g for 10 min and resuspended in 30 µl import buffer supplemented with 5 mM malate, 5 mM glutamate and 2 mM ATP. Where indicated $\Delta\psi$ was dissipated by addition of a mixture of 8 µM antimycin A, 0.5 µM valinomycin and 20 µM oligomycin and mitochondria resuspended in import buffer w/o supplements. Samples were incubated at 30 °C for the indicated times and then separated into mitochondrial pellet and soluble fraction at 12,000 x g for 10 min. The soluble fraction was TCA- precipitated and all samples finally resuspended in SDS-PAGE sample buffer. After separation by SDS-PAGE, samples were analyzed by digital autoradiograohy.

4.3.6 Mitochondrial degradation assay

To follow the degradation of newly imported radiolabeled proteins by mitochondrial proteases, *in vitro* import was conducted as described for 40 min. After completion of the import reaction, mitochondria were re-isolated, washed once in import buffer to remove

unbound preproteins and resuspended in 30 µl fresh import buffer, supplemented with 1 mM creatine phosphate, 75 µg/ml creatine kinase and 7.5 µg/ml BSA. Where indicated, mitochondria were depleted of $\Delta\psi$ by addition of 8 µM antimycin A, 0.5 µM valinomycin and 20 µM oligomycin. For degradation in the absence of ATP, mitochondria were pre-incubated with 0.01 U/µl apyrase and 20 µM oligomycin for 10 min at 30 °C and then incubated in import buffer w/o glutamate, malate and ATP-regenerating system but supplemented with 10 mM EDTA. Degradation reactions were incubated at 30 °C and after different time points, samples were withdrawn and mixed directly with SDS-PAGE sample buffer. All samples were analyzed by SDS-PAGE and digital autoradiography.

4.3.7 Cellular degradation assay

To monitor cellular degradation of Pink1 under different conditions, SH-SY5Y cells transiently expressing Pink1-FLAG, were subjected to radioactive cellular pulse/chase labeling, followed by immunoprecipitation specifically of Pink1-FLAG using an anti-FLAG antibody.

4.3.7.1 Cellular pulse/chase labeling

24 h post-transfection with pPINK1-FLAG, cells were incubated for 1 h in depletion medium (Met/Cys free DMEM supplemented with 10 % FCS dialyzed against PBS and 1 mM L-glutamine) under normal culture conditions to deplete intracellular methionine and cysteine. For pulse labeling, cells were incubated in depletion medium containing [^{35}S]-Met/Cys-labeling mix with a specific activity of 22 mCi/ml in the medium for 30 min. After washing once with complete DMEM, cells were further incubated in depletion medium supplemented with 30 mg/L cold methionine and 25 mg/L cold cysteine. After different chase incubation times, cells were scarped off from culture dished in PBS and whole cell suspensions subjected to TCA precipitation before proceeding with immunoprecipitation.

4.3.7.2 Immunoprecipitation of Pink1-FLAG

For immunoprecipitation, TCA precipitated proteins were lysed by boiling samples in denaturing lysis buffer (1 % SDS, 50 mM Tris-HCl, pH 7.4, 5 mM EDTA, 8 M urea). Lysates were diluted 1:10 in IP buffer (1 % Triton X-100, 50 mM Tris-HCl, pH 7.4,

150 mM NaCl, 50 mM EDTA, 1 mM PMSF, 1 x protease inhibitors) and subjected to a clarifying spin at 14,000 x g for 10 min. After determination of the protein concentration by BCA assay, equal amounts of protein were mixed with 25 µl of anti-FLAG antibody coupled to agarose beads (Anti-FLAG M2 affinity gel, Sigma A220) equibrilated in IP-buffer and incubated on a tube rotator at 4 °C o/N. Samples were washed three times in wash buffer (0.1 % Triton X-100, 50 mM Tris-HCl, pH 7.4, 300 mM NaCl, 5 mM EDTA, 1 mM PMSF) before adding 40 µl SDS-PAGE sample buffer, shaking for 10 min, and boiling the samples at 95 °C for 5 min to elute bound proteins. Samples were analyzed by SDS-PAGE and digital autoradiography.

4.3.8 Measurement of mitochondrial membrane potential (Δψ) in cultured cells by TMRE staining and flow cytometry

The potential-sensitive fluorescent dye tetramethylrhodamine ethyl ester (TMRE) was used to assess Dy in intact SH-SY5Y cells. Following incubation in complete growth medium containing 0.5 µM TMRE for 20 min, cells were harvested by trypsinization and washed twice in PBS containing 0.2 % BSA. The red fluorescence of 20,000 cells per sample was analyzed by flow cytometry. Untreated cells and cells treated with the mitochondrial uncoupler carbonyl cyanide *m*-chlorophenyl hydrazone (CCCP) were analyzed as controls.

4.3.9 Measurement of Δψ in isolated mitochondria by TMRE staining and fluorescence intensity measurement

For determination of Dy in isolated mitochondria, mitochondria were resuspended in potential buffer (0.6 M sorbitol, 0.1 % BSA, 10 mM $MgCl_2$, 20 mM KP_i, pH 7.2, 5 mM malate, 10 mM glutamate) and incubated with 1 µM TMRE for 30 min at 30 °C and protected from light. Samples were washed once to remove excess TMRE and the TMRE fluorescence (excitation: 540 nm, emission: 585 nm) was measured in a microplate reader (Tecan Infinite M200 PRO, Tecan).

4.3.10 Measurement of oxygen radicals in cultured cells by MitoSOX staining and flow cytometry

The superoxide indicator MitoSOX™ Red was utilized to detect superoxide radicals in living SH-SY5Y cells. Cells were treated with 10 µM menadione for 16 h and then incubated with Hank's buffered salt solution (HBSS) containing 1 µM MitoSOX™ for 10 min at 37 °C. After harvesting by trypsinization, cells were washed twice in HBSS containing 0.2 % BSA. The red fluorescence of 20,000 cells per sample was analyzed by flow cytometry. Untreated cells were analyzed as a control.

4.3.11 Determination of cellular and mitochondrial ATP content

The cellular and mitochondrial ATP content was measured by means of a luciferase based ATP assay. Cells were detached from culture plates by trypsinization, diluted to a final concentration of 1 x 10^6 cells/ml in PBS and permeabilized by incubation with 0.005 % digitonin for 5 min at 25 °C. Mitochondrial fractions were obtained by centrifugation of permeabilized cells at 12,000 x g for 5 min and washing once in PBS to remove cytosolic components. 0.5 x 10^4 cells or mitochondrial fractions of 1 x 10^6 cells per reaction were used for the ATP assay according to the manufacturer's instructions and luminescence was measured in a microplate reader. An ATP standard curve was generated from reactions containing 0 to 160 picomoles ATP to confirm that the obtained values were in the linear range.

4.3.12 Analysis of life cells by fluorescence microscopy

For fluorescence microscopic analysis of living SH-SY5Y cells, transiently expressing SU9-GFP, SU9-GFP-DHFR or SU9-GFP-dsDHFR, 4 x 10^4 cells per well were seeded in 24-well plates and transfected as described in 4.2.3. 48 h post-transfection, cells were incubated for 10 min in serum-free medium containing the mitochondria-specific dye MitoTracker Red at 250 nM and one drop per ml NucBlue Hoechst 33342 reagent for DNA specific staining of nuclei. After replacing the medium by PBS, cells were analyzed by fluorescence microscopy.

4.3.13 RT-PCR

Cells were scraped off from culture dishes using a cell scraper and total RNA was isolated with the RNeasy Mini Kit (Qiagen) according to the manufacturer's instructions, including an optional DNA digestion step. Random primed cDNA was produced by trancription of 1 µg RNA of each sample using the iScript Select cDNA synthesis kit (Bio-Rad). mRNA expression of *PINK1* was determined by quantitative Real-time PCR. PCR reactions were performed on an iQ5 qPCR system (Bio-Rad) using iQ SYBR Green Supermix (Bio-Rad) under the following conditions: 95 °C for 5 min, and 45 cycles of 95 °C for 15 s and 62.5 °C for 1 min. CT values were defined at the inflection points of fitted sigmoid curves (4-parameter Chapman curves) and were compared with those of the reference gene *GAPDH* (ΔCt-method).

5 Results

5.1 Pink1 protein levels under mitochondrial stress conditions

It is well established, that Pink1 accumulates at mitochondria upon uncoupling of the mitochondrial membrane potential ($\Delta\psi$) upon exposure of cells to CCCP (Matsuda et al., 2010). However, it was not clear if a complete dissipation of $\Delta\psi$ occurs under physiological conditions or during the etiology of PD. Thus, the question, if other mitochondria-specific stress conditions also lead to an accumulation of Pink1, was addressed in the following experiments.

Note that all figures marked with an asterisk were prepared in collaboration with Nadja Schröder as part of an unpublished manuscript (Rüb, C., Schröder, N., Hallmann, K., Kunz, W. and Voos, W.: "Damage-related mitochondrial accumulation of Pink1 is based on a transcriptional induction reaction independent of the membrane potential").

5.1.1 Pink1 levels in response to inhibitors of oxidative phosphorylation

The generation of ATP through oxidative phosphorylation is a key metabolic function of mitochondria. Accordingly, perturbation of this process should represent a state of severe mitochondrial dysfunction. Thus, SHSY-5Y cells were incubated with different inhibitors of respiratory chain complexes and the F_1/F_0-ATPase or CCCP as a control. Pink1 protein levels were then analyzed in total cell lysates by SDS-PAGE and Western blot (Figure 4). In accordance with previously reported results (Matsuda et al., 2010), the full-length form of Pink1 (Pink1-FL), with an apparent molecular weight of 64 kDa, was detected in CCCP-treated cells already after 8 h and further accumulated during 8 to 24 h of treatment. When cells were exposed to oligomycin, an inhibitor of the F_1/F_o-ATPase, Pink1 also accumulated over time, although at a lower level compared to CCCP treatment. By comparison, Pink1 accumulation in cells treated with the complex III inhibitor antimycin A was similar to the CCCP control. Furthermore, high levels of Pink1 after 16 h of CCCP treatment and 24 h of oligomycin treatment, respectively, correlated with decreasing levels of the mitochondrial markers MPP and Tim23, while the amount of GAPDH as a cytosolic loading control remained unchanged under all conditions (Figure 4, lanes 3, 4 and 10). This decline in specifically mitochondrial proteins is consistent with

removal of mitochondria by Pink1-induced mitophagy. Notably, an accumulation of the 53 kDa processed form of Pink1 (Pink1-PF) was not observed at any time point tested.

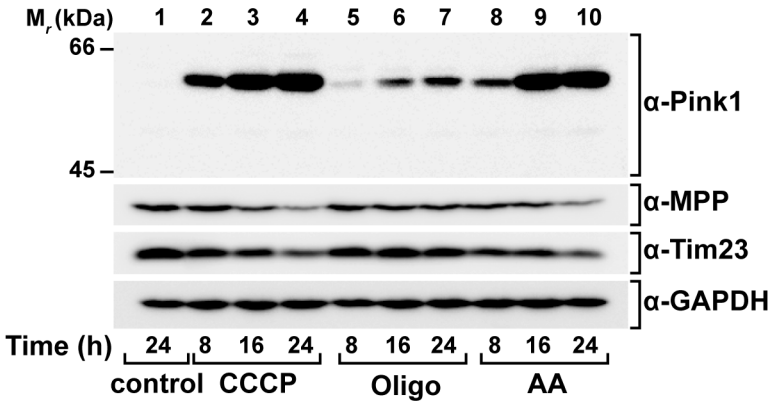

Figure 4*: Effect of inhibitors of oxidative phosphorylation on cellular Pink1 protein levels. SH-SY5Y cells were incubated with DMSO/EtOH (control), 10 µM CCCP, 50 µM oligomycin (Oligo) or 200 M antimycin A (AA) for 8 to 24 h, respectively. Total cell lysates were analyzed by SDS-PAGE and Western blot using antibodies against Pink1, the mitochondrial processing peptidase (MPP), the TIM subunit Tim23 and glyceraldehyde-3-phosphate dehydrogenase (GAPDH) as cytosolic control.

To assess the effect of the OXPHOS inhibitors on mitochondria, measurements of the mitochondrial membrane potential ($\Delta\psi$) and mitochondrial ATP levels were performed. First, to monitor $\Delta\psi$, live cells were stained with the potential-sensitive fluorescent dye tetramethylrhodamine ethyl ester (TMRE) and analyzed by flow-cytometry (Figure 5). TMRE binds to the outer mitochondrial membrane (OMM) only in the presence of $\Delta\psi$. In cells exposed to antimycin A, TMRE fluorescence was strongly reduced, indicating a dissipation of $\Delta\psi$, almost identical to the CCCP control (Figure 5A). By contrast, the membrane potential of mitochondria in oligomycin-treated cells were even higher compared to untreated control cells (Figure 5B).

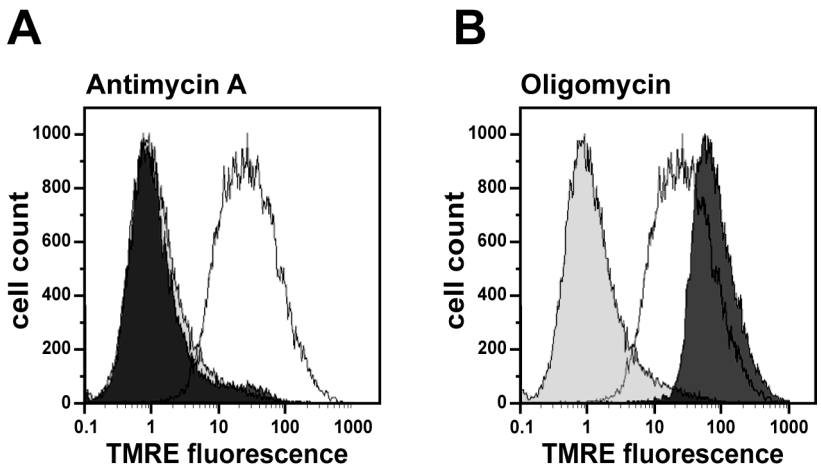

Figure 5*: Mitochondrial membrane potential measurements. After treatment with oligomycin or antimycin A for 16 h, mitochondrial membrane potential was determined in intact SH-SY5Y cells by TMRE staining and flow-cytometry. White: untreated, light grey: CCCP, dark grey: antimycin A (A) or oligomycin (B). Results are representative for at least three independent experiments per treatment. Note that for better visualization control plots for untreated and CCCP-treated cells are shown in both panels.

Secondly, as a direct measure for oxidative phosphorylation, mitochondrial ATP content in cells exposed to the OXPHOS inhibitors was analyzed (Figure 6). To this end, mitochondrial fractions were obtained from digitonized cells and ATP levels determined by means of a luciferase-based ATP assay. As shown in Figure 6A, mitochondrial ATP levels in cells exposed to CCCP, oligomycin or antimycin A were strongly reduced to about 10 to 30 % of the untreated control. By contrast, cellular ATP levels were largely unchanged under the same conditions, confirming a mitochondria-specific effect of the cell treatment (Figure 6B).

In order to determine, if the accumulation of Pink1 observed in Figure 3 occurred at mitochondria, cell homogenates from SH-SY5Y cells treated as above for 16 h, were separated into cytosolic and mitochondrial fractions (Figure 7). When Pink1 accumulated in response to CCCP, oligomycin and antimycin A, the protein completely co-fractionated with the mitochondrial markers MPP and Tom40 and was undetectable in the cytosolic fraction. As judged by GAPDH signals, a small amount of cytosolic proteins was present in the mitochondrial fraction. Accordingly, a minor fraction of the Pink1 signal in mitochondrial fractions may represent cytosolic Pink1, while the vast majority of Pink1 was associated with mitochondria.

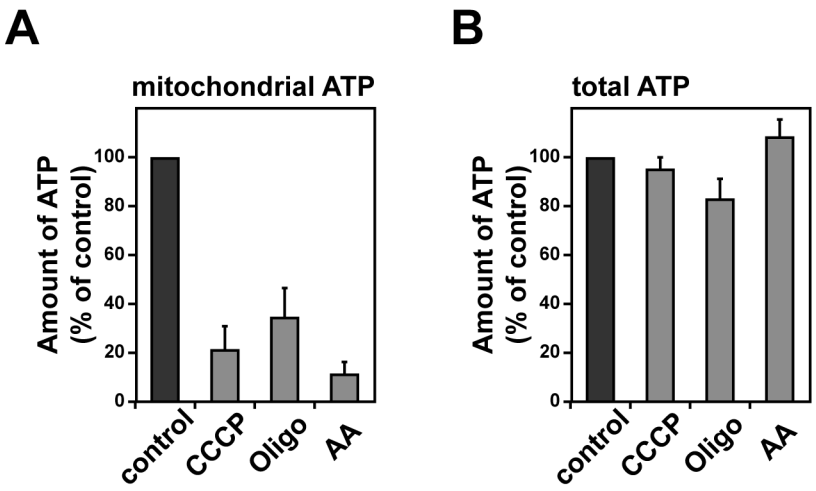

Figure 6*: Determination of mitochondrial (A) and cellular (B) ATP levels. After incubation with DMSO/EtOH, CCCP, oligomycin or antimycin A as described above for 16 h, a luciferase based ATP assay was performed. ATP amounts are given in percentage relative to untreated cells and represent the mean of three independent experiments for each condition tested. Error bars indicate the standard error of the mean (SEM).

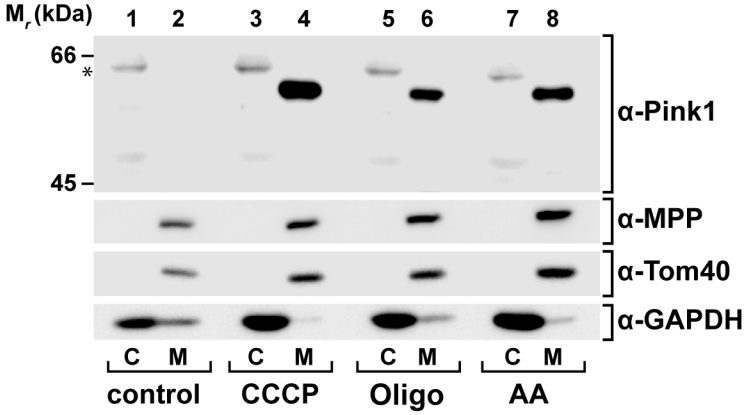

Figure 7: Subcellular localization of Pink1. After treatment of SH-SY5Y cells as described for Figure 3 for 16 h, SH-SY5Y cell homogenates were separated into cytosolic (C) and mitochondrial (M) fraction by differential centrifugation and analyzed by SDS-PAGE and Western blot. Signals indicated with an asterisk most likely represent nonspecific signals from the Pink1 antibody.

In Figure 4 Pink1 was already detectable at the earliest time point tested. Thus, the kinetics of Pink1 accumulation in response to CCCP and oligomycin was monitored more closely from 0.5 to 16 h of treatment (Figure 8). Pink1 started to become detectable after 1 h of CCCP treatment or 4 h of exposure to oligomycin, respectively, and Pink1 protein levels strongly increased over the 16 h period tested. Interestingly, the decrease in MPP and Tim23 levels already observed in Figure 4 became evident only after 12 h of treatment

with CCCP or oligomycin. These results suggest, that either Pink1 levels need to reach a certain threshold to induce detectable mitophagy or that removal of mitochondria by mitophagy becomes detectable only after several hours upon induction.

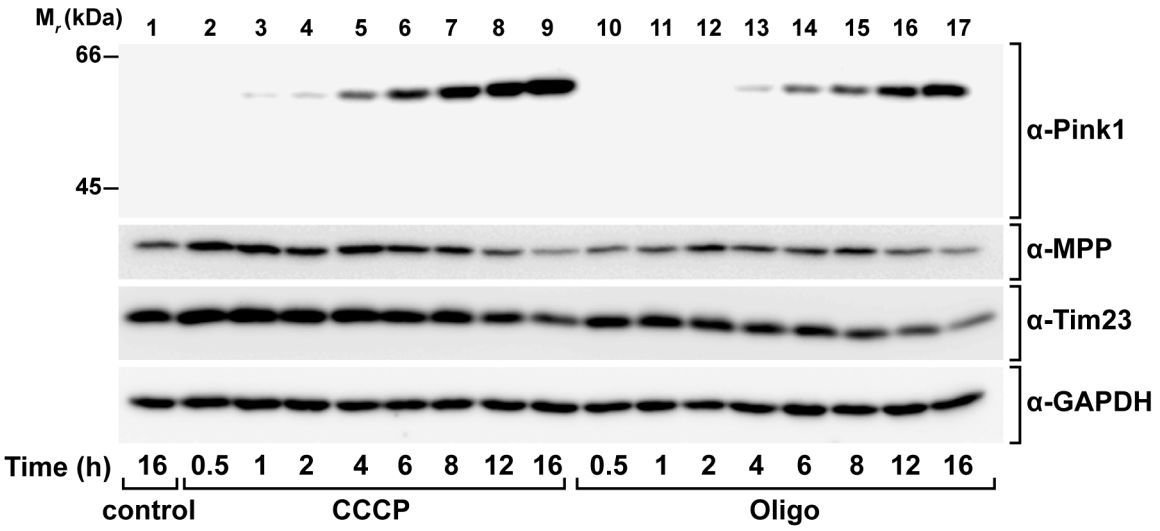

Figure 8: Time course of Pink1 accumulation after CCCP and oligomycin treatment. SH-SY5Y cells were incubated with CCCP or oligomycin as above for 0.5 to 16 h and Pink1 protein levels in total cell lysates analyzed by SDS-PAGE and Western blot.

In summary, mitochondrial accumulation of Pink1 was observed under conditions that inhibit oxidative phosphorylation. This accumulation showed a rather slow kinetics and did not strictly correlate with the loss of $\Delta\psi$. Mitochondrial localization of Pink1, together with a decline in mitochondrial proteins, which was dependent on high levels of Pink, corresponds to Pink1-mediated induction of mitophagy.

5.1.2 Mfn2 ubiquitination

Mitofusin2 (Mfn2) was previously reported to be ubiquitinated in a Pink1/Parkin-dependent manner upon CCCP-induced mitophagy and is also a direct phosphorylation substrate of Pink1 (Gegg et al., 2010). Hence, ubiquitinated Mfn2 may indicate Pink1 and Parkin activity. To analyze Mfn2 ubiquitination, Western blot analysis with immunodetection of Mfn2 was performed with total lysates of cells, exposed to the OXPHOS inhibitors as above (Figure 9). Under control conditions, the Mfn2-specific antibody recognized a single protein band. An additional band, at a slightly higher

apparent molecular weight, was detected in cell lysates of cells exposed to CCCP or antimycin A for 16 h. According to the molecular weight of a single ubiquitin molecule, monoubiquitination of Mfn2 would result in a size shift of 8.5 kDa. Thus, the additional band may correspond to monoubiquitinated Mfn 2. The additional Mfn2 signal was not detected in lysates from oligomycin-treated cells. Hence, the presence of the putatively ubiquitinated Mfn2 correlated with high levels of Pink1 as well as a decrease in mitochondrial proteins consistent with mitophagy. In conclusion, putative ubiquitination of Mfn2 may reflect the Pink1-dependent enzymatic activity of Parkin under conditions where Pink1 accumulates.

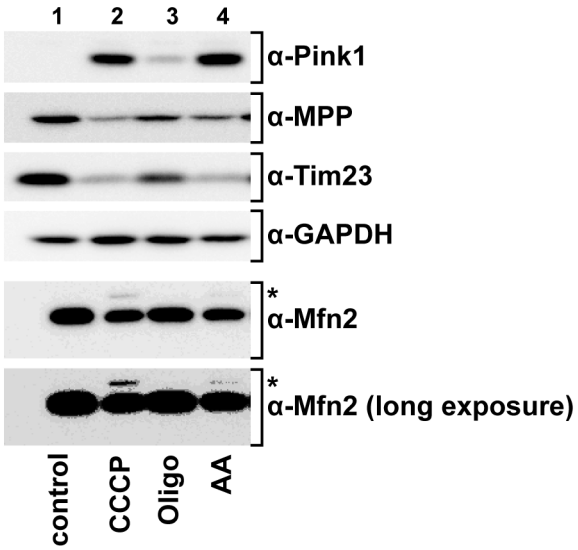

Figure 9: Effect of Pink1 accumulation on Mitofusin 2. SH-SY5Y cells were exposed to DMSO/EtOH (control), CCCP, oligomycin or antimycin A at concentrations as above for 8 h and total cell lystaes analyzed by SDS-PAGE and Western blot using an antibody against Mitofusin 2 (Mfn2). Signals indicated with an asterisk represent putatively mo-noubiquitinated Mfn2.

5.1.3 Pink1 levels in response to inhibition of respiratory chain complex I

When considering the respiratory chain in the context of Pink1 and Parkinson's disease, complex I plays an exceptional role, as exposure to complex I inhibitiors has been shown to cause PD-like symptoms in humans and animal models Pickrell & Youle, 2015). Thus, the effect of complex I inhibition on Pink1 levels was investigated next. When SH-SY5Y cells were exposed to the complex I inhibitor rotenone at different concentrations for 2 to 16 h, Pink1 did not accumulate at any time point tested (Figure 10A). As a control, mitochondrial and cellular ATP levels were determined as above. A reduction of mitochondrial ATP content by about 50 % relative to untreated cells (Figure 10B) and unchanged total ATP levels (Figure 10C) confirmed a mitochondria-specific effect of rotenone, under the experimental conditions tested here.

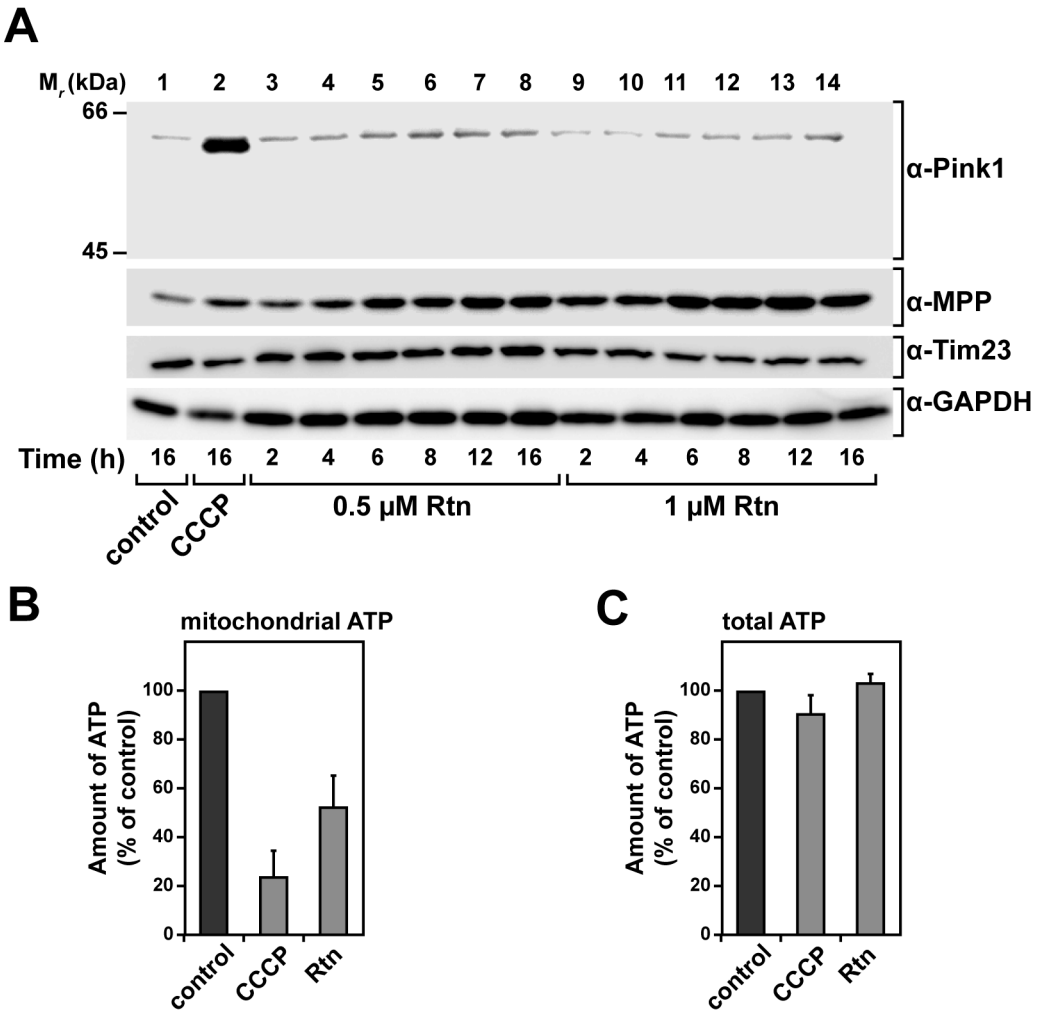

Figure 10: Effect of rotenone on cellular protein levels of Pink1, and ATP levels. Effect of rotenone on Pink1 levels. SH-SY5Y cells were treated with DMSO (control), CCCP or 0.5 or 1 µM rotenone (Rtn) for 2 to 16 h. Pink1 levels in total cell lysates were analyzed by SDS-PAGE and Western blot. (B, C) Measurement of mitochondrial (B) or cellular (C) ATP levels. Cells were incubated in the presence 0.5 µM rotenone and ATP levels determined by luciferase assay as in Figure 6.

Since the observation of unaltered Pink1 levels clearly distinguishes rotenone from the other inhibitors of OXPHOS (see Figure 4), cells were treated with an alternative complex I inhibitor. The drug 1-methyl-4-phenylpyridinium (MPP^+) is the metabolite of the PD-related neurotoxin 1-methyl-4-phenyl-1,2,3,6-tetrahydropyridine (MTPT) (Singer, Ramsay et al., 1988).

As seen in Figure 11A, Pink1 did not accumulate in response to MPP^+ even after 24 h, while TMRE staining of cells treated with MPP^+ for 24 h, indicated a strong reduction of the Dy (Figure 11B). Hence, inhibition of complex I by MPP^+ reflects a condition, where

a diminished Δψ does not result in the accumulation of Pink1. The failure of rotenone and MPP^+ treatment to promote an accumulation of Pink1 raised the question, if inhibition of complex I interfered with the accumulation of Pink1 observed upon exposure of cells to the other OXPHOS inhibitors. Thus, SH-SY5Y cells were treated with CCCP or oligomycin as in Figure 4 but in the presence or absence of 0.5 µM rotenone for 8 and 16 h, respectively. As shown in Figure 12, accumulation of Pink1 in response to CCCP, oligomycin and antimycin A was not affected by rotenone.

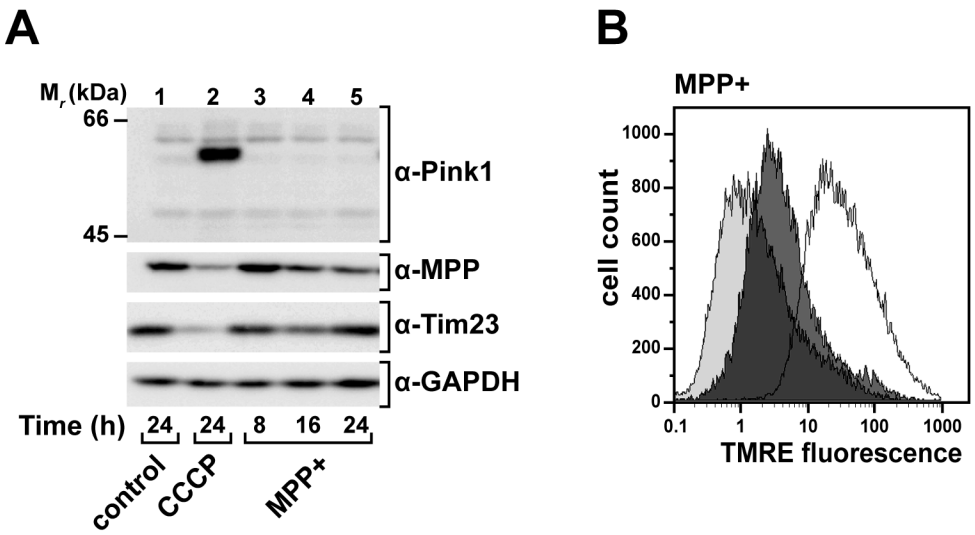

Figure 11: Effect of MPP^+ on Pink1 levels and Δψ. (A) Cells were treated with 2.5 mM 1-Methyl-4-phenylpyridinium iodode (MPP^+) for 8 to 24 h and Pink1 levels in whole cell lysates analyzed as above. (B) Mitochondrial membrane potential (Δψ) was determined in intact cells treated with DMSO (control), 10 µM CCCP or MPP^+ for 24 h determined by TMRE staining and flow cytometry as in Figure 5. White: control, light grey: CCCP, dark grey: MPP^+.

Taken together, inhibition of complex I neither resulted in elevated protein levels of Pink1 nor prevented accumulation of the protein in response to other stress conditions.

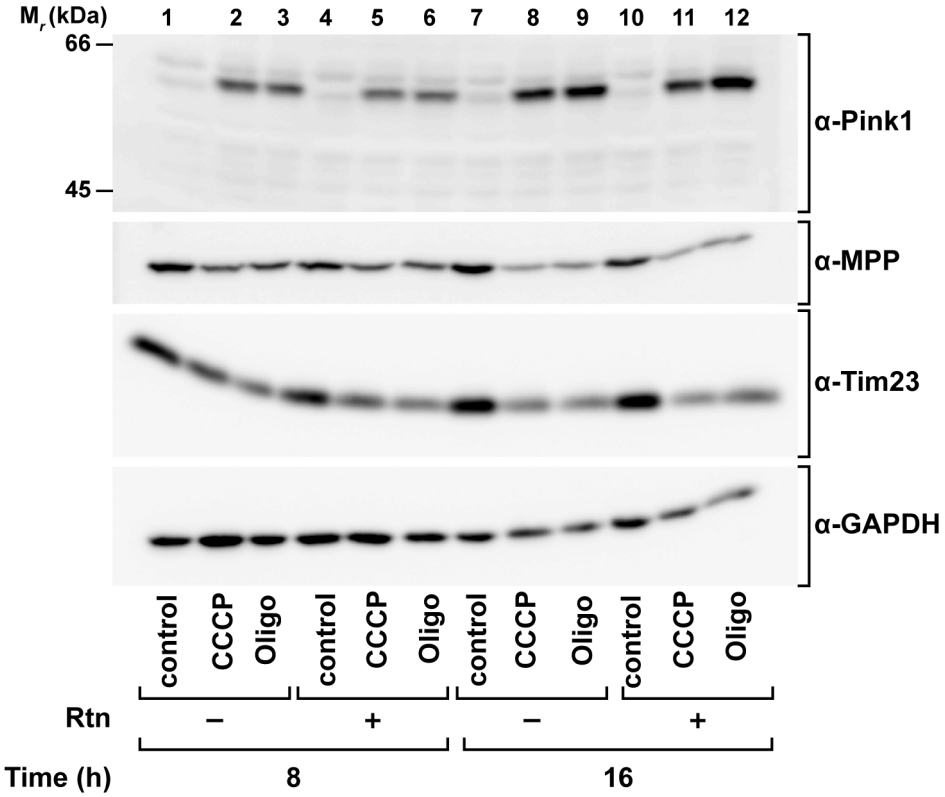

Figure 12: Effect of rotenone on Pink1 accumulation in response to CCCP and oligomycin. SH-SY5Y cells were treated with DMSO/EtOH (control), CCCP or oligomycin as above for 8 or 16 h in the presence or absence of 0.5 µM rotenone in serum-free medium. Total cell lysates were analyzed by SDS-PAGE and Western blot as above.

5.1.4 Δψ-dependent protein complexes of Pink1

Under native conditions, Pink1 has previously been found in two distinct membrane potential dependent protein complexes (Becker et al., 2012a). Presumably, these complexes comprise Pink1 and interacting proteins and may therefore harbor important information about functional consequences of Pink1 accumulation. A protein that is part of a complex with Pink1 should co-migrate with the respective Pink1 signal in Blue Native polyacrylamide gel electrophoresis (BN-PAGE). To revisit Pink1 complex formation, SH-SY5Y cells were incubated in the presence or absence of CCCP for 16 h. Mitochondria isolated from these cells were solubilized in digitonin buffer and analyzed by BN-PAGE and Western blot (Figure 13).

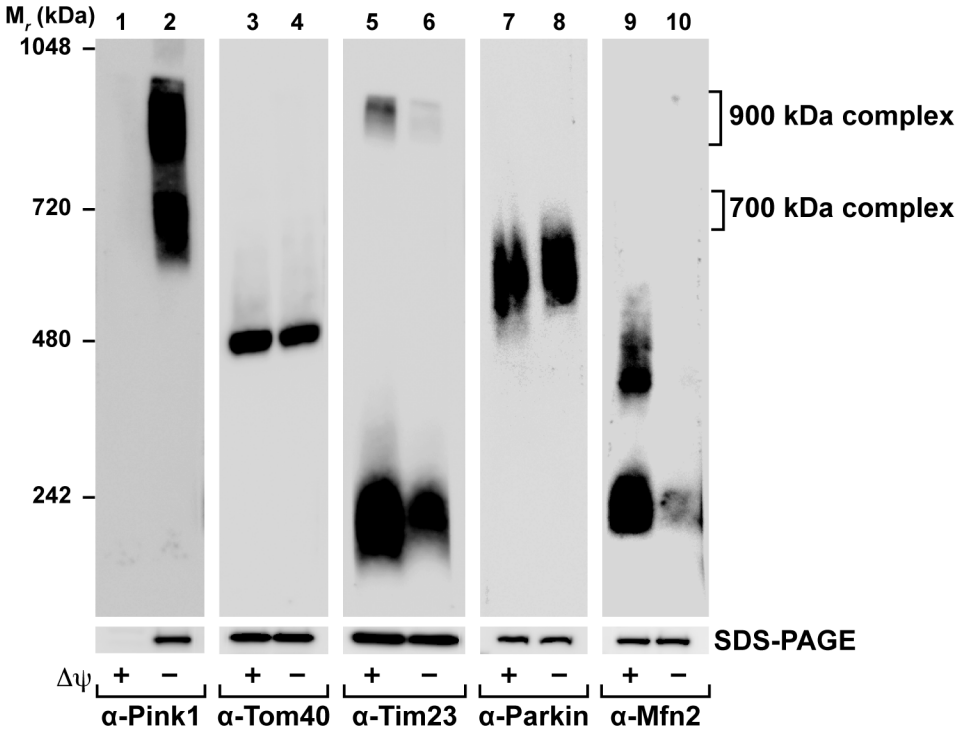

Figure 13: Δψ-dependent protein complexes of Pink1. SH-SY5Y cells were incubated with DMSO (control) or 10 µM CCCP for 16 h to dissipate Δψ, followed by isolation of mitochondria. Mitochondrial proteins and protein complexes were separated by BN-PAGE or standard SDS-PAGE as a control and analyzed by Western blot.

In accordance with previously published results (Becker et al., 2012a), two complexes of about 700 and 900 kDa in mitochondria from CCCP-treated but not untreated control cells were detectable by a Pink1-specific antiserum (Figure 13, lanes 1 and 2). Immunodetection of Tom40 and Tim23, the core components of the TOM and TIM23 translocase complexes, resulted in signals at about 450 and 240 kDa, corresponding to the fully assembled TOM and TIM complexes. However, no co-migration of the Tom40 or Tim23 signal with either Pink1 complex was observed. The anti-Tim23 antibody recognized an additional band, approximately in the range of the 900 kDa Pink1 complex but as opposed to the Pink1 signal, this band was strongly reduced in depolarized mitochondria. Thus, Pink1 did not form a complex with Tom40 or Tim23 under the tested experimental conditions. As Parkin is a phosphorylation substrate of Pink1 (Kondapalli et al., 2012, Shiba-Fukushima et al., 2012), it is a candidate for complex formation with Pink1. In mitochondrial fractions from control cells and CCCP-exposed cells, the anti-Parkin antibody recognized a complex at around 600 kDa, which did not co-migrate with either Pink1 complex (Figure 13, lanes 5 and 6). The proposed Pink1 substrate Mfn2 (Chen & Dorn, 2013) was detected in two complexes of about 240 and 400 kDa,

respectively, in mitochondria from untreated control cells (Figure 13, lanes 7 and 8). No co-migration with either of the two Pink1 complexes was observed. Interestingly, in depolarized mitochondria, the amount of the 240 kDa complex was strongly reduced, similarly as observed for the TIM23 complex. The 400 kDa Mfn2 containing complex was undetectable in depolarized mitochondria. Since SDS-PAGE analysis revealed similar Mfn2 protein levels in both polarized and depolarized mitochondria, this decrease was not due to reduced protein amounts of Mfn2 but rather reflected a Δψ-dependent characteristic of the Mfn2 containing complexes.

In summary Pink1 was found in two Δψ-dependent protein complexes of 700 and 900 kDa when it accumulated under mitochondrial stress conditions. These two Pink1 containing complexes did neither co-migrate with the fully-assembled TOM or TIM23 complex nor with the Pink1 substrates Parkin and Mfn2.

5.2 Effect of protein stress conditions on Pink1 levels

5.2.1 Overexpression of destabilized DHFR

Challenging the protein quality control system reflects a mitochondrial stress condition that may elicit Pink1 accumulation and the downstream mitophagy process. Therefore, the effect of mitochondrial protein stress on Pink1 levels was investigated. In a first approach a mitochondrially targeted, destabilized form of the usually cytosolic protein dihydrofolate reductase (DHFR) was transiently expressed in HeLa or SH-SY5Y cells. The mutant protein comprises the full DHFR amino acid sequence with three point mutations that prevent folding of the protein ($DHFR_{ds}$), fused to GFP and an N-terminal mitochondrial translocation signal (SU9-GFP-$DHFR_{ds}$). The corresponding fusion construct of normal DHFR (SU9-GFP-DHFR) and mitochondrially targeted GFP (SU9-GFP) alone were used as controls. All three constructs are schematically shown in the appendix (Figure 36).

In order to confirm mitochondrial localization of the fusion proteins and aggregation of the destabilized DHFR, HeLa cells were transiently transfected with the $DHFR_{ds}$ construct or control constructs, respectively. Fluorescence microscopic analysis of live cells, stained with the fluorescent dyes Mitotracker Red and Hoechst for visualization of nuclei and mitochondria, 48 h post-transfection, is shown in Figure 14. In SU9-GFP-transfected cells,

GFP fluorescence showed perinuclear, filamentous structures, which co-localized with Mitotracker staining, indicating mitochondrial localization of the control protein. A very similar picture was obtained for cells expressing the SU9-GFP-DHFR protein. By contrast, in cells expressing SU9-GFP-DHFR$_{ds}$, GFP fluorescence was restricted to more condensed, dot like structures in proximity to the nucleus that predominantly co-localized with mitochondrial staining. This observation is consistent with aggregation of the destabilized DHFR protein inside mitochondria.

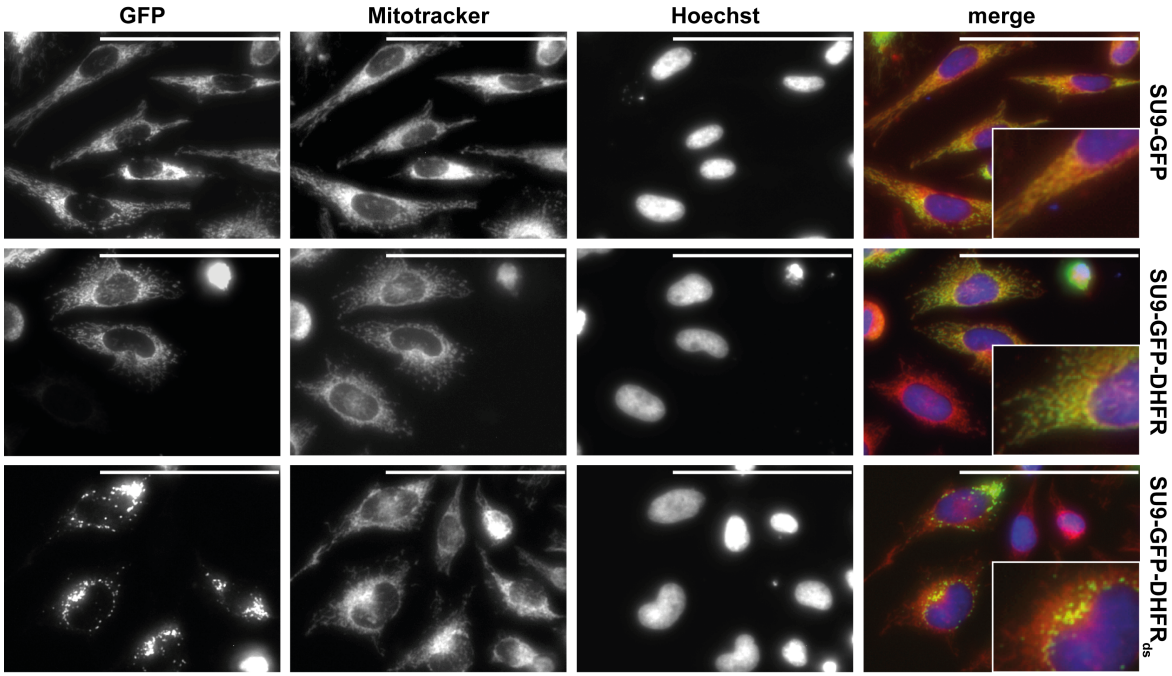

Figure 14: Fluorescence microscopic analysis of cells expressing mitochondria-targeted destabilized DHFR or control constructs. HeLa cells were transiently transfected with the indicated construct. 48 h post-transfection, living cells were stained with MitoTracker Red and the DNA-specific dye Hoechst and analyzed by fluorescence microscopy. Scale bars indicate 100 µM.

To test, if aggregation of the destabilized DHFR protein had an effect on Pink1 protein levels, SH-SH5Y cells were transfected with the different constructs for 24 to 48 h and total cell lysates were analyzed by SDS-PAGE and Western blot (Figure 15). Expression of all three fusion proteins was confirmed by immunodetection of GFP. The major signals at 30 kDa for SU9-GFP and 52 kDa for SU9-GFP-DHFR and SU9-GFP-DHFR$_{ds}$, respectively, correspond to the processed proteins, after cleavage of the mitochondrial targeting signal by the matrix processing peptidase (MPP). This observation indicates, that a major fraction of all proteins was translocated to the mitochondrial matrix. Additional bands, representing the full-length forms, were detected for SU9-GFP and

SU9-GFP-DHFR, respectively. The presence of the unprocessed fragments correlated with high expression levels, which likely exceeded the capacity of the import machinery. Compared to the DHFR construct, the $DHFR_{ds}$ fusion protein was expressed at lower levels and its expression further declined over time, which was confirmed by immunodetection using a DHFR-specific antiserum. Since no apparent degradation fragments were detected with either the anti-GFP or the anti-DHFR antibody, comparatively low levels of the destabilized DHFR protein, were due to less efficient expression of the protein, rather than proteolytic degradation. Pink1 was not detectable, upon expression of $DHFR_{ds}$ or the control constructs at any time point tested, as compared to Pink1 accumulation in SH-SY5Y cells treated with CCCP for 16 h

In conclusion mitochondrially targeted destabilized DHFR as well as the two control proteins did localize to mitochondria. The SU9-GFP-$DHFR_{ds}$ protein but not SU9-GFP-DHFR or SU9-GFP aggregated inside mitochondria. Thus, SU9-GFP-$DHFR_{ds}$ is a suitable model protein for mitochondrial protein aggregation in human cells. However, aggregation of destabilized DHFR did not elicit an accumulation of Pink1.

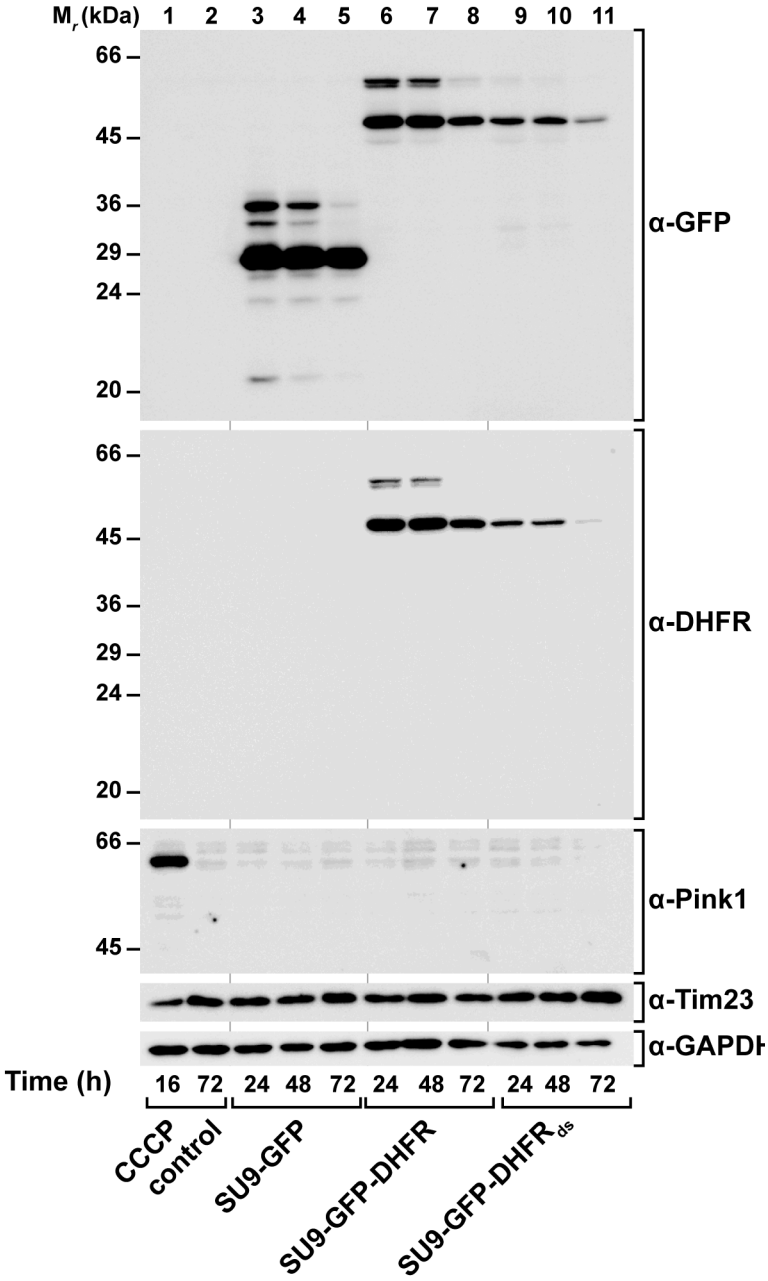

Figure 15: Pink1 levels in cells overexpressing mitochondria-targeted destabilized DHFR or control constructs. SH-SY5Y cells were transiently transfected with the indicated construct. Cells were lysed 24 to 72 h post-transfection and analyzed by SDS-PAGE and Western blot. Controls: Mock transfection containing no plasmid DNA and cells treated with 10 mM CCCP for 16 h.

5.2.2 Knock-down of Mortalin

In a second approach, knock-down of the mitochondrial Hsp70 chaperone Mortalin (Grp75) was utilized to induce mitochondrial protein stress. Mortalin locates to the mitochondrial matrix, and is indispensible for protein import, folding of newly imported proteins and stress protection (Voos, 2013). Thus, SH-SY5Y cells were transiently transfected with Mortalin specific siRNA for 24 to 48 h or control siRNA and total cell lysates analyzed as above (Figure 16).

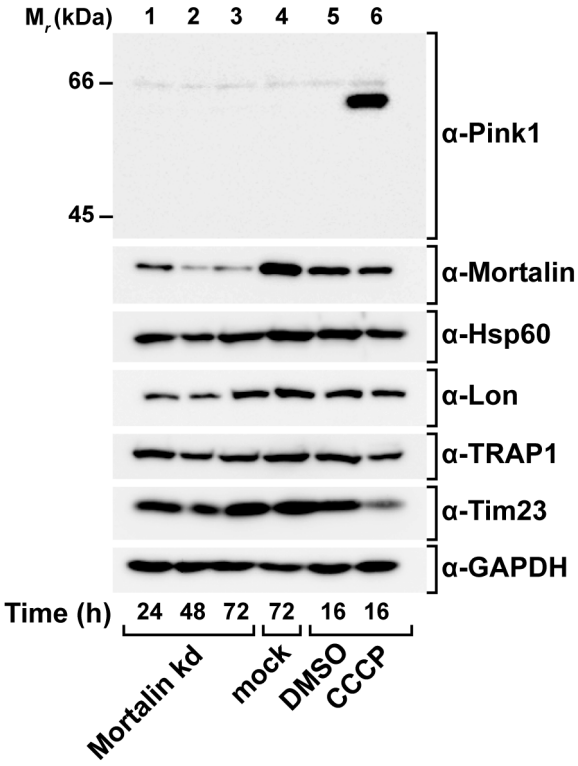

Figure 16: Effect of Mortalin knock-down on Pink1 levels. SH-SY5Y cells were transiently transfected with siRNA specific for the mitochondrial Hsp70 chaperone Mortalin (Grp75). 24 to 72 h post-transfection, total cell lysates were analyzed by SDS-PAGE and Western blot using antibodies against Pink1, Mortalin, the mitochondrial chaperones Hsp60 and TRAP1 (mtHsp90) and the Lon protease.

Successful knock-down was evident by strongly reduced protein levels of Mortalin already after 24 h and a further decrease to about 15 % after 48 h, as compared to cells transfected with unspecific control siRNA (mock). Notably, cells analyzed 72 h post-transfection with control siRNA showed increased Mortalin levels as compared to cells exposed to DMSO or CCCP for 16 h. (Figure 16, lane 4). This effect may reflect a stress situation due to prolonged incubation of the cells. Protein levels of other members of the mitochondrial protein quality system were analyzed as a control. A correlation between diminished Mortalin levels and amounts of the mitochondrial chaperones Hsp60 and TRAP1, the mitochondrial Hsp90 homologue, was not evident. By comparison, the level of the matrix protease Lon was slightly increased after 72 h of Mortalin knock-down,

compared to shorter time points. As compared to cells treated with CCCP for 16 h, Pink1 did not accumulate in response to reduced levels of Mortalin.

In conclusion, mitochondrial proteotoxic stress induced either by the ectopic expression of a destabilized mitochondria-targeted protein or knock-down of Mortalin did not result in an accumulation of Pink1.

5.3 Effect of cellular stress conditions on Pink1 levels

5.3.1 Oxidative stress

Having observed an accumulation of Pink1 under specific mitochondrial stress conditions, the effect of general, cellular stress conditions on Pink1 levels was assessed next. Oxidative stress has previously been related to mitochondrial dysfunction and Parkinson's disease (Lin & Beal, 2006). Thus, SH-SY5Y cells were treated with the superoxide-generating compound menadione for 16 h, and Pink1 protein levels in total cell extracts were analyzed as above. As seen in Figure 17A, menadione did not cause elevated levels of Pink1 at any concentration tested. To monitor the presence of superoxide radicals, cells exposed to 10 μM menadione for 16 h, were stained with the mitochondria-specific superoxide-sensitive fluorescent dye MitoSOX and analyzed by flow-cytometry (Figure 17B). A significantly higher MitoSOX fluorescence of menadione-treated cells compared to control cells clearly indicated an increase in superoxide radicals.

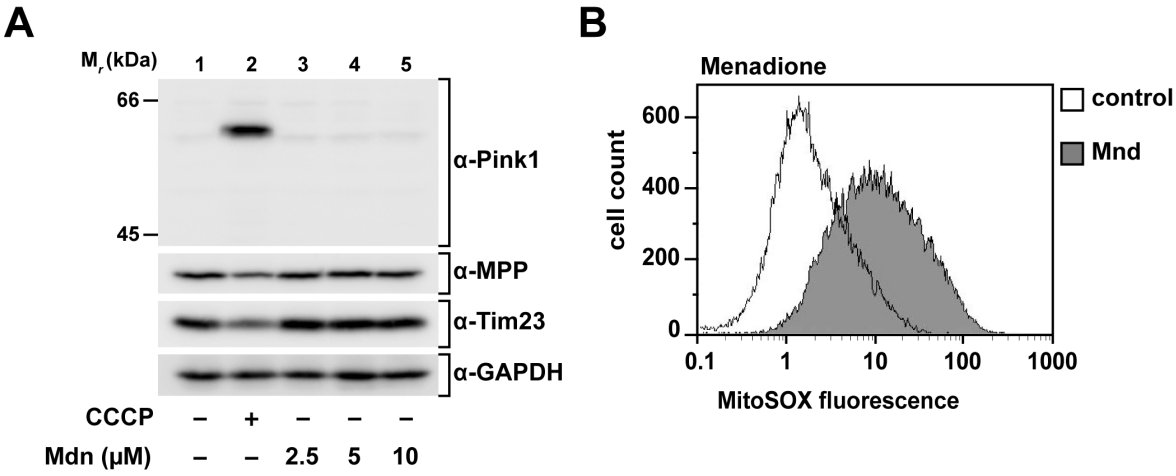

Figure 17*: Protein levels of Pink1 and superoxide radicals in menadione-treated cells.

(A) SH-SY5Y cells were incubated with EtOH/DMSO or 10 µM CCCP (controls) or 2.5-5 µM menadione (Mnd) for 16 h and total cell lysates analyzed by SDS-PAGE and Western blot as above. (B) After treatment with EtOH (control) or 10 µM menadione for 16 h, superoxide radicals were detected in living SH-SY5Y cells by staining with the mitochondria-specific superoxide-reactive dye MitoSOX™ and flow cytometry. Grey: menadione, white: control.

5.3.2 ER protein stress

Within the cell, mitochondria and the endoplasmatic reticulum (ER) are functionally connected through processes like calcium homeostasis and lipid metabolism. Moreover, mitochondria and ER have been reported to share common structures, the so-called mitochondria-associated ER membranes (MAM) (Paillusson, Stoica et al., 2016). Accordingly, ER stress conditions might be propagated to mitochondria and cause an accumulation of Pink1. To test this hypothesis, SH-SY5Y cells were exposed to tunicamycin, a compound that causes unfolded protein stress in the ER by blocking N-linked glycosylation, which is required for the proper folding of specific proteins. As seen in Figure 18A, cellular Pink1 amounts were not increased after 16 h of incubation with tunicamycin at different concentrations. Under the same conditions, levels of the ER chaperone BiP (immunoglobulin heavy chain binding protein) were elevated even at 1 µg/ml tunicamycin, indicating an ER-specific effect of the tunicamycin treatment (Figure 18B) Upregulation of BiP is part of the unfolded protein response (UPR) in the ER (Behnke, Feige et al., 2015).

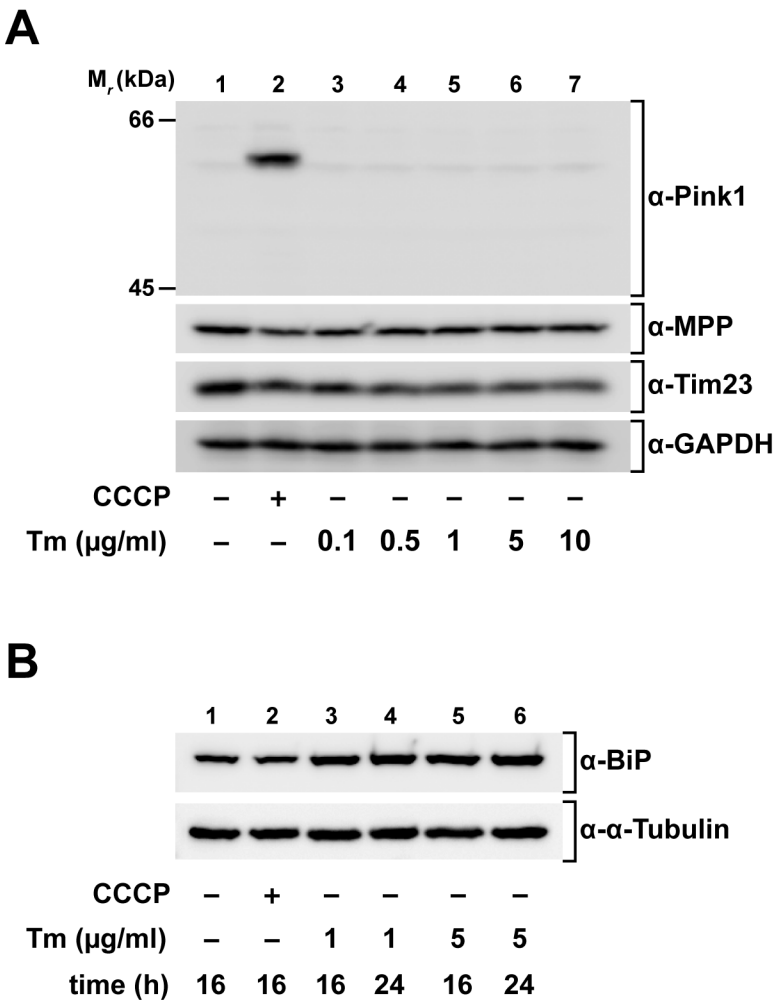

Figure 18*: Effect of tunicamycin on cellular levels of Pink1 and BiP.

(A) Cells were incubated with tunicamycin (Tm) at the indicated concentrations for 16 h and total cell lysates analyzed by SDS-PAGE and Western blot as above.

(B) Cells were treated with tunicamycin at the concentrations indicated for 16 or 24 h and total cell lysates analyzed as above, using an antibody against the ER chaperone BiP/Grp78.

5.3.3 Inhibition of mitochondrial ATP transport

Accumulation of Pink1 in response to OXPHOS inhibitors in Figure 4 was concurrent with decreased mitochondrial ATP levels and largely unchanged cellular ATP amounts. It was reasoned that an altered ATP transport rate might also affect the overall energy state of the cell, influencing quality control reactions. Therefore, cells were treated with atractyloside, an inhibitor of the ADP/ATP carrier in the inner mitochondrial membrane (Figure 19). First, atractyloside treatment alone did not result in elevated cellular Pink1 levels. Secondly, atractyloside did not interfere with Pink1 accumulation when cells were simultaneously exposed to atractyloside and the OXPHOS inhibitors. Thus, the observed increase in Pink1 levels indeed represented a mitochondria-specific event.

Taken together, an increase in the cellular levels of Pink1 was only observed under mitochondrial but not cellular stress conditions.

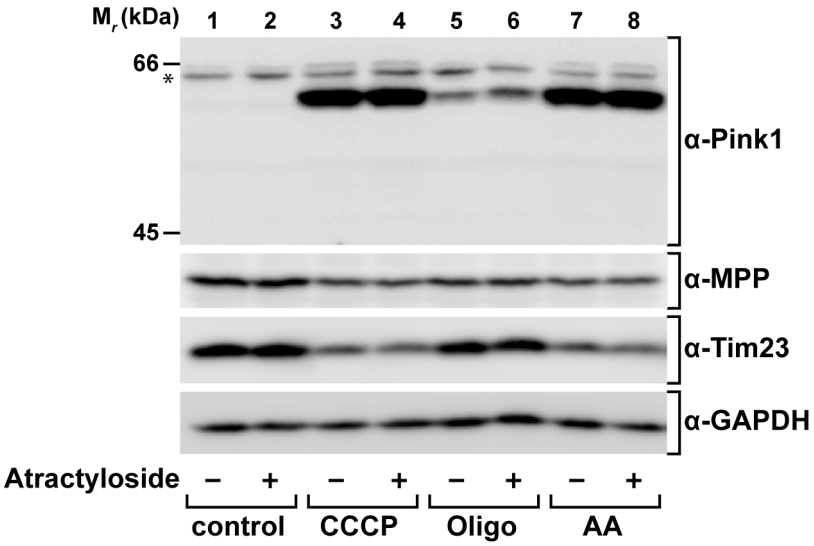

Figure 19*: Effect of atractyloside on Pink1 accumulation. Cells were treated for 16 h as above but in the presence or absence of the ADP/ATP translocase inhibitor atractyloside at 200 µM. Total cell lysates were analyzed as above.

5.4 Pink1 levels in muscle tissue of a *COX8A* patient

In all experiments described so far, Pink1 protein levels were monitored in the time frame of hours upon induction of an acute stress condition. By contrast, there are pathological conditions, in which mitochondrial function is permanently impaired due to a genetic defect. In a specific case, a homozygous splice-site mutation in the *COX8A* gene, encoding the smallest nuclear-encoded complex IV subunit was shown to cause a severe neurological disorder termed Leigh-like syndrome and epilepsy (Hallmann, Kudin et al., 2016). While functional consequences of the *COX8A* mutation, including reduced levels of complex IV were characterized in detail by Hallmann et al., native PAGE analysis is shown here to illustrate the effect of the mutation.

To assess the effect of the *COX8A* mutation on total levels of complex IV mitochondrial fractions isolated from muscle biopsies of the *COX8A* patient and a healthy control, were analyzed by native PAGE and Western blot (Figure 20A). Antibodies specific for the complex IV subunits COX1, COX4 and COX5a all recognized a complex with an apparent relative molecular mass of 250 kDa, suggesting that this signal corresponded to the fully assembled complex IV. Compared to the control, the signal intensity was strongly reduced in the patient sample. This observation illustrates, that the *COX8A* mutation results in a severely decreased level of the entire complex IV. By comparison, levels of the succinate dehydrogenase complex (complex II), detected by an antibody

against the complex II subunit A (SDHA), were similar in patient and control sample. This observation confirmed a complex IV-specific effect of the mutation.

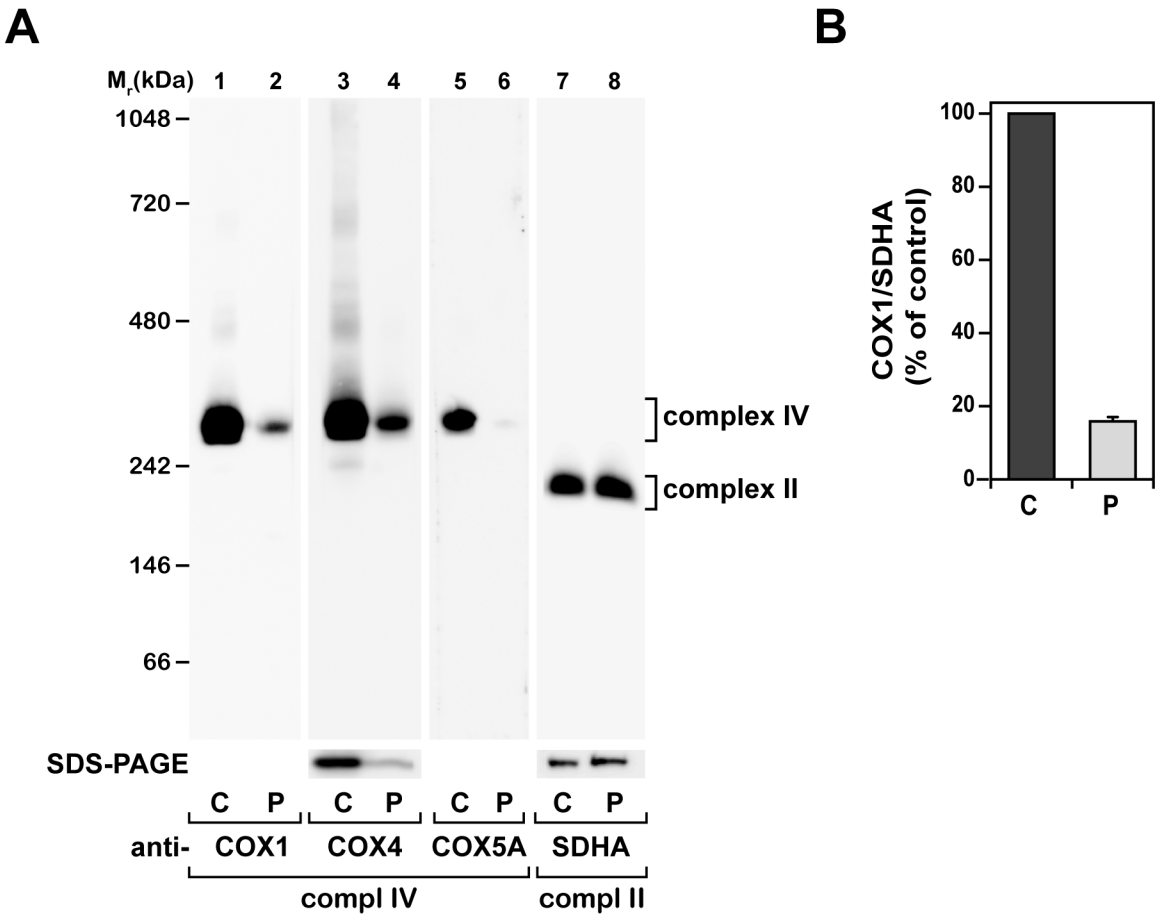

Figure 20: BN-PAGE analysis of mitochondrial fractions from skeletal muscle of a *COX8A* patient and healthy control. (A) Mitochondrial fractions from muscle biopsies were analyzed by BN-PAGE or standard SDS-PAGE and Western blot. Antibodies against the complex IV subunits COX1, COX4 and COX5A and the complex II subunit SDHA as a control were used. C: control, P: patient. (B) Complex IV levels in patient and control mitochondria. The major BN-PAGE signals for COX1, representative for complex IV, and SDHA in (A) were quantified. The signal intensities for COX1, normalized to SDHA are shown relative to the control. Results represent the mean of three experiments and the error bar indicates the standard error of the mean (SEM). This figure was published in (Hallmann et al., 2016).

Quantification of the native PAGE signals for COX1, normalized to SDHA signals, revealed a residual complex IV level of 18 % in mitochondrial fractions isolated from the patient tissue, compared to the control (Figure 20B). Notably, antibodies against COX1 and COX4 recognized two additional complexes of around 480 and 720 kDa, respectively, in control mitochondria. These signals putatively represent high molecular weight complexes, comprising complex IV and other respiratory chain complexes. Strongly

reduced levels of complex IV due to the *COX8A* mutation were shown to result in a severe isolated complex IV deficiency (Hallmann et al., 2016). In order to assess if this defect had an effect on Pink1 levels, total homogenates from patient and control skeletal muscle tissue were analyzed by SDS-PAGE and Western blot (Figure 21). As compared to total cell extracts from SH-SY5Y cells, exposed to CCCP for 16 h, the 64 kDa full-length form of Pink1 was not detectable in patient or control sample. Interestingly, a faint band corresponding to the 53 kDa processed Pink1 species, was detected in muscle homogenates of patient and control, respectively.

In conclusion, a genetic complex IV deficiency did not result in elevated levels of Pink1.

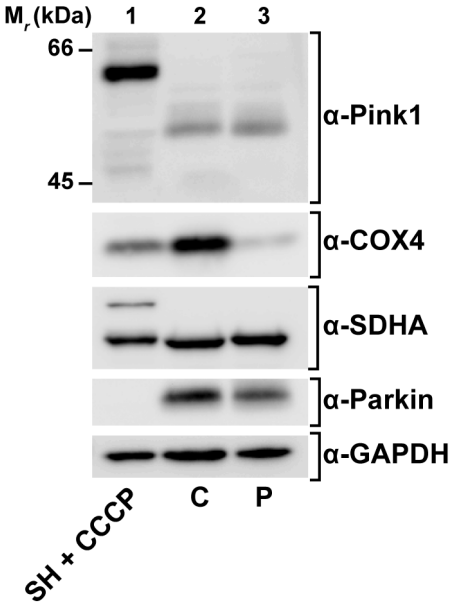

Figure 21: Pink1 levels in muscle tissue of a COX8A patient and a healthy control. Total homogenates from muscle biopsies were analyzed by SDS-PAGE and Western blot. SH-SY5Y cells exposed to 10 µM CCCP for 16 h were analyzed as a control.

5.5 Import and processing of Pink1

The existence of two forms of Pink1, the 64 kDa full-length (FL) and the 53 kDa processed form (PF), is a striking characteristic of Pink1. Thus, the import and processing events converting Pink1-FL into Pink1-PF and the differential behavior of both forms were addressed in the following.

5.5.1 Import of Pink1 into PARL-deficient mitochondria

Processing of Pink1 by different mitochondrial proteases, including the presenilin-associated rhomboid-like protease (PARL) has previously been reported (Deas, Wood et al., 2010b, Greene et al., 2012). To revisit PARL-mediated processing of Pink1, *in vitro*

import of [^{35}S]-methionine/cysteine-labeled full-length Pink1 into mitochondria isolated from homozygous PARL-deficient (PARL -/-) mouse embryonic fibroblasts (MEF) and corresponding wild-type cells was conducted (Figure 22).

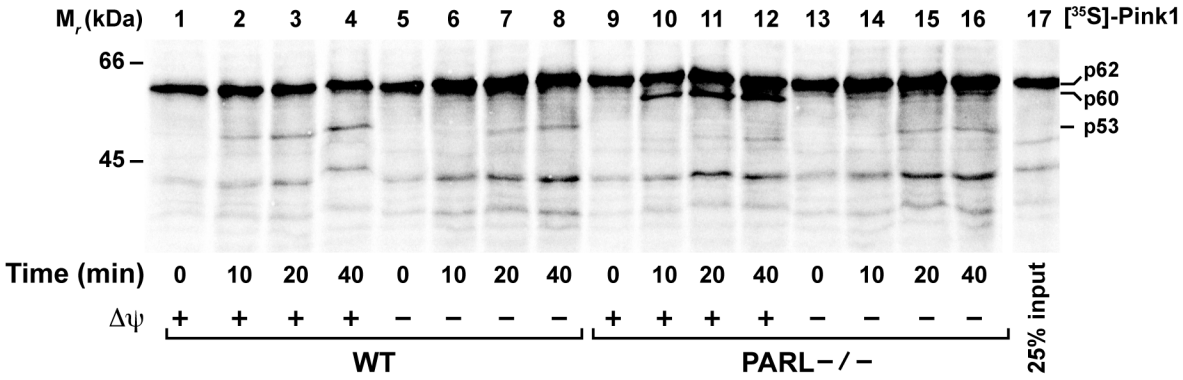

Figure 22: *In vitro* import of Pink1 into mitochondria from PARL-deficient cells or control cells. [^{35}S]-methionie/cysteine-labeled Pink1 was incubated with energized mitochondria isolated from PARL -/- mouse embryonic fibroblasts or corresponding wild-type cells, for the times indicated. Where indicated, Dy was dissipated prior to the import reaction. Re-isolated mitochondria were analyzed by SDS-PAGE and digital autoradiography.

When the Pink1-FL protein was incubated with energized wild-type mitochondria in the presence of Δψ, it associated with mitochondria and two protein bands, one of about 53 kDa and another of about 44 kDa, accumulated over time (Figure 22, lanes 1-4). While the 44 kDa fragment was also detectable in the reticulocyte lysate (Figure 22, lane 17) and therefore likely represents an abnormal translation product, the 53 kDa band corresponds to the major processing product Pink1-PF. The 64 kDa Pink1 precursor likewise associated with wild-type mitochondria depleted of Δψ. The formation of the 53 kDa Pink1-PF was reduced in depolarized mitochondria, as compared to energized mitochondria, but not completely abolished (Figure 22, lanes 5-8). When the 64 kDa Pink1 precursor was incubated with polarized PARL-deficient mitochondria, another major Pink1 fragment of about 60 kDa, putatively representing the MPP cleavage product and PARL substrate, accumulated over time. Notably, a faint signal corresponding to the 53 kDa Pink1-PF was also detected, albeit at a lower intensity compared to polarized wild-type mitochondria (Figure 22, lanes 9-12). In PARL-deficient mitochondria depleted of Dy, the 60 kDa fragment was not detectable, indicating that generation of this fragment requires the presence of an inner membrane potential. Importantly, a Pink1 species

indistinguishable from the 53 kDa Pink1-PF was generated in these mitochondria, at levels very similar to depolarized wild-type mitochondria.

Taken together, generation of Pink1-PF was not strictly dependent on the presence of a Dy. Moreover, a fragment that was indistinguishable from Pink1-PF was generated in mitochondria isolated from PARL -/- cells, which were reported to have no detectable PARL mRNA (Cipolat, Rudka et al., 2006). Thirdly, the effect of the PARL deficiency on Pink1 processing was restricted to polarized mitochondria, as in depolarized mitochondria from both wild-type and PARL -/- cells, similar levels of the apparent Pink1-PF fragment were detected.

5.5.2 Membrane association of full-length and processed forms of Pink1

As a consequence of its proteolytic cleavage within the hydrophobic transmembrane domain (see Figure 1A), the 53 kDa processed Pink1 fragment may be less firmly associated with or integrated into the OMM than its 64 kDa full-length precursor. To address the membrane interaction properties of both Pink1 species, alkaline extraction was performed after *in vitro* import of radiolabeled full-length Pink1 into isolated HeLa mitochondria (Figure 23). During alkaline extraction, proteins that stably interact with membranes remain in the pellet fraction, while peripheral membrane proteins are found in the supernatant. Even under harsh conditions, at pH 12,about 93 % of Pink1-FL remained in the particulate, membrane-associated fraction (Figure 22, lane 4). By contrast, the amount of processed Pink1 in the pellet declined at pH 11.5 and Pink1-PF started to be detectable in the supernatant. At pH 12, only about 46 % of Pink1-PF remained in the pellet. As a control, immunodetection of the mitochondrial proteins MPP, VDAC (voltage-dependent anion channel) and Smac was performed. MPP and Smac, as soluble proteins of the matrix and intermembrane space compartment, respectively, were already detectable in the supernatant at pH 7.3. By contrast, the integral outer membrane protein VDAC resisted the extraction procedure almost entirely. In conclusion, Pink1-PF was less strongly membrane associated, compared to Pink1-FL in this assay.

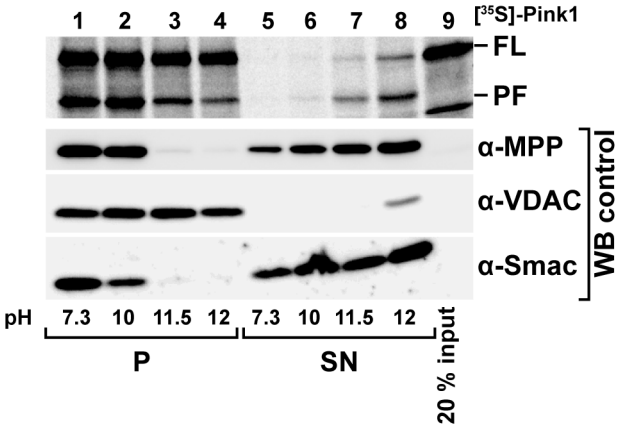

Figure 23: Sensitivity of newly imported [^{35}S]-Pink1 to alkaline extraction. Following *in vitro* import of radiolabeled Pink1 into isolated HeLa mitochondria for 40 min, mitochondria were subjected to alkaline extraction in 0.1 M Na_2CO_3 at the indicated pH. Samples were separated into pellet (P) and supernatant (SN) at 100,000 x g and analyzed by SDS-PAGE and digital autoradiography. As a control, immunodecoration of the endogenous mitochondrial proteins MPP, VDAC and Smac was performed. This figure was published in (Fedorowicz, de Vries-Schneider et al., 2014).

5.5.3 Re-translocation of processed Pink1 to the cytosolic fraction

A variation of the radioactive *in vitro* import assay was utilized, to follow the fate of newly generated Pink1-PF. To this end, after completion of the import reaction in polarized mitochondria, re-isolated, intact mitochondria were further incubated in the presence or absence of Δψ and then separated into mitochondrial and cytosolic fractions (Figure 23). In the presence of Δψ a fraction of about 6 % of Pink1-PF was detected in the soluble fraction after four minutes, and the intensity of this signal slightly increased over time (Figure 24 lanes 5-8). By contrast, when mitochondria were depleted of Δψ, Pink1-PF was only detected in mitochondrial fractions at all time points tested. Although in the presence of Δψ, a faint signal for Pink1-FL was also visible in the supernatants, the relative amount, judged by Pink1-FL signals in the pellet fractions, was lower compared to Pink1-PF. The integrity of mitochondrial membranes over the time period of the translocation assay was assessed by immunodetection of the soluble mitochondrial proteins MPP and Smac. Both proteins were exclusively present in the mitochondrial fractions, indicating that the Pink1-PF signal in the soluble fraction did indeed reflect re-translocation of the protein and was not due to disruption of the mitochondrial membranes. Transferred to the cellular situation, this observation is consistent with re-translocation of a fraction of Pink1-PF from mitochondria to the cytosol.

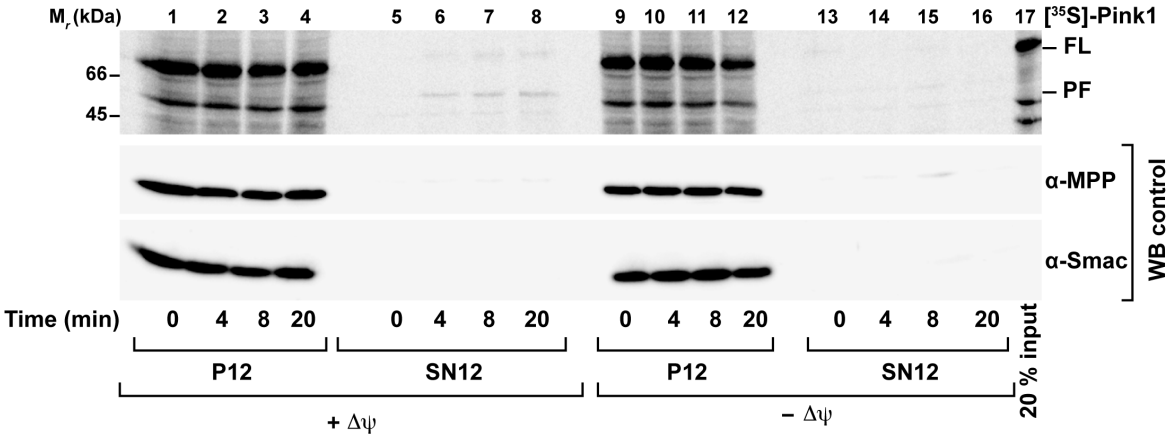

Figure 24: Release of newly imported Pink1 from mitochondria. Following *in vitro* import of radiolabeled Pink1 into energized isolated HeLa mitochondria for 40 min, mitochondria were re-isolated and further incubated for the times indicated. Where indicated, Δψ was dissipated after completion of the import reaction. At the time points indicated, samples were separated into mitochondrial pellets and soluble fractions at 12,000 x g. Proteins were separated by SDS-PAGE and detected by digital autoradiography, followed by control immunodetection of the mitochondrial proteins MPP and Smac.

5.5.4 Effect of OXPHOS inhibitors on Pink1 import

According to the current model, import of Pink1 into mitochondria and therefore indirectly processing of Pink1 by mitochondrial-resident proteases is dependent on Dy. By this mechanism, Pink1-FL is thought to accumulate at depolarized mitochondria. Thus, it was investigated next, if the accumulation of Pink1 in response to OXPHOS inhibitors observed in Figure 4 was the result of diminished Pink1 import and processing. Mitochondria isolated from SH-SY5Y cells were treated with the respective OXPHOS inhibitors prior to import of [^{35}S]-methionine/cysteine-labeled Pink1 as above (Figure 25A). Under control conditions, the 53 kDa Pink1-PF accumulated from 5 to 40 minutes of incubation. By contrast, the formation of Pink1-PF was completely abolished in mitochondria pre-treated with CCCP or antimycin A (Figure 25A, lanes 3-6). Furthermore, pre-treatment with either oligomycin or rotenone alone resulted in a slightly reduced formation of Pink1-PF, as compared to control conditions, but as opposed to mitochondria treated with CCCP or antimycin A, the processed fragment was clearly generated (Figure 25A, lanes 7-10). By contrast, when mitochondria were incubated with a combination of oligomycin and rotenone prior to import, Pink1-PF was not detectable even after 40 minutes of import (Figure 25A, lane 12). Notably, in mitochondria treated with CCCP or the respective OXPHOS inhibitors, a diminished accumulation of the 53 kDa Pink1-PF correlated with an increased formation of yet another Pink1 fragment of

about 56 kDa. In these mitochondria, the formation of this putative processing intermediate showed a different kinetics, since compared to the 53 kDa form of Pink1, it was already detected after five min. To a smaller extent, the 56 kDa Pink1-fragment was also detectable after 40 min of import under control conditions.

To monitor the effect of the pre-treatment on Δψ, mitochondria incubated under the same conditions were subjected to TMRE staining and measurement of TMRE fluorescence (Figure 25B). Similar to the results obtained in intact cells in 4.1.1, Δψ was strongly diminished under all conditions tested with the exception of oligomycin treatment, which resulted in an increased Δψ, compared to mitochondria incubated under control conditions.

Taken together, two observations from the import experiment strongly argue against a strict correlation between an intact Δψ and Pink1 import and processing: First, a considerable amount of Pink1-PF was still formed when Δψ was strongly diminished by the complex I inhibitor rotenone. Secondly, while Δψ was either increased or strongly reduced in mitochondria pre-treated with oligomycin or rotenone, respectively, the efficiency of Pink1 processing was similar under both conditions. Transferred to the cellular level, impaired import and processing of Pink1 were likely not the only reason for an increase in protein levels of Pink1-FL.

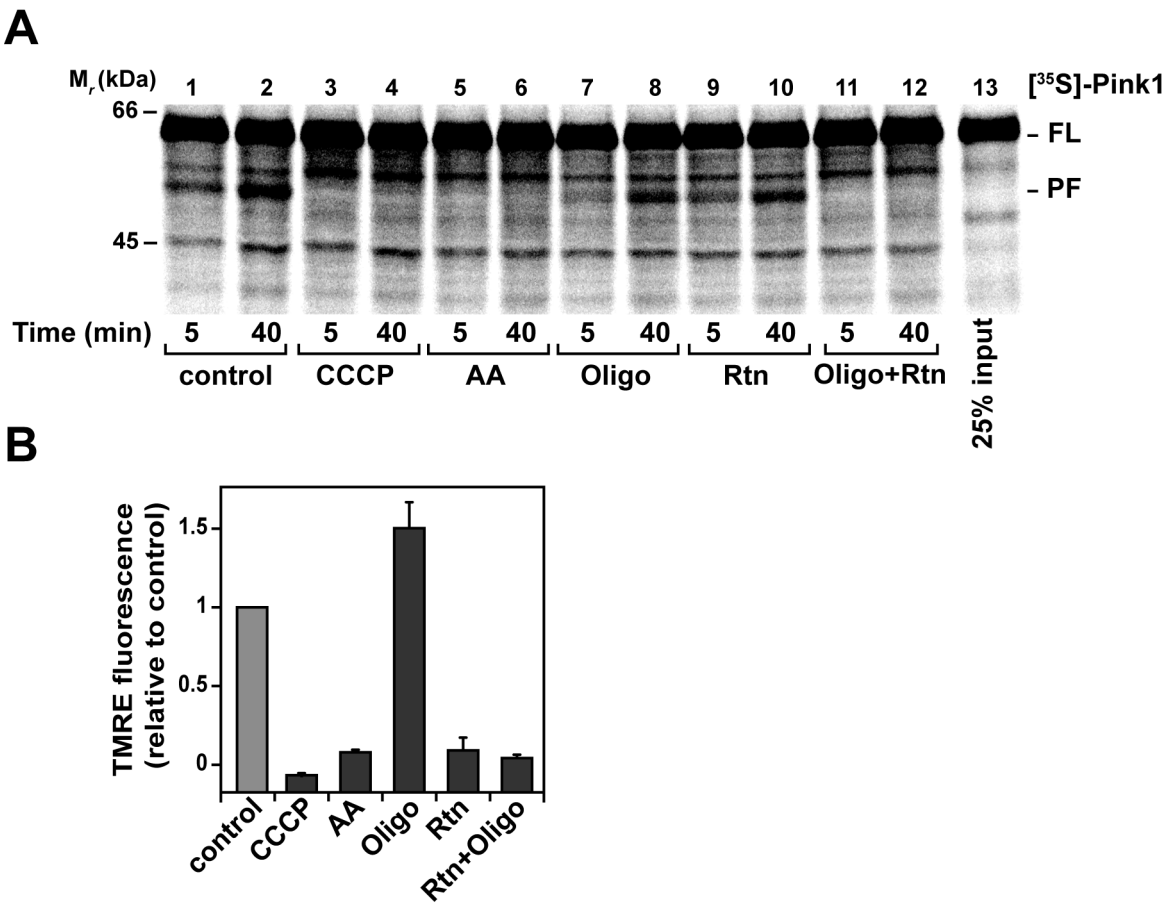

Figure 25: *In vitro* import of Pink1 and Δψ measurements in mitochondria treated with inhibitors of oxidative phosphorylation. (A) *In vitro* import of Pink1. Mitochondria isolated from SH-SY5Y cells were incubated with EtOH (control), 1 µM CCCP, 8 µM antimycin A, 20 µM oligomycin, 0.5 µM rotenone or a combination of 20 µM oligomycin and 0.5 µM rotenone for 5 min, followed by import of radiolabeled Pink1 for 5 or 40 min, respectively. After re-isolation of mitochondria, proteins were separated by SDS-PAGE and detected by digital autoradiography. (B) Measurement of Δψ in isolated mitochondria. Mitochondria treated as in (A) were incubated with 1 µM TMRE for 30 min and TMRE fluorescence was measured in a microplate reader. TMRE fluorescence intensities are shown relative to EtOH-treated control cells. Results represent the mean of three independent experiments and two technical replicates per experiment. Error bars indicate the standard error of the mean (SEM).

5.6 Degradation of Pink1 under normal and stress conditions

In general, the energetic state of mitochondria affects both import and degradation of mitochondrial proteins (Voos, 2013). Since the import experiments shown so far, revealed only a partial effect of the mitochondrial membrane potential on import and processing of Pink1, degradation of the protein was monitored.

5.6.1 Cellular turnover of Pink1

To assess Pink1 turnover on the cellular level, radioactive pulse/chase-labeling and subsequent immunoprecipitation was conducted, using Pink1-FLAG transiently expressed in SH-SHSY cells (Figure 26). Under these experimental conditions, both the 64 kDa Pink1-FL and the 53 kDa Pink1-PF were detectable by autoradiography (Figure 26A). At the starting point of the chase period (t=0) the 53 kDa Pink1-PF accounted for about 45 % of the total cellular amount of Pink1.

Over the course of 5 h incubation under control conditions, both Pink1-FL and Pink1-PF were gradually degraded to about 26 % and 36 %, respectively, relative to the starting value. Quantitative analysis of the degradation experiment resulted in half-life values of approximately 125 min for full-length Pink1 and 175 min for the processed form of Pink1 (Figure 26B). To monitor the effect of mitochondrial perturbation on Pink1 stability, cells were exposed to CCCP during the chase period. The resulting turnover rates for both full-length and processed forms were very similar to those in untreated cells. Small differences in the relative ratios between full-length and processed forms under control and CCCP conditions, respectively, are consistent with a reduced processing of Pink1 in the absence of $\Delta\psi$ as observed in Pink1 import experiments described above (see Figures 22 and 25). In conclusion, changes in $\Delta\psi$ did not affect the overall cellular degradation rates of Pink1. By comparison, treatment of cells with the proteasome inhibitor MG132 during the chase period resulted in a significantly increased stability of the processed form of Pink1. However, turnover of PINK1-FL was only marginally affected, extending its half-life from 125 to 180 min. This indicates, that at least the processed form of Pink1 is degraded by the proteasome.

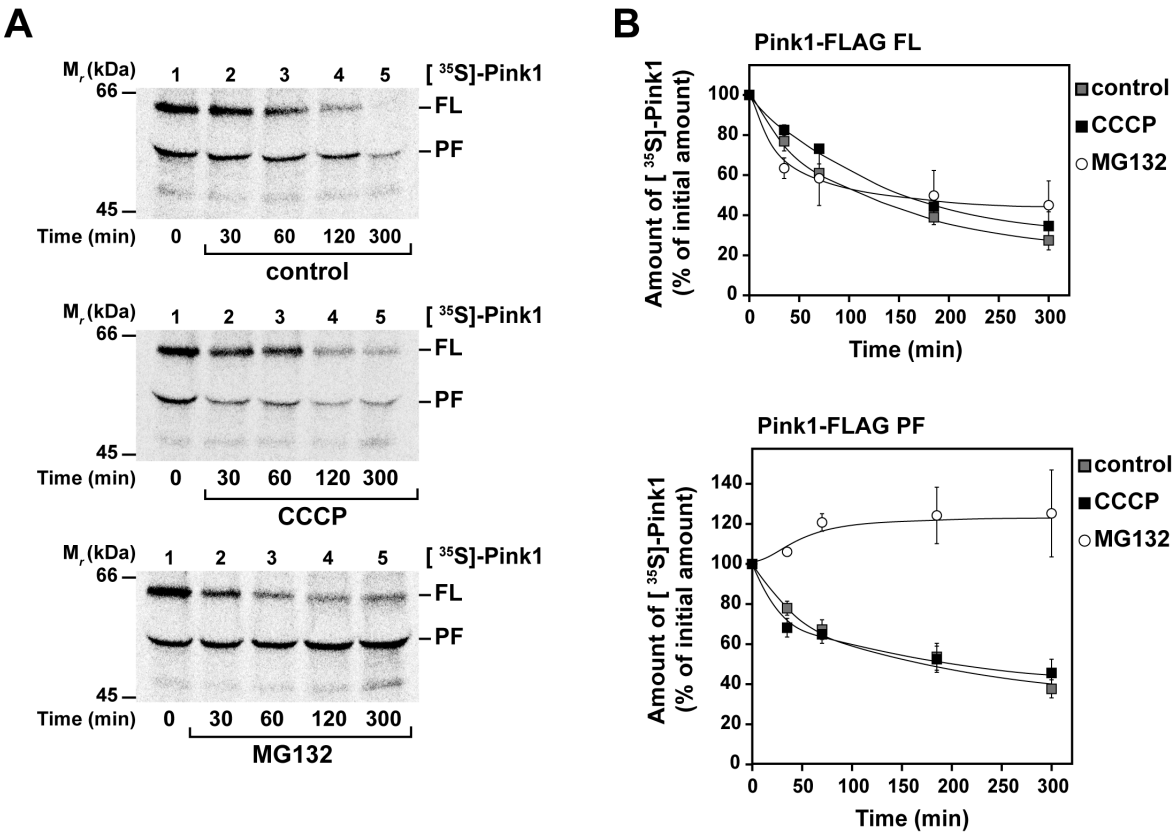

Figure 26: Cellular degradation of overexpressed [^{35}S]-labeled Pink1-FLAG. SH-SY5Y cells transiently expressing Pink1-FLAG were subjected to [^{35}S]-Met/Cys pulse labeling for 30 min and chase incubation with excess cold Met/Cys for the times indicated. Following immunoprecipitation of Pink1-FLAG, proteins were separated by SDS-PAGE and detected by digital autoradiography. (A) Representative autoradiograms of pulse/chase experiments, with chase under normal conditions and in the presence of 10 µM CCCP or 10 µM MG132. FL and PF indicate the 64 kDa full-length Pink1 and the 53 kDa processed form, respectively. (B) Quantification of cellular Pink1 degradation. Amounts of Pink1-FL and Pink1-PF are given as percentage of the respective initial Pink1 amount at t=0. Results represent the mean of three independent experiments per condition tested. Error bars indicate the standard error of the mean (SEM).

5.6.2 Mitochondrial turnover of Pink1

Reasoning that Pink1 at least partially enters mitochondria, it may be degraded by mitochondrial proteases as was previously postulated (Greene et al., 2012). To address this possibility, radiolabeled Pink1 was imported into isolated SH-SY5Y mitochondria for 40 min. After re-isolation of mitochondria the fate of the different Pink1 fragments was followed over a period of 4 h (Figure 27). At the start of the degradation time (t=0) both, the Pink1-FL and the Pink1-PF species were detected while Pink1-FL was the more abundant form, similar to the cellular degradation assay. As evident by the respective signal intensities, 20 % of the total mitochondria-associated Pink1 had been processed to

Pink1-PF during the import time (Figure 27A, lane 1). In energized mitochondria, the total amount of Pink1 declined by about 40 % over the 4 h course of the degradation experiment (Figure 27C). The relatively constant apparent amounts of Pink1-PF detected during this time are consistent with a continuing conversion of mitochondria-bound or already imported Pink1-FL to Pink1-PF. A very similar degradation rate was obtained, when $\Delta\psi$ was dissipated by the addition of CCCP after completion of the import reaction (Figure 27D). Hence, the presence of $\Delta\psi$ had no detectable effect on mitochondrial degradation of Pink1. Notably, total degradation reactions were analyzed in this experiment, to account also for the fraction of Pink1 that was shown to be released from mitochondria in the translocation assay (see Figure 24). The processed form Pink1-PF was previously postulated to be the main target of mitochondrial proteases (Greene et al., 2012). To assess the degradation of the processed Pink1 fragment alone, by circumventing the continuing conversion of Pink1-FL to Pink1-PF, the mutant Pink1Δ103 was used as a substrate in the degradation assay as above (Figure 26E). Pink1Δ103 mimics the proposed PARL-cleavage product (Deas et al., 2010a) and associates with mitochondria similar to the wild-type protein *in vitro* (Becker et al., 2012a). However, the degradation rate of about 40 % over 4 h of incubation was almost identical to the value obtained for combined Pink1-FL and Pink1-PF signals in the degradation assay with wild-type Pink1. In conclusion, the processed form of Pink1 did not show a higher sensitivity to degradation by mitochondrial proteases compared to full-length Pink1.

In a next approach, the degradation assay was repeated under ATP depletion conditions, to assess the involvement of ATP-dependent processes in the observed reduction of the Pink1 signal over time (Figure 27F). The resulting degradation rate of about 40 % over 4 h was virtually indistinguishable from the value obtained in energized mitochondria, arguing against a role of one of the ATP-dependent proteases of the mitochondrial matrix or inner membrane compartment in the degradation of Pink1.

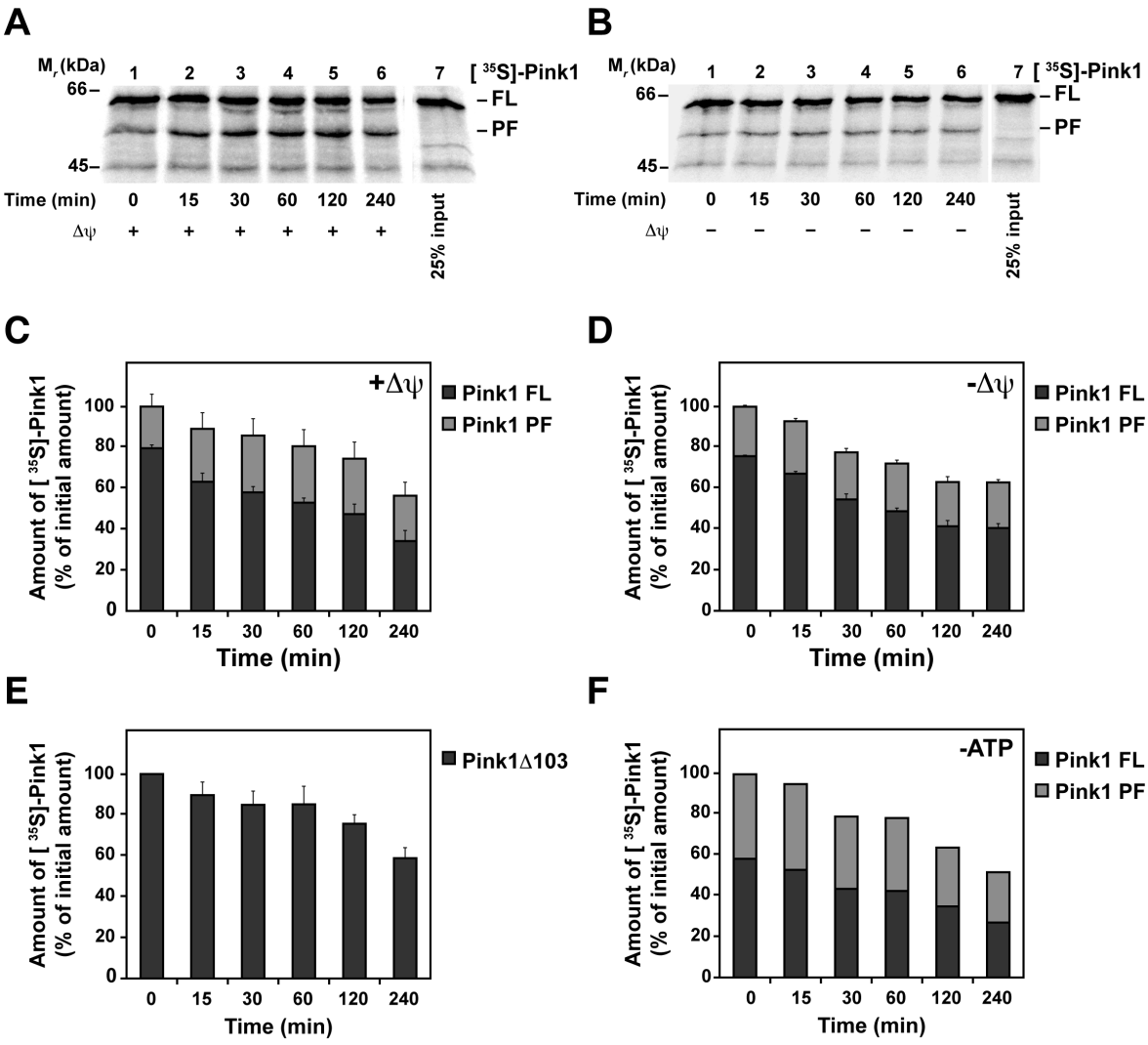

Figure 27: Mitochondrial degradation of newly imported [^{35}S]-Pink1. After *in vitro* import of [^{35}S]-Pink1 into energized isolated SH-SY5Y mitochondria, a degradation assay was performed as described in 2.4.6. Total samples were analyzed by SDS-PAGE and digital autoradiography. For quantification, the combined initial amount of full length (FL) and processed (PF) [^{35}S]-Pink1 was set to 100 % and results for each time point calculated as percentage of the initial amount. Percentages of FL and PF for each time point are indicated by different grey scale. Results represent the mean of three independent experiments per condition tested. Error bars indicate the standard error of the mean (SEM). (A, B) Representative autoradiograms for mitochondrial degradation of Pink1 under normal conditions (A) or after depletion of Δψ (B). (C) Degradation under normal conditions. (D) Degradation after depletion of Δψ after completion of the import reaction. (E) Degradation of [^{35}S]-Pink1Δ103 (F). Degradation of [^{35}S]-Pink1 in mitochondria depleted of ATP by apyrase treatment and the addition of oligomycin after completion of the import reaction.

Taken together, the results of the degradation assays imply, that the vast accumulation of Pink1, observed upon depletion of $\Delta\psi$, is not due to a diminished cellular or mitochondrial turnover of the protein. Moreover, the processing state of Pink1 did not determine its sensitivity towards degradation.

5.7 Regulation of Pink1 gene expression

If the accumulation of Pink1 under mitochondrial stress conditions is not the result of a decrease in processing and turnover of the protein, cellular amounts of Pink1 must be regulated on another level. Thus, the requirement of protein biosynthesis for Pink1 accumulation was assessed.

5.7.1 Effect of transcription and translation inhibitors on Pink1 protein levels

In a first approach, SH-SY5Y cells were exposed to the inhibitors of oxidative phosphorylation as before, but in the presence or absence of the translation inhibitor cycloheximide (Figure 28).

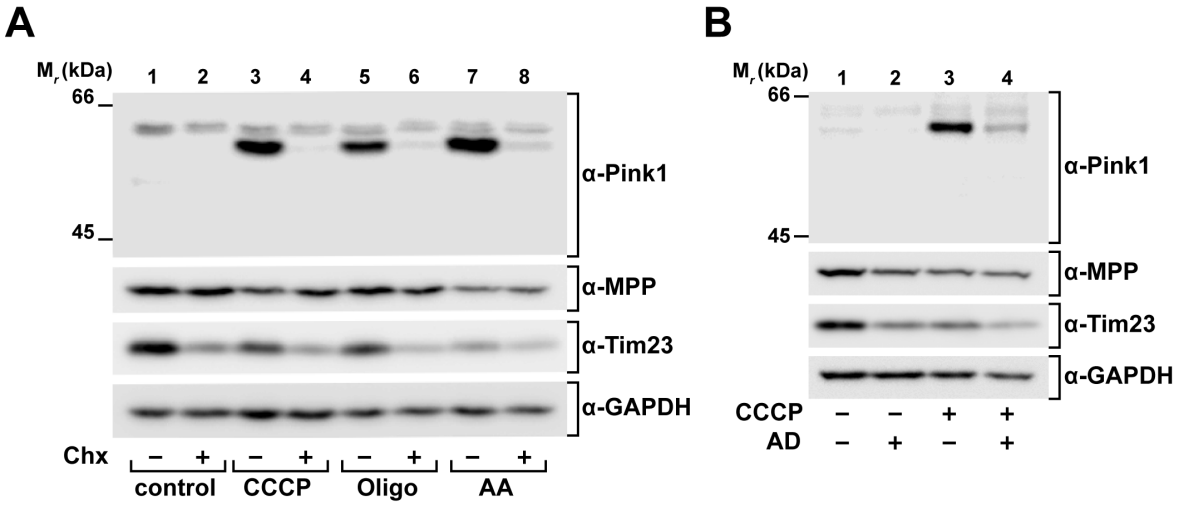

Figure 28: Effect of cycloheximide and actinomycin D on Pink1 protein expression.

(A) Effect of translation inhibition on Pink1 expression. SH-SY5Y cells were treated with DMSO/EtOH (control), CCCP, oligomycin or antimycin A at concentrations described for Figure 4 for 16 h but in the presence or absence of 50 µg/ml cycloheximide. (B) Effect of transcription inhibition on Pink1 expression. Cells were incubated with DMSO/EtOH or CCCP for 16 h as above but in the presence or absence of 5 µg/ml actinomycin D.

As shown in Figure 28A, accumulation of Pink1 in response to CCCP, oligomycin or antimycin A was almost completely blocked by cycloheximide. This observation implies, that the *de novo* synthesis of Pink1 molecules is indispensible for an increase in cellular Pink1 levels. To further elucidate, which step of protein biosynthesis is crucial for Pink1 accumulation, actinomycin D was used to inhibit transcription during exposure of cells to CCCP. As evident from Figure 28B, Pink1 accumulation was almost completely abolished in the presence of actinomycin D. This observation indicates the regulation of Pink1 protein amounts on the transcriptional level.

5.7.2 Pink1 mRNA levels in response to OXPHOS inhibitors

In order to verify the observations from actinomycin D experiments, quantitative real-time PCR (qRT-PCR) was performed. In detail, Pink1 mRNA amounts, relative to mRNA levels of GAPDH as a control were analyzed. After exposure of cells to CCCP, antimycin A or oligomycin for 8 h, an approximately two-fold increase in Pink1 mRNA expression, relative to samples treated with the respective compound for 0.5 h was observed (Figure 29 A-C). Relative amounts of Pink1mRNA further increased in cells treated with CCCP or antimycin A, reaching approximately four-fold of the starting value (0.5 h). A slight increase in Pink1 mRNA expression was also observed between 8 and 16 h of oligomycin treatment, respectively. After 24 h of exposure to all three inhibitors, Pink1 mRNA levels started to decline. Compared to the other inhibitors, Pink1 mRNA amounts measured in cells treated with the complex 1 inhibitor MPP^+ were lower, reaching a maximum of approximately 1.5-fold after 16 h (Figure 29D).

In conclusion, the sensitivity of Pink1 accumulation to an inhibition of protein biosynthesis together with elevated Pink1 mRNA levels in response to mitochondrial perturbations imply, that cellular amounts of Pink1 are determined by transcriptional regulation of *PINK1* gene expression.

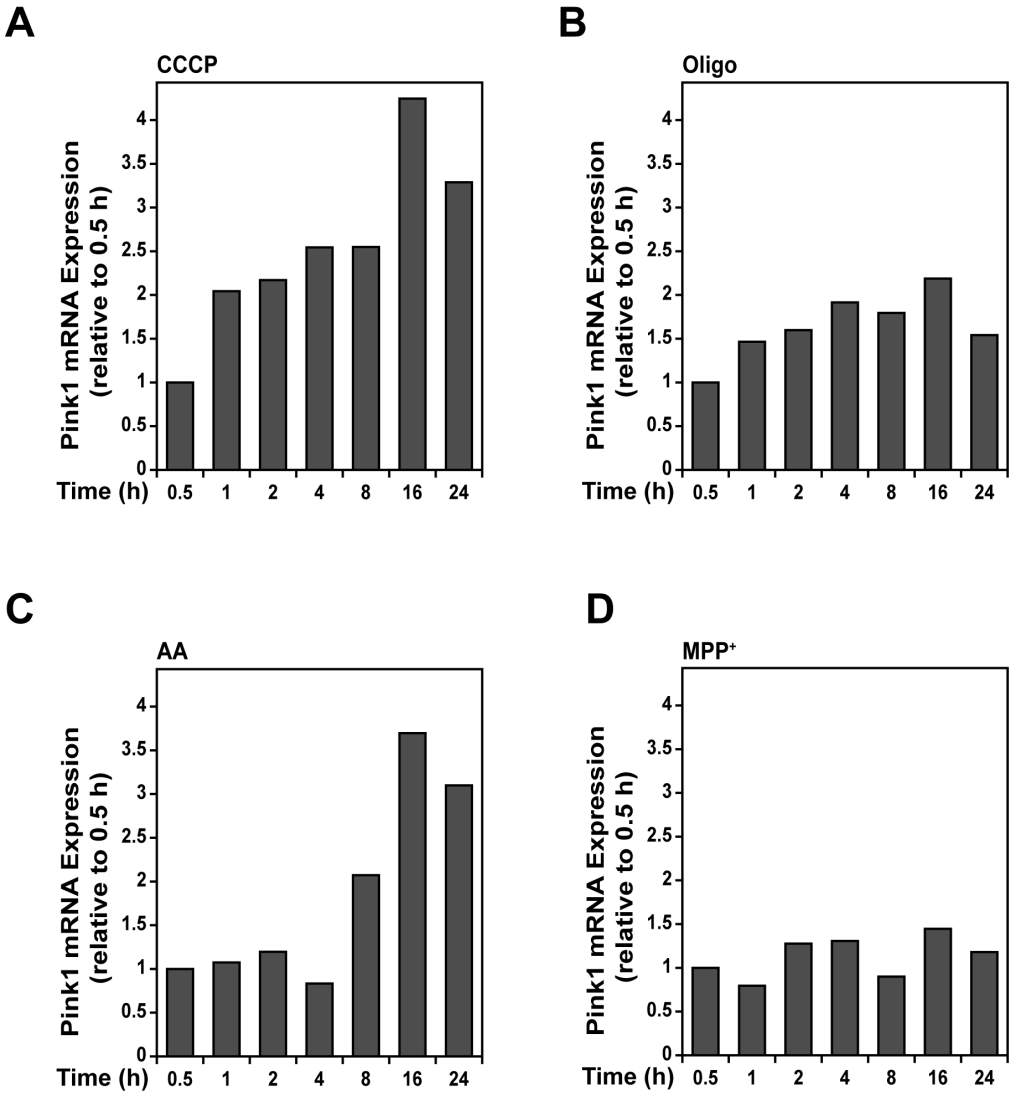

Figure 29: Analysis of Pink1 mRNA levels by qRT-PCR. After treatment of cells with 10 µM CCCP, 50 µM oligomycin, 200 µM antimycin A or 2.5 mM MPP^+, Pink1 mRNA levels were determined by quantitative RT-PCR and normalized to mRNA levels of GAPDH for each sample. Results are shown relative to mRNA levels in cells exposed to the respective compound for 0.5 h and represent the mean of two technical replicates. mRNA measurements were performed by Kerstin Hallmann (Life and Brain Center, University of Bonn).

5.7.3 Candidate regulators of Pink1 transcription

Several factors have previously been discussed in the context of Pink1 gene expression. One candidate, the transcription factor c-Fos (Gomez-Sanchez, Gegg et al., 2014), is responsive to elevated intracellular calcium levels. To revisit calcium-dependent regulation of Pink1 expression, SH-SY5Y cells were treated with thapsigargin at different concentrations. By inhibiting the sarcoplasmic/endoplasmic Ca^{2+} ATPase (SERCA), thapsigargin prevents calcium uptake into intracellular storage compartments, which results in an increase in cytosolic Ca^{2+}-levels (Lytton, Westlin et al., 1991, Thastrup, Cullen et al., 1990). However, no increase in Pink1 protein levels was detected after exposure of cells to thapsigargin even at high concentrations (Figure 30). This observation implies, that intracellular Ca^{2+}-levels do not affect Pink1 expression under the conditions tested here.

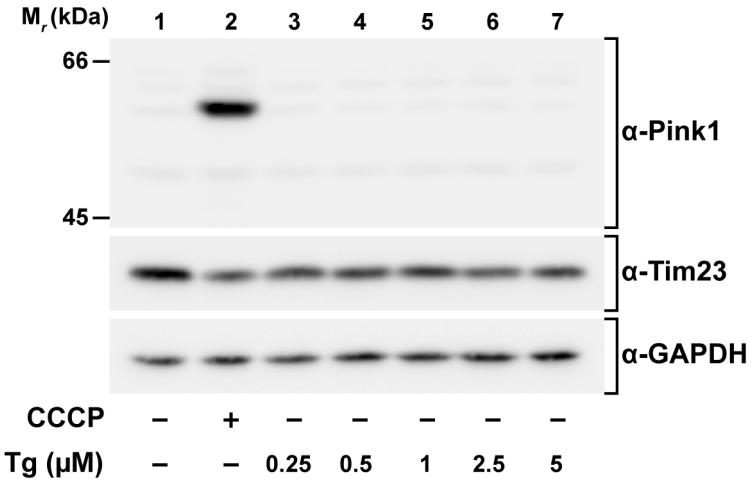

Figure 30*: Effect of thapsigargin on Pink1 expression. SH-SY5Y cells were treated with the inhibitor of the sarco/endoplasmatic reticulum Ca^{2+}-ATPase (SERCA) thapsigargin, at 0.25 to 5 µM or with DMSO or 10 µM CCCP as controls for 16 h. Total cell lysates were analyzed by SDS-PAGE and Western blot.

Another previous study, examining the Pink1 promoter, proposed the transcription factor NF-kB (nuclear factor kappa-light-chain-enhancer of activated B-cells) as an activator of Pink1 gene expression (Duan, Tong et al., 2014). Thus, the effect of three different inhibitors of NF-kB signaling, NG25, BI605906 and MLN4924 on Pink1 induction in response to CCCP was tested. BI605906 prevents activation of NF-kB signaling by inhibiting the I-kB kinase (IKK) complex, which usually phosphorylates the inhibitor I-kB under inductive conditions, marking it for ubiquitination and proteasomal degradation. MLN4924 inhibits both the canonical and non-canonical activation of NF-kB by affecting the proteasomal degradation of the I-kB inhibitor. NG25 is an inhibitor of the TAK1

kinase, which is involved in the intracellular propagation of NF-kB-related signaling events. As shown in Figure 31, MLN4924 and, to a smaller extent, BI605906 led to a decrease in Pink1 levels after CCCP-treatment (by about 30 % for MLN4929) but did not completely abolish Pink1 induction. By comparison, Pink1 induction in response to CCCP was slightly increased in the presence of NG25.

In summary, both inhibitors with an effect on I-kB reduced Pink1 expression levels, indicating at least a partial dependence of Pink1 induction on regulation via the NF-kB signaling pathway.

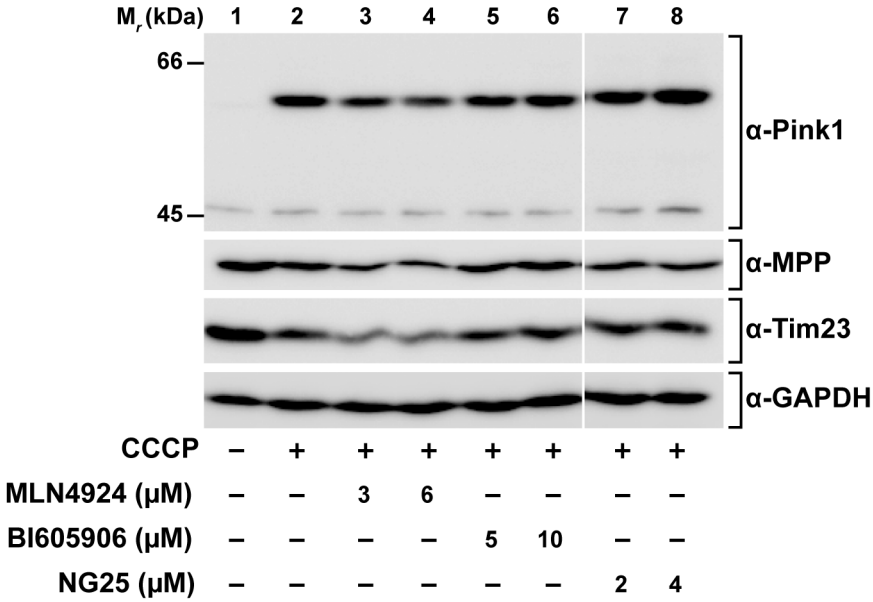

Figure 31*: NF-kB dependence of Pink1 expression. Cells were pre-treated with inhibitors of NF-kB signaling MLN4924, BI605906 or NG25 for 2 h followed by 16 h incubation in the presence of the respective inhibitor and 10 µM CCCP.

Through mediating degradation of the endogenous NF-kB inhibitor Ik-B, the ubiquitin-proteasome system is directly involved in NF-kB signaling. Accordingly, the proteasome inhibitior MG132 blocks NF-kB activation (Lee & Goldberg, 1998). Therefore, MG132 was used as an alternative way to study involvement of NF-kB in transcriptional regulation of Pink1 (Figure 32). Pink1 induction in response to CCCP, oligomycin or antimycin A was almost completely abolished in the presence of the proteasome inhibitor. The accumulation of the 53-kDa Pink1-PF observed after MG132 treatment is in consistence with the notion, that the processed Pink1 fragment is a target of the 26S proteasome, as was observed in the cellular degradation assay (see Figure 26) and has been described previously (Lin & Kang, 2008).

Taken together, the effect of specific NF-kB inhibitors as well as the strong inhibitory effect of MG132 on the induction of Pink1 are consistent with an involvement of NF-kB signaling in Pink1 gene expression under mitochondrial stress conditions.

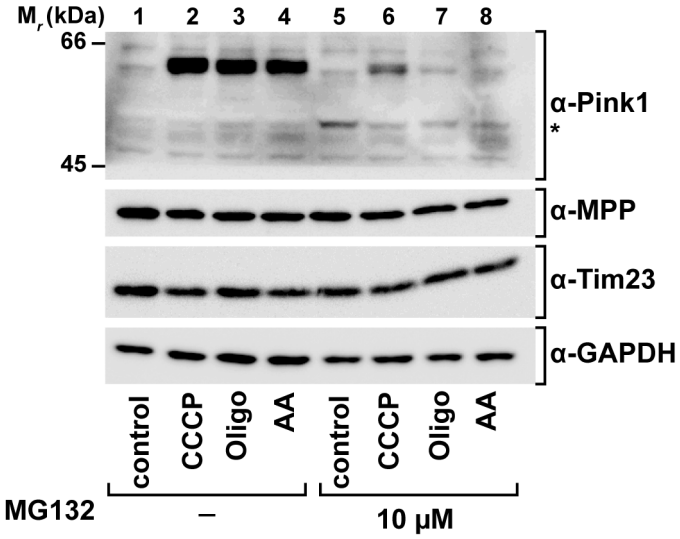

Figure 32: Effect of MG132 on Pink1 expression. Cells were treated with CCCP, oligomycin or antimycin A as described for Figure 4, but in the presence or absence of the proteasome inhibitor MG132 at 10 µM for 8 h. Total cell lysates were analyzed by SDS-PAGE and Western blot. Pink1-PF is indicated with an asterisk.

5.8 Association of wild-type and mutant α-synuclein with mitochondria

Albeit its predominantly cytosolic localization, several studies have demonstrated α-synuclein to be localized in or at mitochondria (Devi et al., 2008, Li et al., 2007). An intra-mitochondrial localization of the nuclear-encoded α-synuclein would require its insertion into or translocation over the mitochondrial membranes. To directly address this hypothesis, an *in vitro* import assay of [^{35}S]-Met/Cys-labeled wild-type and mutant (A30P and A53T) α-synuclein was performed (Figure 33). The two pathogenic point mutations in α-synuclein, A30P and A53T, respectively, are associated with autosomal-dominant PD (Klein & Westenberger, 2012). Mitochondrial malate dehydrogenase 2 (Mdh2), which is imported into the mitochondrial matrix via the TOM and TIM23 translocase complexes, was used as a control (Figure 33).

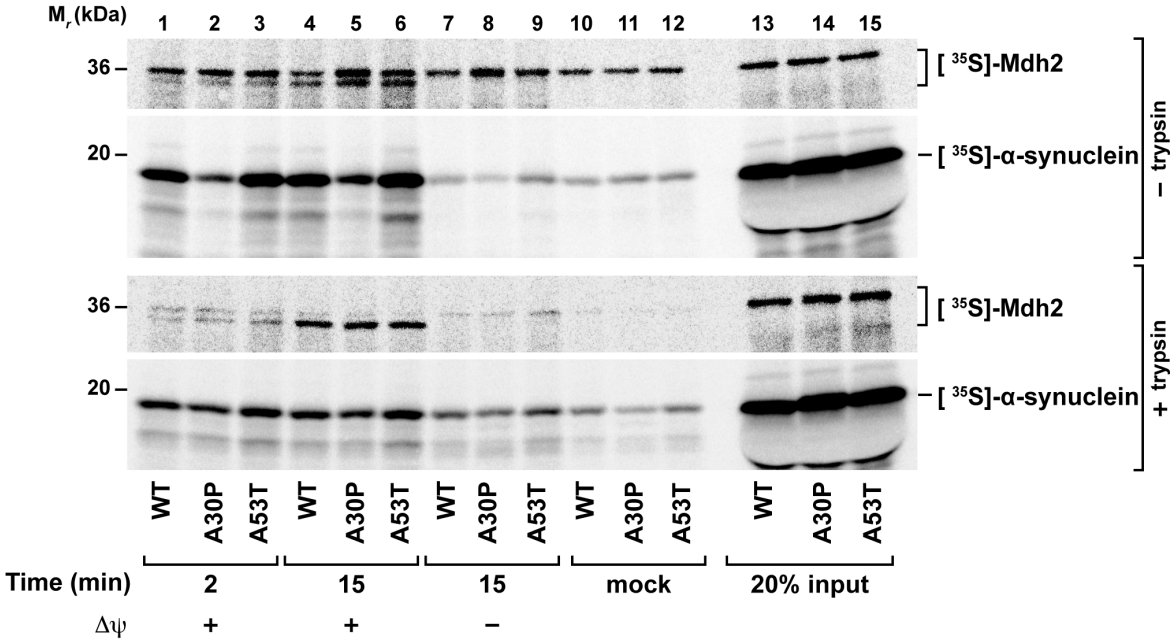

Figure 33: *In vitro* import assay with [^{35}S]-labeled α -synuclein. *In vitro* import of [^{35}S]-Met/Cys-labeled Mdh2 and either wild-type a-synuclein, α -synuclein$_{A30P}$ or a-synuclein$_{A53T}$ into energized isolated HeLa mitochondria for 2 or 15 minutes was performed under standard conditions. Where indicated, Δψ was dissipated prior to the import reaction. Protease-accessible proteins were digested by incubation with 100 µg/ml trypsin after the import (lower panel). Mock samples contained no mitochondria. Following re-isolation of mitochondria, proteins were separated by Tricine-SDS-PAGE and detected by digital autoradiography. This figure was published in (Guardia-Laguarta, Area-Gomez et al., 2014).

When the Mdh2 precursor protein was incubated with energized isolated HeLa cell mitochondria, it associated with mitochondria. The appearance of a second band, representing the mature form after cleavage of the presequence by the matrix processing peptidase (MPP), was observed after 15 min of import (Figure 33 lanes 4-6). In consistence with import into the mitochondrial matrix, processing of Mdh2 was dependent on the mitochondrial membrane potential (Δψ) (Figure 33, lanes 7-9) and the processed Mdh2 but not the full-length form was resistant to trypsin treatment of mitochondria re-isolated after import (Figure 33, lanes 1-6, lower panel). As compared to the Mdh2 control, wild-type α-synuclein also associated with mitochondria and this association was reduced in the absence of Δψ. However, neither an increase in mitochondria-bound α-synuclein over time, nor the appearance of a cleaved fragment was observed (Figure 33, lanes 1 and 4). While a fraction of the mitochondria-associated α-synuclein was apparently resistant to protease treatment a similar amount of trypsin-resistant a-synuclein was detected in the absence of mitochondria in “mock” samples (Figure 33, lane 10). This observation may be explained by aggregation of a fraction of α-synuclein,

which would reduce the accessibility of the protein to trypsin. The α-synuclein aggregates would then sediment during re-isolation of mitochondria by centrifugation.

As compared to the wild-type protein, less α-synuclein$_{A30P}$ associated with mitochondria, while the binding efficiency of α-synuclein$_{A35T}$ was slightly increased over the WT protein. Moreover, binding of both mutant proteins was partially dependent on Δψ and a fraction of a-synuclein$_{A30P}$ and a-synuclein$_{A53T}$, respectively, was resistant to trypsin even in the absence of mitochondria, similar to the wild-type protein (Figure 33, lanes 7-12).

Most mitochondrial proteins require the TOM complex for insertion into or crossing of the outer mitochondrial membrane (OMM) (Becker et al., 2012b). Thus, in a second approach, isolated mitochondria were incubated with proteinase K (PK) to digest the cytosol-exposed peripheral receptors Tom20 and Tom70 prior to *in vitro* import as above (Figure 34). Import of Mdh2, as evident by the appearance of the processed form, was strongly reduced even at 5 µg /ml PK. By contrast, the binding of both α-synuclein and the Mdh2 precursor to mitochondria was unaffected by PK pre-treatment (Figure 34, lanes 1-8). This observation implies, that a-synuclein association with mitochondria does not occur through the TOM receptors. In case of the Mdh2 control, import but not binding of the Mdh2 precursor was dependent on TOM receptors at the outer face of the OMM. The effect of the PK pre-treatment was confirmed by Western blot analysis of Tom70 and Tom40 (Figure 34, lower panel). According to their respective positions, the partially peripheral Tom70 receptor was readily cleaved by PK, while the pore-forming integral membrane protein Tom40 was digested only by a combination of pre- and post-treatment (Figure 34, lanes 5-8).

In summary, WT and mutant α-synuclein associated with mitochondria in a Δψ-dependent manner. Since this binding was independent of TOM receptors and did not confer protease-resistance, α-synuclein is likely not imported into the mitochondrial membranes or matrix compartment.

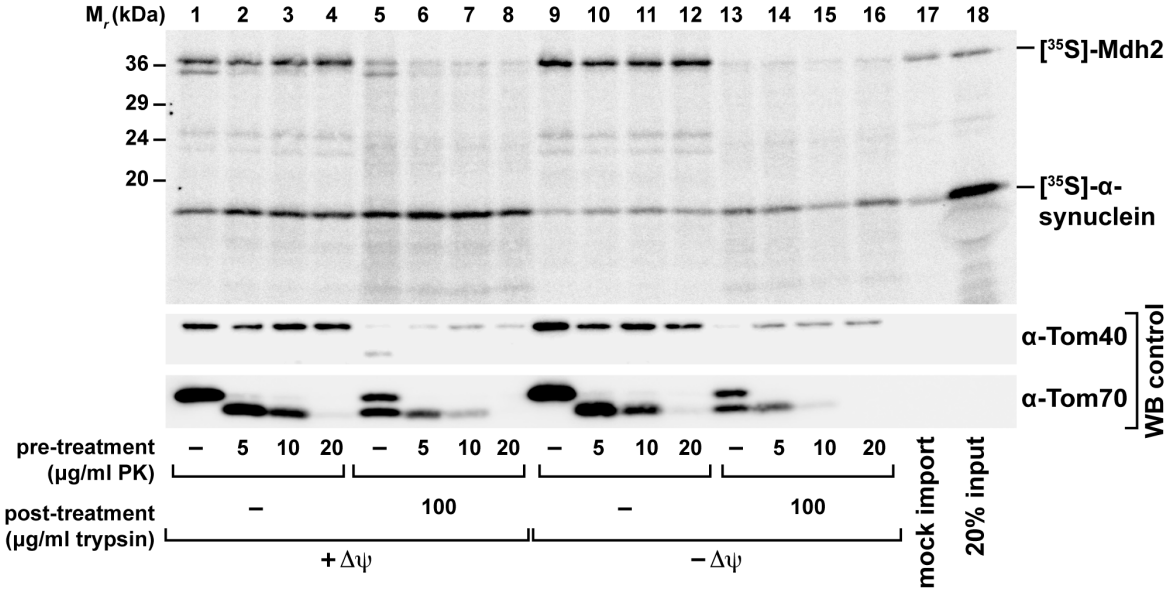

Figure 34: Dependence of α-synuclein association with mitochondria on mitochondrial outer membrane receptors. Isolated mitochondria were incubated with proteinase K at the indicated concentrations (pre-treatment), prior to *in vitro* import of radiolabeled Mdh2 and α-synuclein for 15 min in the presence or absence of Δψ. Protease-accessible proteins were digested by treatment with 100 µg/ml trypsin (post-tratment). After re-isolation of mitochondria, proteins were separated by Tricine-SDS-PAGE. Digital autoradiography and control immunodetection of the TOM subunits Tom40 and Tom70 is shown.

6 Discussion

6.1 Pink1 accumulates upon specific mitochondrial perturbations

The kinase Pink1 accumulates on the surface of defective mitochondria. This event represents a pivotal step in an organellar quality control pathway that mediates the removal of damaged mitochondria by mitophagy. The strong increase in cellular levels of Pink1 is an outstanding characteristic of this protein, seeking its equal among other mitochondrial components. According to current models, Pink1 is constitutively expressed at high levels, while steady-state amounts at healthy mitochondria are kept low by a rapid proteolytic turnover of the protein (Eiyama & Okamoto, 2015, Pickrell & Youle, 2015). Import of Pink1 into mitochondria and processing by mitochondrial proteases is proposed to be a prerequisite for its subsequent degradation. Thus, a reduction of the inner membrane potential ($\Delta\psi$) and the concurrent inhibition of mitochondrial import would result in an accumulation of full-length Pink1 at the mitochondrial surface, which in turn would initiate the downstream mitophagy process. This rather elaborate mechanism is proposed to allow a rapid accumulation of Pink1 upon loss of $\Delta\psi$, a major hallmark of mitochondrial damage (Eiyama & Okamoto, 2015, Pickrell & Youle, 2015). However, the proposed import/turnover model has its shortcomings. First, both full-length Pink1 (Pink1-FL) and its major processing product (Pink1-PF) localize exclusively to the outer face of the OMM (Becker et al., 2012a) and secondly, it is still not clear which protease is responsible for the degradation of Pink1. I therefore aimed at elucidating the connection between mitochondrial dysfunction and the accumulation of Pink1 in my thesis.

In my experiments, the increase in Pink1 protein levels was not strictly correlated with a reduction of $\Delta\psi$, as was previously postulated (Matsuda et al., 2010, Narendra et al., 2010b). By contrast, a significant up-regulation of Pink1 amounts concurrent with an increased $\Delta\psi$ was observed after exposure of cells to the mitochondrial F_1/F_O-ATPase inhibitor oligomycin. Conversely, treatment of cells with the complex I inhibitor MPP^+ resulted in a decreased $\Delta\psi$ but failed to provoke an accumulation of Pink1.

The inhibition of $\Delta\psi$-dependent import, as a prerequisite for Pink1 degradation, has been postulated to account for the accumulation of Pink1-FL selectively at the surface of

depolarized mitochondria. However, the results from my *in vitro* import assay (Figure 25A) argue against this hypothesis. First, Pink1 import was not strictly dependent on Δψ and secondly, inhibition of Pink1 import *in vitro* did not necessarily correlate with elevated cellular amounts of Pink1. Although treatment of mitochondria with rotenone resulted in a strongly reduced Δψ, a considerable amount of Pink1 was still imported and processed. This observation is in line with the previously published finding, that Pink1 import and generation of Pink1-PF *in vitro* is only partially abolished in depolarized mitochondria (Becker et al., 2012a). Moreover, while rotenone and oligomycin inhibited *in vitro* import of Pink1 to a similar degree, oligomycin but not rotenone caused elevated cellular Pink1 levels. When relating the results from the import experiment to cellular Pink1 levels, the different experimental conditions should be taken into account. While protein levels of Pink1 were determined in intact cells exposed to the OXPHOS inhibitors for several hours, isolated mitochondria were incubated with the respective compounds for five minutes prior to the import assay. Still, similar effects of CCCP, antimycin A and oligomycin on Δψ were measured under the respective conditions in intact cells and *in vitro*, arguing for comparable conditions in both assays. It should be noted that rotenone treatment is not compatible with assessing Δψ by TMRE staining of intact cells. Provided that the *in vitro* assay sufficiently reflects the cellular situation, the combined results from both experiments allow two conclusions on the accumulation of Pink1: 1) a reduced membrane potential is likely not the sole trigger for Pink1 accumulation and 2) Δψ-dependent import is not the single mechanism responsible for the regulation of Pink1-FL amounts at the mitochondrial surface. Pink1 was furthermore proposed to form a complex with components of the TOM translocase at the surface of depolarized mitochondria. This association would allow a rapid re-import of the protein to rescue mitochondria from mitophagy (Lazarou, Jin et al., 2012). In the native PAGE experiments shown here, I found Pink1 present in two high molecular weight complexes of about 700 and 900 kDa, respectively, when it accumulated in response to CCCP (Figure 13). However, Pink1 did not co-migrate with the TOM component Tom40, arguing against complex formation between Pink1 and the outer membrane translocase. While this observation questions the model suggested by Lazarou et al. it is in line with another previous study examining Pink1 complexes by native PAGE (Becker et al., 2012a). As two of the known direct Pink1 substrates, Parkin and Mfn2, did also not co-migrate with Pink1, identifying the

actual complex constituents in future experiments may lead to the identification of novel Pink1 interaction partners.

In my experiments, general cellular perturbations, exemplified by tunicamycin-induced ER protein stress and oxidative stress, collectively failed to elicit elevated levels of Pink1. The absence of an effect of atractyloside, an inhibitor of the mitochondrial nucleotide transporter further indicates that the overall cellular energy state is likely not involved in damage-related accumulation of Pink1.

In the experiments shown here, enhanced amounts of Pink1 in response to OXPHOS inhibitors correlated well with reduced levels of mitochondrial proteins. Moreover, a potentially ubiquitinated species of Mfn2 concurrent with high levels of Pink1, may reflect Parkin-dependent ubiquitination of Mfn2 (Gegg et al., 2010). While both observations are consistent with Pink1/Parkin-mediated mitophagy, a direct confirmation for the initiation of mitophagy is missing. It should be noted that a reliable assay to detect mitophagy has not been described so far. Most methods assess the loss of mitochondrial proteins, as also observed here. However, removal of mitochondrial components may occur by several distinct processes. First, addition of specific ubiquitin chains by Parkin was shown to result in the proteasomal degradation of OMM proteins, including Mfn2, which in turn was crucial for mitophagy (Chan, Salazar et al., 2011). Secondly, so-called mitochondria-derived vesicles (MDVs) were proposed to sequester components of the mitochondrial matrix and IMM for delivery to lysosomal degradation (Soubannier, McLelland et al., 2012), and this process possibly involves Pink1 and Parkin (McLelland, Soubannier et al., 2014). Thus, it remains to be clarified, if Pink1 accumulation under the conditions tested here did indeed result in autophagic elimination of mitochondria by mitophagy.

6.2 Pink1 does not accumulate in response to mitochondrial protein stress

Although being restricted to mitochondrial perturbations, Pink1 accumulation appears to occur only in response to a subset of mitochondrial insults. In my hands, potential mitochondrial protein stress generated either through ectopic expression of a destabilized model protein or by reducing the endogenous amount of the mitochondrial Hsp70

chaperone Mortalin, did not result in enhanced Pink1 levels. The first observation contradicts the previously published finding that the expression of a mitochondria-targeted aggregation-prone mutant OTC (ornithine carbamoyltransferase) causes the accumulation of Pink1 and mitophagy (Jin & Youle, 2013). This discrepancy may be due to different aggregation propensities or expression levels of the two model proteins. There are different explanations for the increased Pink1 levels upon expression of mutant OTC observed by Jin et al. First, accumulation of Pink1 could be a direct response to intra-mitochondrial protein aggregates, as it is described for the protein-stress induced mitochondrial unfolded protein response in *C.elegans* (mtUPR, see below). Alternatively, the overexpression of an artificial aggregation-prone protein may indirectly cause mitochondrial damage, which in turn would lead to elevated Pink1 levels. In the latter case, Pink1 accumulation might occur through the same mechanism as the upregulation of Pink1 I observed upon inhibition of OXPHOS. Thus, determining if Pink1 accumulation is a direct or indirect effect of intra-mitochondrial protein aggregates will be an important cue for resolving a putative signaling mechanism responsible for the regulation of Pink1 levels. Importantly, Jin et al. note that Pink1 accumulation occurred in the presence of an intact $\Delta\psi$, supporting my present findings discussed above. Another study showed that the Mortalin knockdown phenotype in cells, namely increased susceptibility to intra-mitochondrial proteolytic stress, mitochondrial fragmentation and reduced mitochondrial mass, could be rescued by overexpression of Pink1 and Parkin (Burbulla, Fitzgerald et al., 2014). However, the authors did not examine levels of endogenous Pink1 in this context. Thus, although Pink1/Parkin-mediated mitophagy may in general counteract mitochondrial damage resulting from loss of Mortalin, it remains elusive if protein stress is a direct trigger for Pink1 accumulation and subsequent mitophagy.

6.3 Inhibition of complex I or a genetic complex IV deficiency do not result in elevated Pink1 levels

I have shown in my thesis, that inhibition of complex I (NADH-ubichinon-oxidoreductase) with either rotenone or MPP^+, a metabolic product of the PD-related neurotoxin MTPT (Singer et al., 1988), reduces both $\Delta\psi$ and mitochondrial ATP levels without promoting an accumulation of Pink1. This observation does not only challenge the current model of $\Delta\psi$-dependent accumulation of Pink1 but prompts an intriguing hypothesis. The failure to elicit an accumulation of Pink1 by complex I inhibitors like

MTPT would also preclude a subsequent activation of the Pink1/Parkin-related quality control pathway, thereby contributing to the development of Parkinson's disease, similar as defects or loss of Pink1 function contribute to hereditary PD (Valente et al., 2004).

Apart from the short-term mitochondrial stress conditions caused by chemical treatment of cells described above, I also examined Pink1 levels under a condition of permanent mitochondrial dysfunction due to a genetic defect. In detail, I analyzed Pink1 levels in muscle tissue samples of a patient carrying a mutation in the gene encoding subunit 8A of respiratory chain complex IV (cytochrome c oxidase). Pink1 was not detectable under-steady state conditions in this tissue. Notably, protein levels of complex IV as well as complex IV-dependent respiratory activity, measured in cultured fibroblasts of the same patient, were dramatically reduced (Hallmann et al., 2016). Thus, the *COX8A* mutation represents yet another condition, where severe mitochondrial dysfunction and Pink1 accumulation are not correlated. However, it remains to be elucidated if *COX8A*-deficient cells do accumulate Pink1 upon treatment with OXPHOS inhibitors, or if Pink1 induction is altogether abolished in these cells. The lack of Pink1 accumulation observed under steady-state conditions also raises the question, if distinct stress-responses exist. Under short-term stress conditions accumulation of Pink1 at defective mitochondria and mitophagy may be beneficial. By contrast, permanent dysfunctions, exemplified by mutations in nuclear-encoded genes for respiratory chain components, affect the whole mitochondrial network. In the latter case, the removal of virtually the entire mitochondrial population would be deleterious. Intriguingly, a direct connection between a genetic respiratory chain defect and Parkinsonism was proposed only for a mutation in the nuclear-encoded cytochrome *c* (De Coo, Renier et al., 1999). A possible explanation is, that at least severe hereditary OXPHOS defects typically cause premature death and these patients simply do not reach the age of even early-onset PD (Schon & Przedborski, 2011). Although a connection between large-scale somatic mtDNA mutations and PD was reported (Bender et al., 2006), it remains to be elucidated if a lack of Pink1 accumulation contributes to the etiology of the disease in these cases, similarly as hypothesized above for complex I inhibition.

6.4 A fraction of processed Pink1 translocates to the cytosol

Sequential proteolytic cleavage of the 64 kDa full-length Pink1 by MPP and PARL was previously proposed to generate the 53 kDa processed Pink1 fragment (Deas et al., 2010a, Greene et al., 2012). By analyzing *in vitro* import of Pink1 into PARL-deficient mitochondria, I confirmed here, that Pink1-PF is indeed generated by PARL. However, low levels of an apparently identical processed Pink1 species accumulating even in the absence of PARL, suggested an alternative, PARL-independent cleavage. In contrast to PARL-dependent processing, generation of this PARL-independent fragment was virtually unaltered in the absence of $\Delta\psi$. However, regarding the low abundance of this fragment, the physiological relevance of a proposed alternative processing reaction is debatable.

In all experiments analyzing Pink1 accumulation in cultured cells discussed so far, only the 64 kDa Pink1-FL was detectable by Western blot analysis, which is consistent with rapid proteasomal degradation of the 53 kDa Pink1-PF species (Lin & Kang, 2008). The previously described increase in endogenous Pink1-PF upon exposure of cells to the proteasome inhibitor MG132 was reproducible in my experiments. The highly sensitive radioactive *in vitro* import assay allowed following the fate of newly processed Pink1 under steady-state conditions. First, the processed Pink1 fragment displayed a weaker membrane association compared to the full-length species, which may result from PARL-mediated cleavage within the hydrophobic N-terminal domain (Deas et al., 2010a). Secondly, I was able to show that a fraction of Pink1-PF is released from mitochondria in the presence of $\Delta\psi$. Re-translocation of the processed Pink1 to the cytosol is a prerequisite for a postulated model, in which Pink1-PF associates with Parkin to prevent its translocation to mitochondria and induction of mitophagy under steady-state conditions (Fedorowicz et al., 2014). In proposing a distinct function for Pink1-PF, this model contradicts the previous notion, that Pink1-FL is the single functional Pink1 species and that cleavage represents degradation rather than processing (Greene et al., 2012, Jin et al., 2010, Matsuda et al., 2010, Narendra et al., 2010b).

6.5 Pink1 turnover rates are independent of the mitochondrial membrane potential

Although protein turnover reactions were proposed to maintain low levels of Pink1 under steady-state conditions (Pickrell & Youle, 2015), the subcellular degradation site and the responsible proteases have not been conclusively identified so far. While the proteasome was shown to degrade the processed Pink1 (Lin & Kang, 2008, Yamano & Youle, 2013), a conflicting study suggested the matrix-resident mitochondrial protease Lon to mediate Pink1 turnover (Thomas et al., 2014). Moreover, a diverse set of endogenous mitochondrial proteases, namely MPP, PARL, ClpXP and the mitochondrial AAA protease have been shown to affect Pink1 stability. The proposed fast degradation was correlated with a Δψ-dependent import of Pink1 (Jin et al., 2010). As discussed above, Pink1 import was not unambiguously dependent on the presence of a Δψ in my experiments. Moreover, by directly assessing Pink1 degradation, I observed only moderate turnover rates under normal conditions, both on cellular and on mitochondrial levels. Remarkably, the degradation rates of Pink1 were not affected by the presence or absence of a Δψ. Using a similar experimental approach to measure cellular turnover of Pink, Lin et al. observed a stabilizing effect of Δψ-depletion on Pink1-FL (Lin & Kang, 2008). However, reasoning that not Pink1-FL but Pink1-PF is the major target of degradation (Yamano & Youle, 2013), their finding reflects a decreased processing efficiency under Δψ-depletion conditions, rather than an effect on degradation as such. As to my mitochondrial degradation assay, the failure of ATP-depletion to affect mitochondrial degradation of Pink virtually precludes an involvement of the collectively ATP-dependent mitochondrial proteases (Voos, 2013). This observation is in line with published results showing that both full-length and processed Pink1 accumulate at the outer face of the OMM independent of the Δψ (Becker et al., 2012a, Zhou et al., 2008) as this localization precludes degradation by mitochondrial proteases.

6.6 Pink1 levels are regulated by a transcriptional mechanism

In the experiments shown here, I observed a rather slow increase in Pink1 protein levels in response to mitochondrial perturbations, as Pink1 became detectable only after 4 h of CCCP treatment in cultured cells. This delayed accumulation was likely not due to the pharmacokinetics of CCCP, as an almost complete dissipation of Δψ occurs already after

15 min of exposing cells to the protonophore (data not shown). The observed time course of Pink1 accumulation is consistent with published results obtained under comparable experimental conditions and analyzing total cellular levels of endogenous Pink1 (Gomez-Sanchez et al., 2014). An accumulation of Pink1 already after 0.5 h was reported elsewhere, but based either on immunofluorescence analysis of ectopically expressed Pink1 or immunodetection of endogenous Pink1 in carbonate extracts of isolated mitochondria (Narendra et al., 2010b). An accumulation of Pink1 in the course of hours is consistent with a transcriptional induction mechanism. In my thesis, I directly confirmed a transcriptional regulation of Pink1 levels. First, inhibitors of transcription or translation completely blocked damage-related mitochondrial accumulation of the protein and secondly Pink1 mRNA levels were elevated after induction of mitochondrial stress conditions. The increase in Pink1 biosynthesis together with its intrinsic targeting properties to the OMM is sufficient to explain the observed accumulation at damaged mitochondria. A complete block of Pink1 accumulation by translational inhibitors after depletion of $\Delta\psi$ was already observed in previous experiments (Narendra et al., 2010b) but not considered important for the downstream mitophagy pathway, due to the apparent absence of an increase in Pink1 mRNA levels. Several other groups reported an involvement of transcriptional induction in the context of a protective function of Pink1 (Duan et al., 2014, Gomez-Sanchez et al., 2014, Priyadarshini, Orosco et al., 2013). An increase in Pink1 expression after cellular insults that were not specific to mitochondria but lead to general autophagy processes, in particular starvation and growth factor deprivation by serum removal (Klinkenberg, Gispert et al., 2012, Mei, Zhang et al., 2009, Uittenbogaard, Baxter et al., 2010) or ischemia/perfusion injury (Sakurai, Kawamura et al., 2009, Sengupta, Molkentin et al., 2011) was also described. Similarly, expression of Parkin as the immediate downstream partner of Pink1 was proposed to be under transcriptional control (Klinkenberg et al., 2012). These observations indicate that Pink1, together with Parkin, may also be involved in integrating mitophagy and cellular autophagy.

In my experiments shown here, treatment of cells with chemicals that induce oxidative stress did not result in elevated protein levels of Pink1. This observation apparently contradicts the reported finding that diverse oxidative stress inducing compounds lead to elevated Pink1 mRNA levels (Murata, Takamatsu et al., 2015). However the increase in

Pink1 transcription described by Murata et al. occurred over the course of days, as opposed to the relatively fast induction of Pink1 in response to OXPHOS inhibitors I observed here. A long-term damage of mitochondria by oxidative stress may provoke cell-protective autophagy reactions that may involve also Pink1 (Wang, Nartiss et al., 2012) but are putatively distinct from the short-term transcriptional response observed here.

Previous reports also indicated a connection between ER stress and mitophagy reactions (Fouillet, Levet et al., 2012, Zhang, Yuan et al., 2014) by a mechanism potentially involving Parkin. In my hands, induction of unfolded protein stress in the ER by tunicamycin did not lead to an induction of Pink1 expression. This observation indicates, that induction of Pink1 expression represents a very specific reaction to mitochondrial damage.

The observed transcriptional up-regulation of Pink1 expression in response to mitochondrial damage raises questions regarding a putative mito-nuclear signaling pathway and a candidate transcription factor. A study published in the course of this work, indicated an effect of calcium ions on Pink1 transcription (Gomez-Sanchez et al., 2014). However, exposure of cells to thapsigargin, which reportedly increases intracellular Ca^{2+}-levels (Thastrup et al., 1990), did not have any effect on Pink1 protein levels in my hands. Supposing that cytosolic calcium levels were indeed increased under the experimental conditions, this observation argues against the involvement of a calcium-responsive factor. Further experiments shown in the present thesis point towards an involvement of the NF-kB signaling pathway in Pink1 transcriptional regulation, which is in line with a recent report showing that the Pink1 promoter is under control of the transcription factor NF-kB (Duan et al., 2014). Intriguingly, calcium may come back in the focus here, as the Ca^{2+}- and calmodulin-dependent phosphatase calcineurin was proposed to promote NF-kB-signaling through dephosphorylation and inactivation of the endogenous NF-kB inhibitor I-kBβ (Biswas, Anandatheerthavarada et al., 2003). Notably, the diminished Pink1 induction I observed in the presence of NF-kB inhibitors may also represent an indirect effect. As was previously reported, the inhibitor of another IkB isoform, I-kBa, directly affects the integrity of the OMM to counteract the induction of apoptosis (Pazarentzos, Mahul-Mellier et al., 2014). Inhibitors that affect IkB activity, as used here, could potentially stabilize mitochondria and may therefore indirectly reduce Pink1 induction. A

recent publication proposed a novel pathway whereby NF-kB positively regulates transcription of the autophagy adaptor p62 to mediate Parkin-dependent mitophagy in macrophages as part of an inflammatory response (Zhong, Umemura et al., 2016). Although the events upstream of Parkin in this pathway may be distinct from damage-related mitophagy, it points towards a connection between NF-kB activity and mitophagy in a broader context.

6.7 Revised model of Pink1/Parkin-mediated mitophagy

The damage-induced transcriptional up-regulation of Pink, which I have demonstrated here calls for a revised model of Pink1/Parkin-mediated mitophagy (Figure 35). In this model, mitochondrial perturbations are signaled to the nuclear transcription machinery, where the expression of the *PINK1* gene is activated. This proposed mito-nuclear signaling pathway putatively involves NF-kB. Upon translation at cytosolic ribosomes, the newly synthesized Pink1 protein associates with the outer mitochondrial membrane through its N-terminal mitochondrial targeting signal. Accumulation of Pink1 results in the recruitment and activation of Parkin, which in turn, initiates the downstream mitophagy pathway. The processes leading from the initial pathologic insult to accumulation of Pink1 may require several hours. As opposed to its previously postulated function in sensing mitochondrial damage by assessing $\Delta\psi$, Pink1 represents a downstream mediator in the removal of generally damaged mitochondria by mitophagy.

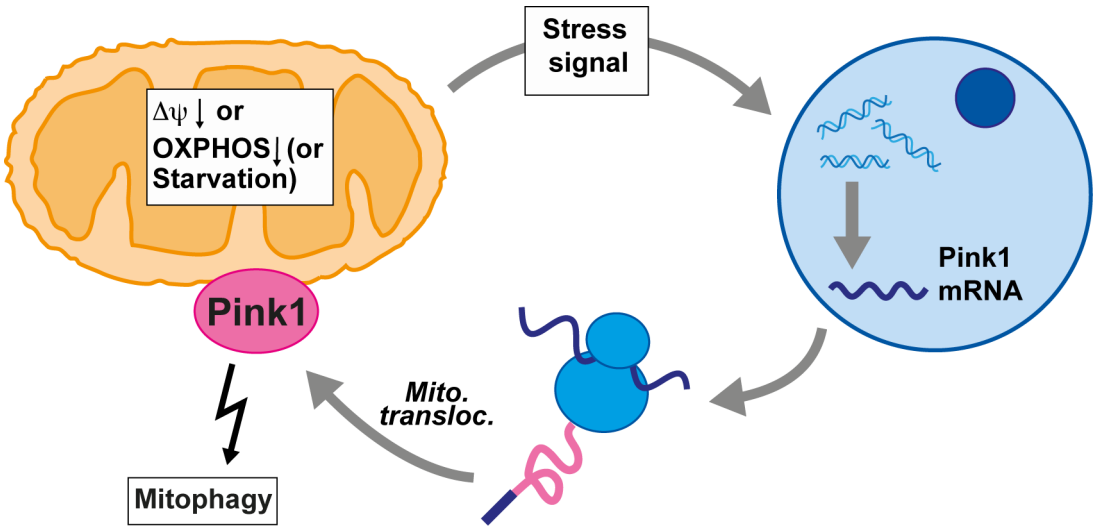

Figure 35: Proposed model for transcriptional regulation of Pink1 protein levels.
Different mitochondrial stress conditions generate as yet unknown mitochondria to nucleus signal, which induces transcription of Pink1. After translation at cytosolic ribosomes, the newly synthesized Pink1 proteins translocate to the outer mitochondrial membrane where they initiate the downstream mitophagy pathway.

Several signaling pathways have been identified that involve a communication between mitochondria and the gene expression machinery in the nucleus. In general, these signaling mechanisms allow adjusting the mitochondrial protein content and accordingly, organellar activity to different internal or external stress situations. In this context, mitochondria and nucleus communicate through a complex network of anterograde (nucleus to mitochondria) and retrograde (mitochondria to nucleus) signaling mechanisms (Quiros, Mottis et al., 2016). The proposed Pink1/Parkin signaling might represent a mammalian variant of a mitochondria-specific stress-signaling pathway. The best-studied example so far is the mitochondrial unfolded protein response (mtUPR) in *C. elegans*. This protective transcriptional response is triggered by mitochondrial proteotoxic stress and promotes the expression of mitochondrial PQC genes (Haynes, Fiorese et al., 2013). The transcriptional mechanism underlying the mtUPR is coordinated by the transcription factor ATFS-1 (activating transcription factor associated with stress 1), which is imported into mitochondria under normal conditions but translocates to the nucleus upon mitochondrial protein stress (Haynes et al., 2013). Similarly, severe mitochondrial damage would be signaled to the nucleus, by a yet unidentified factor and promote Pink1 expression.

6.8 Association of wild-type and mutant α-synuclein with mitochondria

To date, a decline in mitochondrial function is widely recognized as a feature of Parkinson's disease. A pivotal question remains, if mitochondrial damage causes PD or rather occurs as a consequence of other pathological processes. Mutations in the genes encoding Pink1 and Parkin, respectively that cause hereditary PD clearly support a "mitochondrial hypothesis". Considering that the initiation of mitophagy is the foremost function of these two proteins, a genetic defect in the Pink1/Parkin system would result in the accumulation of dysfunctional mitochondria as an early event in the etiology of the disease. By contrast, other PD-related factors may exert mitochondrial damage as part of a broader cellular toxicity and among them is α -synuclein. The aggregation-prone cytosolic protein is thought to form toxic oligomers (Haass & Selkoe, 2007). In its aggregated form, α -synuclein is the major constituent of intra-neuronal Lewy-body inclusions, which are the pathological hallmark of PD (Goedert, 2001). Mutations affecting the α-synuclein amino acid sequence as well as gene multiplications have been implicated in PD (Benskey, Perez et al., 2016). Several groups have reported the presence of α -synuclein at or in mitochondria (Cole, Dieuliis et al., 2008, Devi et al., 2008, Li et al., 2007, Parihar, Parihar et al., 2008, Shavali, Brown-Borg et al., 2008). However, these reports were largely controversial regarding the suborganellar localization of α-synuclein. A proposed interaction of α-synuclein with mitochondria is consistent with data showing mitochondrial abnormalities upon overexpression of wild-type or mutant α -synuclein both *in vivo and in vitro*. The reported defects include inhibition of respiratory chain complexes (Subramaniam, Vergnes et al., 2014) and mitochondrial fragmentation (Plotegher, Gratton et al., 2014).

In my thesis, I directly assessed a putative interaction of α -synuclein with mitochondria using an *in vitro* import assay with isolated intact mitochondria. In this experiment, α-synuclein did not behave like a canonical mitochondrial imported protein. First, both wild-type α-synuclein as well as the two PD-related mutants A30P and A53T readily associated with mitochondria but the amount of mitochondria-bound α-synuclein did not increase over time. Secondly, α-synuclein remained largely accessible to protease treatment in the presence of mitochondria. Thirdly, the association of α-synuclein with

mitochondria occurred independent of cytosol-exposed TOM receptors but was dependent on the presence of an inner membrane potential.

The kinetics of α-synuclein binding to mitochondria together with the observation that the protein did not acquire protease resistance indicate, that it was likely not imported into the mitochondrial matrix compartment or inserted into the IMM but rather peripherally bound to the outer mitochondrial membrane. Unlike the initial association of most mitochondrial preproteins with the OMM, this binding was independent of cytosol-exposed TOM receptors, which further argues against canonical import of α-synuclein. The observed association of α-synuclein with the OMM may reflect the general property of the protein to bind lipid membranes (Kim, Laurine et al., 2006). In this regard, I observed a more efficient binding of α-synuclein$_{A53T}$, whereas less a-synuclein$_{A30P}$ associated with mitochondria compared to the wild-type protein. Both observations correlate well with previously reported characteristics of the two mutant forms of α-synuclein. While the A53T mutation has been demonstrated to enhance the membrane interacting properties of α -synuclein, the A30P mutation was shown to result in reduced affinity for phospholipids (Auluck, Caraveo et al., 2010). A general tendency of α-synuclein to bind lipids raises questions concerning the specificity of its association with mitochondria. In experiments using artificial membrane vesicles, α-synuclein was previously demonstrated to bind acidic lipids, including the mitochondria-specific lipid cardiolipin with a high affinity (Nakamura, Nemani et al., 2008). Although cardiolipin is enriched in the IMM, it is also found in the OMM (Hovius, Thijssen et al., 1993). Thus, the observed binding of α-synuclein to the OMM possibly represents an interaction with cardiolipin.

In my import assay I found that the association of α -synuclein with mitochondria was diminished in the absence of Δψ. While this observation is in line with a previously reported result (Devi et al., 2008), another study came to the contradictive conclusion that α-synuclein binding to mitochondria does not depend on the energetic state of the organelle (Nakamura et al., 2008). Notably, the initial association of authentic mitochondrial preproteins with import receptors of the OMM and the insertion into the TOM channel occurs independent of the membrane potential. The only Δψ-dependent step in the canonical presequence import pathway is the translocation of the preprotein over- or its insertion into the IMM, respectively (Becker et al., 2012b). However, the α-synuclein

sequence lacks a mitochondrial targeting signal (Guardia-Laguarta et al., 2014) and my results strongly suggest that the protein was not imported into any internal mitochondrial subcompartment. Thus, dependency on Δψ was not indicative of import into the matrix compartment or IMM here, but rather reflected a characteristic of the interaction between α-synuclein and the OMM. One plausible explanation for an effect of Δψ would be an altered lipid composition of the OMM upon mitochondrial depolarization. Similarly, exposure of cardiolipin in response to cytosolic acidification has been proposed to facilitate α-synuclein binding to the OMM (Cole et al., 2008).

Further elucidating the observation that α -synuclein did not behave like a canonical mitochondrial-targeted protein in my import assay, Guardia-Laguarta et al. proposed an alternative model for α -synuclein interaction with mitochondria (Guardia-Laguarta et al., 2014). In fractionation assays with total cellular extracts, wild-type and mutant forms of the protein were shown to localize not to mitochondria but rather to so-called mitochondria-associated ER membranes (MAM). These structurally and functionally distinct ER subdomains were previously proposed to facilitate the cooperation between ER and mitochondria in various joint processes, including Ca^{2+} homeostasis, phospholipid biosynthesis and intracellular trafficking (Paillusson et al., 2016). Guardia-Laguarta et al. further showed that the pathogenic mutations A30T and A53P reduced α-synuclein localization to MAM. Diminished amounts of α-synuclein in MAM coincided with an increased spatial distance between ER and mitochondria and mitochondrial fragmentation (Guardia-Laguarta et al., 2014). While the details still need to be worked out, the proposed interaction of α-synuclein with MAM may provide a mechanism whereby α-synuclein affects mitochondrial function in PD. The described interaction of α-synuclein with MAM would explain the apparent association with mitochondria I observed in the *in vitro* import assay, provided that the crude mitochondrial fractions used for this experiment contained mitochondria-associated ER membranes. It will further be interesting, to revisit the effect of Δψ on α-synuclein binding observed in my import assay in the light of the proposed association of the protein with MAM. One possibility is that mitochondrial depolarization destabilizes the mitochondria-ER contacts, which would result in reduced binding sites for α-synuclein.

In light of the Pink1 experiments shown here, α-synuclein is of particular interest as it represents a potential mediator of mitochondrial damage with a direct relevance for PD. Considering the implication of both α-synuclein and the Pink1/Parkin system in PD, a possible connection between them is scarcely described so far. In *Drosophila* models, Pink1 and Parkin can rescue the mitochondrial fragmentation phenotype induced by overexpression of α-synuclein (Kamp 2010). It remains to be clarified, if vise versa, elevated levels of α-synuclein elicit Pink1 accumulation and mitophagy.

In conclusion, genetic and biochemical findings on the Pink1/Parkin system, α-synuclein and other genetic risk factors have impressively advanced PD research over the last years. Yet, a lot of work remains to be done. My own results may exemplify this complexity on the small scale. While the proposed transcriptional regulation of Pink1 may help reconsidering the events leading to the initiation of mitophagy, the underlying signaling mechanism still awaits identification. It should be kept in mind that our present knowledge on the pathology of PD stems from studying the small percentage of hereditary cases. Thus, a major leap in PD research will require translating the gathered information to sporadic forms of the disease. In parts, this transition has already started as illustrated by a recent paper examining the mechanism whereby a single nucleotide polymorphism (SNP) within the α-synuclein-encoding gene *SNCA* increases the risk of developing sporadic PD (Soldner, Stelzer et al., 2016). The authors propose that a certain sequence variant reduces the binding of inhibitory transcription factors, which results in elevated *SNCA* expression. Intriguingly the described gene variant has a much higher prevalence compared to rare point mutations in *SNCA*. From the mitochondrial point of view, a major question remains how, α-synuclein-mediated toxicity, age-related mitochondrial dysfunction and organellar quality control collectively contribute to the pathology of PD.

7 Abstract

Mitochondrial dysfunction is a common feature of many neurodegenerative diseases, in particular Parkinson's disease (PD). Mutations in the genes encoding the mitochondrial kinase Pink1 and the cytosolic E3 ubiquitin ligase Parkin have been associated with familial cases of PD. In healthy cells, the Pink1/Parkin system functions as sensor of mitochondrial damage in an organellar quality control system. High levels of Pink1 accumulate at the surface of damaged mitochondria to recruit and activate Parkin. In turn, Parkin initiates a signaling reaction eventually resulting in the autophagic removal of the organelle, a process termed mitophagy.

In my thesis, I analyzed mitochondrial and cellular stress conditions, resulting in an increase in Pink1 protein levels. I was able to demonstrate that the accumulation of Pink1 was not strictly correlated with a depolarization of the mitochondrial inner membrane potential ($\Delta\psi$) or with changes in mitochondrial ATP levels. Both cellular and mitochondrial protein turnover rates were also not affected by changes in the mitochondrial membrane potential. In contrast, inhibition of cellular transcription or translation reactions completely blocked Pink1 accumulation. Characterization of mRNA levels indicated that the increase of Pink1 amounts after acute mitochondrial perturbations was based on a transcriptional induction reaction. My results demonstrate that the mitochondrial quality control process mediated by the Pink1-Parkin system is based on a transcriptional response triggered independently of reductions in Dy. This yet unknown signaling pathway may involve the transcriptional regulator NFκB. Another factor prominently involved in PD is the aggregation-prone cytosolic protein α-synuclein, which is the major constituent of Lewy body inclusions. Although α-synuclein has previously been proposed to exert mitochondrial damage and localize to mitochondria, its submitochondrial localization remained controversial. In my thesis, I was able to demonstrate that α-synuclein is not imported into mitochondria but apparently associates with the outer mitochondrial membrane in a $\Delta\psi$-dependent manner.

8 Abbreviations

^{35}S	Sulfur isotope with mass number 35
AA	Antimycin A
AD	Autosomal dominant
AR	Autosomal recessive
ATP	Adenosine triphosphate
BN	Blue native
BSA	Bovine serum albumin
C-terminus	Carboxy-terminus
CCCP	Carbonyl cyanide *m*-chlorophenyl hydrazone
Chx	Cycloheximide
CMV	Cytomegalovirus
COX	Cytochrome c oxidase
DHFR	Dihydrofolate reductase
DMSO	Dimethyl sulfoxide
DNA	Deoxy-ribonucleid acid
EDTA	Ethylenediaminetetraacetic acid
ER	Endoplasmatic reticulum
EtOH	Ethanol
FCS	Fetal calf serum
FL	Full-length
FLAG	Octapeptide protein tag
g	Gravity
GAPDH	Glyceraldehyde-3-phosphate dehydrogenase
GFP	Green fluorescent protein
Hsp	Heat shock protein
IgG	Immunoglobulin G
IKK	IkB kinase
IMM	Inner mitochondrial membrane
IMS	Intramembrane space
IkB	Inhibitor of NF-kB
kd	Knock-down

kDa	Kilodalton
Lys	Lysine
MAM	Mitochondria-associated ER membranes
Mdh2	Malate dehydrogenase
MEF	Mouse embryonic fibroblasts
Mfn	Mitofusin
min	Minute
mM	Millimolar
MPP	Matrix processing peptidase
M_r	Relative molecular mass
mRNA	Messenger RNA
N-terminus	Amino-terminus
NF-kB	Nuclear factor kappa-light-chain-enhancer of activated B-cells
nm	Nanometer
nM	Nanomolar
Oligo	Oligomycin
OMM	Outer mitochondrial membrane
OXPHOS	Oxidative phosphorylation
PAGE	Polyacrylamide gel electrophoresis
PD	Parkinson’s disease
PF	Processed form
Pink1	PTEN-induced putative kinase 1
PK	Proteinase K
PQC	Protein quality control
PTEN	Phosphatase and tensin homolog
qRT-PCR	Quantitative real-time polymerase chain reaction
RING	Really interesting new gene domain
RNA	Ribonucleic acid
SDH	Succinate dehydrogenase
SDS	Sodium dodecyl sulfate
SEM	Standard error of the mean
siRNA	small interfering RNA
SU9	Subunit 9 of mitochondrial ATPase

TCA	Trichloroacetic acid
TIM	Translocase of the inner (mitochondrial) membrane
TMRE	Tetramethylrhodamine ethyl ester
TOM	Translocase of the outer (mitochondrial) membrane
Ub	Ubiquitin
WT	Wild-type
α-Tom40	Antibody directed against Tom40
Δψ	Mitochondrial membrane potential
µM	Micromolar

9 Appendix

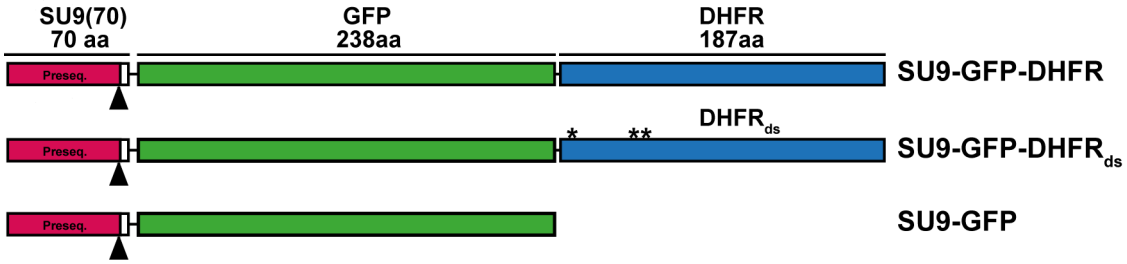

Figure 36: Schematic illustration of DHFR fusion proteins and the SU9-GFP control construct. The first 70 aa of *N.crassa* ATPase subunit 9 (SU9(70)) are fused to green fluorescent protein (GFP) alone or GFP followed by the full mouse dihydrofolate reductase (DHFR). Asterisks indicate the three point mutations in the destabilized DHFR ($DHFR_{ds}$) C7S, S42C, N49C, respectively. The cleavage site for the mitochondrial processing peptidase (MPP) within the SU9 sequence is indicated.

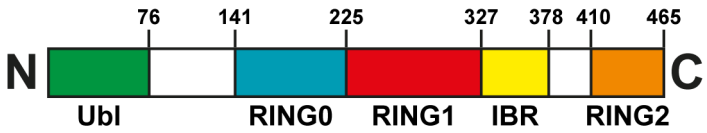

Figure 37: Schematic illustration of the Parkin domain structure. The N-terminal ubiquitin-like (Ubl) domain is followed by RING0 and a RING1 In-between RING2 (RBR) motif. IBR: In between RING. RING: Really interesting new gene domain.

10 References

Andersen JL, Kornbluth S (2013) The tangled circuitry of metabolism and apoptosis. Mol Cell 49: 399-410

Anderson S, Bankier AT, Barrell BG, de Bruijn MH, Coulson AR, Drouin J, Eperon IC, Nierlich DP, Roe BA, Sanger F, Schreier PH, Smith AJ, Staden R, Young IG (1981) Sequence and organization of the human mitochondrial genome. Nature 290: 457-65

Ashrafi G, Schwarz TL (2013) The pathways of mitophagy for quality control and clearance of mitochondria. Cell Death Diff 20: 31-42

Auluck PK, Caraveo G, Lindquist S (2010) alpha-Synuclein: membrane interactions and toxicity in Parkinson's disease. Annual review of cell and developmental biology 26: 211-33

Becker D, Richter J, Tocilescu MA, Przedborski S, Voos W (2012a) Pink1 kinase and its membrane potential (Deltapsi)-dependent cleavage product both localize to outer mitochondrial membrane by unique targeting mode. J Biol Chem 287: 22969-22987

Becker T, Böttinger L, Pfanner N (2012b) Mitochondrial protein import: from transport pathways to an integrated network. Trends Biochem Sci 37: 85-91

Behnke J, Feige MJ, Hendershot LM (2015) BiP and its nucleotide exchange factors Grp170 and Sil1: mechanisms of action and biological functions. J Mol Biol 427: 1589-1608

Beilina A, Van Der Brug M, Ahmad R, Kesavapany S, Miller DW, Petsko GA, Cookson MR (2005) Mutations in PTEN-induced putative kinase 1 associated with recessive parkinsonism have differential effects on protein stability. Proc Natl Acad Sci U S A 102: 5703-8

Bender A, Krishnan KJ, Morris CM, Taylor GA, Reeve AK, Perry RH, Jaros E, Hersheson JS, Betts J, Klopstock T, Taylor RW, Turnbull DM (2006) High levels of mitochondrial DNA deletions in substantia nigra neurons in aging and Parkinson disease. Nat Genet 38: 515-7

Benskey MJ, Perez RG, Manfredsson FP (2016) The contribution of alpha synuclein to neuronal survival and function - Implications for Parkinson's disease. J Neurochem 137: 331-59

Berry C, La Vecchia C, Nicotera P (2010) Paraquat and Parkinson's disease. Cell Death Differ 17: 1115-25

Betarbet R, Sherer TB, MacKenzie G, Garcia-Osuna M, Panov AV, Greenamyre JT (2000) Chronic systemic pesticide exposure reproduces features of Parkinson's disease. Nat Neurosci 3: 1301-1306

Biswas G, Anandatheerthavarada HK, Zaidi M, Avadhani NG (2003) Mitochondria to nucleus stress signaling: a distinctive mechanism of NFkappaB/Rel activation through calcineurin-mediated inactivation of IkappaBbeta. J Cell Biol 161: 507-519

Burbulla LF, Fitzgerald JC, Stegen K, Westermeier J, Thost AK, Kato H, Mokranjac D, Sauerwald J, Martins LM, Woitalla D, Rapaport D, Riess O, Proikas-Cezanne T, Rasse TM, Krüger R (2014) Mitochondrial proteolytic stress induced by loss of mortalin function is rescued by Parkin and PINK1. Cell Death Dis 5

Canet-Aviles RM, Wilson MA, Miller DW, Ahmad R, McLendon C, Bandyopadhyay S, Baptista MJ, Ringe D, Petsko GA, Cookson MR (2004) The Parkinson's disease protein DJ-1 is neuroprotective due to cysteine-sulfinic acid-driven mitochondrial localization. Proc Natl Acad Sci U S A 101: 9103-8

Chan NC, Salazar AM, Pham AH, Sweredoski MJ, Kolawa NJ, Graham RL, Hess S, Chan DC (2011) Broad activation of the ubiquitin-proteasome system by Parkin is critical for mitophagy. Hum Mol Genet 20: 1726-1737

Chen Y, Dorn GW, 2nd (2013) PINK1-phosphorylated mitofusin 2 is a Parkin receptor for culling damaged mitochondria. Science 340: 471-475

Ciechanover A (2005) Proteolysis: from the lysosome to ubiquitin and the proteasome. Nature reviews Molecular cell biology 6: 79-87

Cipolat S, Rudka T, Hartmann D, Costa V, Serneels L, Craessaerts K, Metzger K, Frezza C, Annaert W, D'Adamio L, Derks C, Dejaegere T, Pellegrini L, D'Hooge R, Scorrano L, De Strooper B (2006) Mitochondrial rhomboid PARL regulates cytochrome c release during apoptosis via OPA1-dependent cristae remodeling. Cell 126: 163-75

Clague MJ, Urbe S (2010) Ubiquitin: same molecule, different degradation pathways. Cell 143: 682-5

Clark IE, Dodson MW, Jiang C, Cao JH, Huh JR, Seol JH, Yoo SJ, Hay BA, Guo M (2006) Drosophila pink1 is required for mitochondrial function and interacts genetically with parkin. Nature 441: 1162-6

Cole NB, Dieuliis D, Leo P, Mitchell DC, Nussbaum RL (2008) Mitochondrial translocation of alpha-synuclein is promoted by intracellular acidification. Exp Cell Res 314: 2076-89

Costa AC, Loh SH, Martins LM (2013) Drosophila Trap1 protects against mitochondrial dysfunction in a PINK1/parkin model of Parkinson's disease. Cell Death Dis 4: e467

De Coo IF, Renier WO, Ruitenbeek W, Ter Laak HJ, Bakker M, Schagger H, Van Oost BA, Smeets HJ (1999) A 4-base pair deletion in the mitochondrial cytochrome b gene associated with parkinsonism/MELAS overlap syndrome. Ann Neurol 45: 130-3

de Lau LM, Breteler MM (2006) Epidemiology of Parkinson's disease. Lancet Neurol 5: 525-35

de Vries RL, Przedborski S (2012) Mitophagy and Parkinson's disease: be eaten to stay healthy. Mol Cell Neurosci 55: 37-43

Deas E, Plun-Favreau H, Gandhi S, Desmond H, Kjaer S, Loh SH, Renton AE, Harvey RJ, Whitworth AJ, Martins LM, Abramov AY, Wood NW (2010a) PINK1 cleavage at position A103 by the mitochondrial protease PARL. Hum Mol Genet 20: 867-879

Deas E, Wood NW, Plun-Favreau H (2010b) Mitophagy and Parkinson's disease: the PINK1-parkin link. Biochim Biophys Acta 1813: 623-633

Der-Sarkissian A, Jao CC, Chen J, Langen R (2003) Structural organization of alpha-synuclein fibrils studied by site-directed spin labeling. J Biol Chem 278: 37530-5

Devi L, Raghavendran V, Prabhu BM, Avadhani NG, Anandatheerthavarada HK (2008) Mitochondrial import and accumulation of alpha-synuclein impair complex I in human dopaminergic

neuronal cultures and Parkinson disease brain. J Biol Chem 283: 9089-100

Duan X, Tong J, Xu Q, Wu Y, Cai F, Li T, Song W (2014) Upregulation of human PINK1 gene expression by NF-kB signalling. Mol Brain 7: 57-67

Eiyama A, Okamoto K (2015) PINK1/Parkin-mediated mitophagy in mammalian cells. Curr Opin Cell Biol 33C: 95-101

Fedorowicz MA, de Vries-Schneider RLA, Rub C, Becker D, Huang Y, Zhou C, Wolken DMA, Voos W, Liu YH, Przedborski S (2014) Cytosolic cleaved PINK1 represses Parkin translocation to mitochondria and mitophagy. EMBO Rep 15: 86-93

Fouillet A, Levet C, Virgone A, Robin M, Dourlen P, Rieusset J, Belaidi E, Ovize M, Touret M, Nataf S, Mollereau B (2012) ER stress inhibits neuronal death by promoting autophagy. Autophagy 8: 915-926

Gegg ME, Cooper JM, Chau KY, Rojo M, Schapira AH, Taanman JW (2010) Mitofusin 1 and mitofusin 2 are ubiquitinated in a PINK1/parkin-dependent manner upon induction of mitophagy. Hum Mol Genet 19: 4861-4870

Geisler S, Holmstrom KM, Skujat D, Fiesel FC, Rothfuss OC, Kahle PJ, Springer W (2010a) PINK1/Parkin-mediated mitophagy is dependent on VDAC1 and p62/SQSTM1. Nat Cell Biol 12: 119-131

Geisler S, Holmstrom KM, Treis A, Skujat D, Weber SS, Fiesel FC, Kahle PJ, Springer W (2010b) The PINK1/Parkin-mediated mitophagy is compromised by PD-associated mutations. Autophagy 6: 871-878

Goedert M (2001) Alpha-synuclein and neurodegenerative diseases. Nat Rev Neurosci 2: 492-501

Gomez-Sanchez R, Gegg ME, Bravo-San Pedro JM, Niso-Santano M, Alvarez-Erviti L, Pizarro-Estrella E, Gutierrez-Martin Y, Alvarez-Barrientos A, Fuentes JM, Gonzalez-Polo RA, Schapira AHV (2014) Mitochondrial impairment increases FL-PINK1 levels by calcium-dependent gene expression. Neurobiol Dis 62: 426-440

Greene AW, Grenier K, Aguileta MA, Muise S, Farazifard R, Haque ME, McBride HM, Park DS, Fon EA (2012) Mitochondrial processing peptidase regulates PINK1 processing, import and Parkin recruitment. EMBO Rep 13: 378-385

Grenier K, McLelland GL, Fon EA (2013) Parkin- and PINK1-Dependent Mitophagy in Neurons: Will the Real Pathway Please Stand Up? Front Neurol 4: 100

Guardia-Laguarta C, Area-Gomez E, Rub C, Liu Y, Magrane J, Becker D, Voos W, Schon EA, Przedborski S (2014) alpha-Synuclein is localized to mitochondria-associated ER membranes. J Neurosci 34: 249-59

Haass C, Selkoe DJ (2007) Soluble protein oligomers in neurodegeneration: lessons from the Alzheimer's amyloid beta-peptide. Nature reviews Molecular cell biology 8: 101-12

Halliwell B (2006) Oxidative stress and neurodegeneration: where are we now? J Neurochem 97: 1634-58

Hallmann K, Kudin AP, Zsurka G, Kornblum C, Reimann J, Stuve B, Waltz S, Hattingen E, Thiele H, Nurnberg P, Rub C, Voos W, Kopatz J, Neumann H, Kunz WS (2016) Loss of the smallest subunit of cytochrome c oxidase,

COX8A, causes Leigh-like syndrome and epilepsy. Brain 139: 338-45

Hampe C, Ardila-Osorio H, Fournier M, Brice A, Corti O (2006) Biochemical analysis of Parkinson's disease-causing variants of Parkin, an E3 ubiquitin-protein ligase with monoubiquitylation capacity. Hum Mol Genet 15: 2059-75

Hao LY, Giasson BI, Bonini NM (2010) DJ-1 is critical for mitochondrial function and rescues PINK1 loss of function. Proc Natl Acad Sci U S A 107: 9747-52

Haynes CM, Fiorese CJ, Lin YF (2013) Evaluating and responding to mitochondrial dysfunction: the mitochondrial unfolded-protein response and beyond. Trends Cell Biol 23: 311-8

Hovius R, Thijssen J, van der Linden P, Nicolay K, de Kruijff B (1993) Phospholipid asymmetry of the outer membrane of rat liver mitochondria. Evidence for the presence of cardiolipin on the outside of the outer membrane. FEBS letters 330: 71-6

Javitch JA, Snyder SH (1984) Uptake of MPP(+) by dopamine neurons explains selectivity of parkinsonism-inducing neurotoxin, MPTP. Eur J Pharmacol 106: 455-6

Jin SM, Lazarou M, Wang C, Kane LA, Narendra DP, Youle RJ (2010) Mitochondrial membrane potential regulates PINK1 import and proteolytic destabilization by PARL. J Cell Biol 191: 933-942

Jin SM, Youle RJ (2013) The accumulation of misfolded proteins in the mitochondrial matrix is sensed by PINK1 to induce PARK2/Parkin-mediated mitophagy of polarized mitochondria. Autophagy 9: 1750-1757

Kane LA, Lazarou M, Fogel AI, Li Y, Yamano K, Sarraf SA, Banerjee S, Youle RJ (2014) PINK1 phosphorylates ubiquitin to activate Parkin E3 ubiquitin ligase activity. J Cell Biol 205: 143-153

Kazlauskaite A, Kondapalli C, Gourlay R, Campbell DG, Ritorto MS, Hofmann K, Alessi DR, Knebel A, Trost M, Muqit MMK (2014) Parkin is activated by PINK1-dependent phosphorylation of ubiquitin at Ser(65). Biochem J 460: 127-139

Kim YS, Laurine E, Woods W, Lee SJ (2006) A novel mechanism of interaction between alpha-synuclein and biological membranes. J Mol Biol 360: 386-97

Kitada T, Asakawa S, Hattori N, Matsumine H, Yamamura Y, Minoshima S, Yokochi M, Mizuno Y, Shimizu N (1998) Mutations in the parkin gene cause autosomal recessive juvenile parkinsonism. Nature 392: 605-8

Klein C, Westenberger A (2012) Genetics of Parkinson's disease. Cold Spring Harb Perspect Med 2: a008888

Klinkenberg M, Gispert S, Dominguez-Bautista JA, Braun I, Auburger G, Jendrach M (2012) Restriction of trophic factors and nutrients induces PARKIN expression. Neurogenetics 13: 9-21

Kondapalli C, Kazlauskaite A, Zhang N, Woodroof HI, Campbell DG, Gourlay R, Burchell L, Walden H, Macartney TJ, Deak M, Knebel A, Alessi DR, Muqit MM (2012) PINK1 is activated by mitochondrial membrane potential depolarization and stimulates Parkin E3 ligase activity by phosphorylating Serine 65. Open Biol 2: 120080

Koyano F, Okatsu K, Kosako H, Tamura Y, Go E, Kimura M, Kimura Y, Tsuchiya H, Yoshihara H, Hirokawa T, Endo T, Fon EA, Trempe JF, Saeki Y, Tanaka K, Matsuda N (2014) Ubiquitin is

phosphorylated by PINK1 to activate parkin. Nature 510: 162-166

Lang AE, Lozano AM (1998a) Parkinson's disease. First of two parts. N Engl J Med 339: 1044-53

Lang AE, Lozano AM (1998b) Parkinson's disease. Second of two parts. N Engl J Med 339: 1130-43

Langston JW, Ballard P, Tetrud JW, Irwin I (1983) Chronic Parkinsonism in humans due to a product of meperidine-analog synthesis. Science 219: 979-80

Lazarou M, Jin SM, Kane LA, Youle RJ (2012) Role of PINK1 binding to the TOM complex and alternate intracellular membranes in recruitment and activation of the E3 ligase Parkin. Dev Cell 22: 320-333

Lazarou M, Sliter DA, Kane LA, Sarraf SA, Wang C, Burman JL, Sideris DP, Fogel AI, Youle RJ (2015) The ubiquitin kinase PINK1 recruits autophagy receptors to induce mitophagy. Nature 524: 309-314

Lee DH, Goldberg AL (1998) Proteasome inhibitors: valuable new tools for cell biologists. Trends Cell Biol 8: 397-403

Li WW, Yang R, Guo JC, Ren HM, Zha XL, Cheng JS, Cai DF (2007) Localization of alpha-synuclein to mitochondria within midbrain of mice. Neuroreport 18: 1543-6

Lin MT, Beal MF (2006) Mitochondrial dysfunction and oxidative stress in neurodegenerative diseases. Nature 443: 787-795

Lin W, Kang UJ (2008) Characterization of PINK1 processing, stability, and subcellular localization. J Neurochem 106: 464-474

Luoma P, Melberg A, Rinne JO, Kaukonen JA, Nupponen NN, Chalmers RM, Oldfors A, Rautakorpi I, Peltonen L, Majamaa K, Somer H, Suomalainen A (2004) Parkinsonism, premature menopause, and mitochondrial DNA polymerase gamma mutations: clinical and molecular genetic study. Lancet 364: 875-82

Lytton J, Westlin M, Hanley MR (1991) Thapsigargin inhibits the sarcoplasmic or endoplasmic reticulum Ca-ATPase family of calcium pumps. J Biol Chem 266: 17067-71

Matsuda N, Sato S, Shiba K, Okatsu K, Saisho K, Gautier CA, Sou YS, Saiki S, Kawajiri S, Sato F, Kimura M, Komatsu M, Hattori N, Tanaka K (2010) PINK1 stabilized by mitochondrial depolarization recruits Parkin to damaged mitochondria and activates latent Parkin for mitophagy. J Cell Biol 189: 211-221

McLelland GL, Soubannier V, Chen CX, McBride HM, Fon EA (2014) Parkin and PINK1 function in a vesicular trafficking pathway regulating mitochondrial quality control. EMBO J 33: 282-295

Mei Y, Zhang Y, Yamamoto K, Xie W, Mak TW, You H (2009) FOXO3a-dependent regulation of Pink1 (Park6) mediates survival signaling in response to cytokine deprivation. Proc Natl Acad Sci USA 106: 5153-5158

Meissner C, Lorenz H, Weihofen A, Selkoe DJ, Lemberg MK (2011) The mitochondrial intramembrane protease PARL cleaves human Pink1 to regulate Pink1 trafficking. J Neurochem 117: 856-867

Murata H, Takamatsu H, Liu S, Kataoka K, Huh NH, Sakaguchi M (2015) NRF2 regulates PINK1 expression under oxidative stress conditions. PLoS ONE 10: e0142438

Nakamura K (2013) alpha-Synuclein and mitochondria: partners in crime? Neurotherapeutics : the journal of the American Society for Experimental NeuroTherapeutics 10: 391-9

Nakamura K, Nemani VM, Wallender EK, Kaehlcke K, Ott M, Edwards RH (2008) Optical reporters for the conformation of alpha-synuclein reveal a specific interaction with mitochondria. J Neurosci 28: 12305-17

Narendra D, Kane LA, Hauser DN, Fearnley IM, Youle RJ (2010a) p62/SQSTM1 is required for Parkin-induced mitochondrial clustering but not mitophagy; VDAC1 is dispensable for both. Autophagy 6: 1090-1106

Narendra D, Tanaka A, Suen DF, Youle RJ (2008) Parkin is recruited selectively to impaired mitochondria and promotes their autophagy. J Cell Biol 183: 795-803

Narendra DP, Jin SM, Tanaka A, Suen DF, Gautier CA, Shen J, Cookson MR, Youle RJ (2010b) PINK1 is selectively stabilized on impaired mitochondria to activate Parkin. PLoS Biol 8: e1000298

Nicklas WJ, Vyas I, Heikkila RE (1985) Inhibition of NADH-linked oxidation in brain mitochondria by 1-methyl-4-phenyl-pyridine, a metabolite of the neurotoxin, 1-methyl-4-phenyl-1,2,5,6-tetrahydropyridine. Life Sci 36: 2503-8

Ordureau A, Sarraf SA, Duda DM, Heo JM, Jedrychowski MP, Sviderskiy VO, Olszewski JL, Koerber JT, Xie T, Beausoleil SA, Wells JA, Gygi SP, Schulman BA, Harper JW (2014) Quantitative proteomics reveal a feedforward mechanism for mitochondrial PARKIN translocation and ubiquitin chain synthesis. Mol Cell 56: 360-75

Orenstein SJ, Kuo SH, Tasset I, Arias E, Koga H, Fernandez-Carasa I, Cortes E, Honig LS, Dauer W, Consiglio A, Raya A, Sulzer D, Cuervo AM (2013) Interplay of LRRK2 with chaperone-mediated autophagy. Nat Neurosci 16: 394-406

Paillusson S, Stoica R, Gomez-Suaga P, Lau DH, Mueller S, Miller T, Miller CC (2016) There's Something Wrong with my MAM; the ER-Mitochondria Axis and Neurodegenerative Diseases. Trends Neurosci 39: 146-57

Parihar MS, Parihar A, Fujita M, Hashimoto M, Ghafourifar P (2008) Mitochondrial association of alpha-synuclein causes oxidative stress. Cellular and molecular life sciences : CMLS 65: 1272-84

Park J, Lee SB, Lee S, Kim Y, Song S, Kim S, Bae E, Kim J, Shong M, Kim JM, Chung J (2006) Mitochondrial dysfunction in Drosophila PINK1 mutants is complemented by parkin. Nature 441: 1157-61

Pazarentzos E, Mahul-Mellier AL, Datler C, Chaisaklert W, Hwang MS, Kroon J, Qize D, Osborne F, Al-Rubaish A, Al-Ali A, Mazarakis ND, Aboagye EO, Grimm S (2014) IκBα inhibits apoptosis at the outer mitochondrial membrane independently of NF-κB retention. EMBO J 33: 2814-2828

Pickrell AM, Youle RJ (2015) The roles of PINK1, parkin, and mitochondrial fidelity in Parkinson's disease. Neuron 85: 257-273

Plotegher N, Gratton E, Bubacco L (2014) Number and Brightness analysis of alpha-synuclein oligomerization and the associated mitochondrial morphology alterations in live cells. Biochimica et biophysica acta 1840: 2014-24

Plun-Favreau H, Klupsch K, Moisoi N, Gandhi S, Kjaer S, Frith D, Harvey K, Deas E, Harvey RJ, McDonald N, Wood

NW, Martins LM, Downward J (2007) The mitochondrial protease HtrA2 is regulated by Parkinson's disease-associated kinase PINK1. Nat Cell Biol 9: 1243-1252

Pridgeon JW, Olzmann JA, Chin L-S, Li L (2007) PINK1 protects against oxidative stress by phosphorylating mitochondrial chaperone TRAP1. PLoS Biol 5: 1494-1503

Priyadarshini M, Orosco LA, Panula PJ (2013) Oxidative stress and regulation of Pink1 in zebrafish (Danio rerio). PLoS ONE 8: e81851

Quiros PM, Mottis A, Auwerx J (2016) Mitonuclear communication in homeostasis and stress. Nature reviews Molecular cell biology 17: 213-26

Ryan BJ, Hoek S, Fon EA, Wade-Martins R (2015) Mitochondrial dysfunction and mitophagy in Parkinson's: from familial to sporadic disease. Trends Biochem Sci 40: 200-210

Sakurai M, Kawamura T, Nishimura H, Suzuki H, Tezuka F, Abe K (2009) Induction of Parkinson disease-related proteins in motor neurons after transient spinal cord ischemia in rabbits. J Cereb Blood Flow Metab 29: 752-758

Sarraf SA, Raman M, Guarani-Pereira V, Sowa ME, Huttlin EL, Gygi SP, Harper JW (2013) Landscape of the PARKIN-dependent ubiquitylome in response to mitochondrial depolarization. Nature 496: 372-6

Schon EA, Przedborski S (2011) Mitochondria: the next (neurode)generation. Neuron 70: 1033-53

Seirafi M, Kozlov G, Gehring K (2015) Parkin structure and function. The FEBS journal 282: 2076-88

Sengupta A, Molkentin JD, Paik JH, DePinho RA, Yutzey KE (2011) FoxO transcription factors promote cardiomyocyte survival upon induction of oxidative stress. J Biol Chem 286: 7468-7478

Shavali S, Brown-Borg HM, Ebadi M, Porter J (2008) Mitochondrial localization of alpha-synuclein protein in alpha-synuclein overexpressing cells. Neurosci Lett 439: 125-8

Shendelman S, Jonason A, Martinat C, Leete T, Abeliovich A (2004) DJ-1 is a redox-dependent molecular chaperone that inhibits alpha-synuclein aggregate formation. PLoS Biol 2: e362

Shiba-Fukushima K, Imai Y, Yoshida S, Ishihama Y, Kanao T, Sato S, Hattori N (2012) PINK1-mediated phosphorylation of the Parkin ubiquitin-like domain primes mitochondrial translocation of Parkin and regulates mitophagy. Sci Rep 2: 1002

Silvestri L, Caputo V, Bellacchio E, Atorino L, Dallapiccola B, Valente EM, Casari G (2005) Mitochondrial import and enzymatic activity of PINK1 mutants associated to recessive parkinsonism. Hum Mol Genet 14: 3477-92

Singer TP, Ramsay RR, McKeown K, Trevor A, Castagnoli NE, Jr. (1988) Mechanism of the neurotoxicity of 1-methyl-4-phenylpyridinium (MPP+), the toxic bioactivation product of 1-methyl-4-phenyl-1,2,3,6-tetrahydropyridine (MPTP). Toxicology 49: 17-23

Soldner F, Stelzer Y, Shivalila CS, Abraham BJ, Latourelle JC, Barrasa MI, Goldmann J, Myers RH, Young RA, Jaenisch R (2016) Parkinson-associated risk variant in distal enhancer of alpha-synuclein modulates target gene expression. Nature 533: 95-9

Soubannier V, McLelland GL, Zunino R, Braschi E, Rippstein P, Fon EA, McBride HM (2012) A vesicular transport pathway shuttles cargo from mitochondria to lysosomes. Curr Biol 22: 135-141

Strauss KM, Martins LM, Plun-Favreau H, Marx FP, Kautzmann S, Berg D, Gasser T, Wszolek Z, Muller T, Bornemann A, Wolburg H, Downward J, Riess O, Schulz JB, Kruger R (2005) Loss of function mutations in the gene encoding Omi/HtrA2 in Parkinson's disease. Hum Mol Genet 14: 2099-111

Subramaniam SR, Vergnes L, Franich NR, Reue K, Chesselet MF (2014) Region specific mitochondrial impairment in mice with widespread overexpression of alpha-synuclein. Neurobiol Dis 70: 204-13

Takatori S, Ito G, Iwatsubo T (2008) Cytoplasmic localization and proteasomal degradation of N-terminally cleaved form of PINK1. Neurosci Lett 430: 13-17

Tanaka A, Cleland MM, Xu S, Narendra DP, Suen DF, Karbowski M, Youle RJ (2010) Proteasome and p97 mediate mitophagy and degradation of mitofusins induced by Parkin. J Cell Biol 191: 1367-1380

Thastrup O, Cullen PJ, Drobak BK, Hanley MR, Dawson AP (1990) Thapsigargin, a tumor promoter, discharges intracellular Ca2+ stores by specific inhibition of the endoplasmic reticulum Ca2(+)-ATPase. Proc Natl Acad Sci USA 87: 2466-2470

Thomas RE, Andrews LA, Burman JL, Lin WY, Pallanck LJ (2014) PINK1-Parkin pathway activity is regulated by degradation of PINK1 in the mitochondrial matrix. PLoS Genet 10

Trempe JF, Fon EA (2013) Structure and Function of Parkin, PINK1, and DJ-1, the Three Musketeers of Neuroprotection. Front Neurol 4: 38

Uittenbogaard M, Baxter KK, Chiaramello A (2010) The neurogenic basic helix-loop-helix transcription factor NeuroD6 confers tolerance to oxidative stress by triggering an antioxidant response and sustaining the mitochondrial biomass. ASN Neuro 2: e00034

Unoki M, Nakamura Y (2001) Growth-suppressive effects of BPOZ and EGR2, two genes involved in the PTEN signaling pathway. Oncogene 20: 4457-4465

Valente EM, Abou-Sleiman PM, Caputo V, Muqit MM, Harvey K, Gispert S, Ali Z, Del Turco D, Bentivoglio AR, Healy DG, Albanese A, Nussbaum R, Gonzalez-Maldonado R, Deller T, Salvi S, Cortelli P, Gilks WP, Latchman DS, Harvey RJ, Dallapiccola B et al. (2004) Hereditary early-onset Parkinson's disease caused by mutations in PINK1. Science 304: 1158-60

Vande Walle L, Lamkanfi M, Vandenabeele P (2008) The mitochondrial serine protease HtrA2/Omi: an overview. Cell Death Differ 15: 453-60

Vives-Bauza C, Zhou C, Huang Y, Cui M, de Vries RL, Kim J, May J, Tocilescu MA, Liu W, Ko HS, Magrane J, Moore DJ, Dawson VL, Grailhe R, Dawson TM, Li C, Tieu K, Przedborski S (2010) PINK1-dependent recruitment of Parkin to mitochondria in mitophagy. Proc Natl Acad Sci USA 107: 378-383

Voos W (2013) Chaperone-protease networks in mitochondrial protein homeostasis. Biochim Biophys Acta 1833: 388-399

Wang K, Klionsky DJ (2011) Mitochondria removal by autophagy. Autophagy 7: 297-300

Wang X, Winter D, Ashrafi G, Schlehe J, Wong YL, Selkoe D, Rice S, Steen J, LaVoie MJ, Schwarz TL (2011) PINK1 and Parkin target Miro for phosphorylation and degradation to arrest mitochondrial motility. Cell 147: 893-906

Wang Y, Nartiss Y, Steipe B, McQuibban GA, Kim PK (2012) ROS-induced mitochondrial depolarization initiates PARK2/PARKIN-dependent mitochondrial degradation by autophagy. Autophagy 8: 1462-1476

Yamano K, Youle RJ (2013) PINK1 is degraded through the N-end rule pathway. Autophagy 9: 1758-1769

Youle RJ, van der Bliek AM (2012) Mitochondrial fission, fusion, and stress. Science 337: 1062-1065

Zhang X, Yuan Y, Jiang L, Zhang J, Gao J, Shen Z, Zheng Y, Deng T, Yan H, Li W, Hou WW, Lu J, Shen Y, Dai H, Hu WW, Zhang Z, Chen Z (2014) Endoplasmic reticulum stress induced by tunicamycin and thapsigargin protects against transient ischemic brain injury: Involvement of PARK2-dependent mitophagy. Autophagy 10: 1801-1813

Zhong Z, Umemura A, Sanchez-Lopez E, Liang S, Shalapour S, Wong J, He F, Boassa D, Perkins G, Ali SR, McGeough MD, Ellisman MH, Seki E, Gustafsson AB, Hoffman HM, Diaz-Meco MT, Moscat J, Karin M (2016) NF-kappaB Restricts Inflammasome Activation via Elimination of Damaged Mitochondria. Cell 164: 896-910

Zhou C, Huang Y, Shao Y, May J, Prou D, Perier C, Dauer W, Schon EA, Przedborski S (2008) The kinase domain of mitochondrial PINK1 faces the cytoplasm. Proc Natl Acad Sci USA 105: 12022-12027

Ziviani E, Tao RN, Whitworth AJ (2010) Drosophila parkin requires PINK1 for mitochondrial translocation and ubiquitinates mitofusin. Proc Natl Acad Sci USA 107: 5018-5023

Danksagung

Ich möchte mich an dieser Stelle besonders bei Prof. Wolfgang Voos bedanken, der mir diese Arbeit ermöglicht hat und mir während der letzten vier Jahre mit Rat und Tat zur Seite stand.

Außerdem danke ich Prof. Jörg Höhfeld für die Übernahme des Zweitgutachtens, sowie allen anderen Mitgliedern der Prüfungskommission.

Nadja Schröder danke ich besonders für die gemeinsame und produktive Arbeit am Pink1 Projekt. Prof. Wolfram Kunz und Kerstin Hallmann gilt mein Dank für die Durchführung der RT-PCR Messungen und die COX8A Kollaboration. Bedanken möchte ich mich auch bei Prof. Serge Przedborski, Dr. Maja A. Fedorowicz und Dr. Cristina Guardia-Laguarta für die interessante Zusammenarbeit zu Beginn meiner Doktorarbeit.

Mein besonderer Dank gilt Dr. Giovanna Cenini, Michael Bruderek, Anne Wilkening und Witold Jaworek. Es war und ist ein großes Glück euch als Kollegen zu haben und unsere gemeinsame Zeit wird immer Teil dieser Arbeit sein.

Mein Dank gilt auch allen anderen ehemaligen Mitarbeitern der AG Voos und nicht zuletzt denen, die gerade erst anfangen.